



Evidence for the $VH, H \rightarrow \tau\tau$ process with the ATLAS detector in Run 2

The ATLAS Collaboration

A search for the Standard Model Higgs boson produced in association with a W or Z boson and decaying into a pair of τ -leptons is presented. This search is based on proton-proton collision data collected at $\sqrt{s} = 13$ TeV by the ATLAS experiment at the LHC corresponding to an integrated luminosity of 140 fb^{-1} . For the Higgs boson candidate, only final states with at least one τ decaying hadronically ($\tau \rightarrow \text{hadrons} + \nu_\tau$) are considered. For the vector bosons, only leptonic decay channels are considered: $Z \rightarrow \ell\ell$ and $W \rightarrow \ell\nu_\ell$, with $\ell = e, \mu$. An excess of events over the expected background is found with an observed (expected) significance of 4.2 (3.6) standard deviations, providing evidence of the Higgs boson produced in association with a vector boson and decaying into a pair of τ -leptons. The ratio of the measured cross-section to the Standard Model prediction is $\mu_{VH}^{\tau\tau} = 1.28^{+0.30}_{-0.29}$ (stat.) $^{+0.25}_{-0.21}$ (syst.).

Contents

1	Introduction	2
2	The ATLAS detector	3
3	Data and simulation samples	4
4	Object reconstruction and event selection	5
4.1	Object reconstruction	5
4.2	Event categorization and selection	6
5	Background estimation	9
6	Analysis strategy	10
6.1	Neural network analysis	11
6.2	Mass-based analysis	13
7	Systematic uncertainties	13
8	Results	14
8.1	Results of the neural network analysis	15
8.2	Results of the mass-based analysis	19
9	Conclusion	20

1 Introduction

This paper presents a search for the associated production of the Higgs boson with a vector boson in which the Higgs boson decays to a pair of τ -leptons. This process is referred to as $VH(\tau\tau)$, where V represents either a W or Z boson. Two possible final states are considered for the $H \rightarrow \tau^+\tau^-$ decay: either both τ -leptons decay hadronically to one or more hadrons ($\tau_{\text{had}}\tau_{\text{had}}$), or one τ -lepton decays leptonically ($\tau \rightarrow \ell\nu_\tau\bar{\nu}_\ell$, $\ell = e, \mu$) and one hadronically ($\tau_{\text{lep}}\tau_{\text{had}}$). The combination in which both τ -leptons from the Higgs boson decay leptonically ($\tau_{\text{lep}}\tau_{\text{lep}}$) is not included in order to ensure an event selection that is independent from analyses such as the one presented in Ref. [1].

The events associated with the $VH(\tau\tau)$ process are classified by the leptonically-decaying vector boson candidate (either a W or Z boson) and by the Higgs boson decay channel ($\tau_{\text{had}}\tau_{\text{had}}$ or $\tau_{\text{lep}}\tau_{\text{had}}$) into four channels. Each channel is independently optimised to achieve sensitivity to these rare events in the context of their relevant background processes. The vector boson decaying to light leptons provides an efficient trigger option for these events that does not require relying on the Higgs boson decay products. Both the VH production [2, 3] and the $H \rightarrow \tau\tau$ decay channels [4, 5] have separately been observed by the ATLAS and CMS experiments in recent years. Recently, the CMS collaboration measured a signal strength relative to the SM prediction of the inclusive $VH(\tau\tau)$ process to be 1.79 ± 0.45 [6].

A similar search was performed by the ATLAS collaboration using 20.3 fb^{-1} of LHC Run 1 data at $\sqrt{s} = 8 \text{ TeV}$ [7]. Because of the smaller size of the dataset used in this search, it was only able to set

a 95% confidence level (C.L.) upper limit on the overall $VH(\tau\tau)$ cross section of 5.6 times the SM prediction. Compared with the Run 1 result, the analysis presented in this paper uses nearly seven times the total integrated luminosity. This analysis also benefits from the higher center-of-mass energy of Run 2 ($\sqrt{s} = 13$ TeV), providing an increase in the Higgs boson production cross section [8] of a factor of about 2, and from improved physics object reconstruction and calibration. The event selection is expanded through the addition of several channels, and the overall analysis strategy is improved via a neural network (NN) discriminant that enhances the signal vs. background selection efficiency.

2 The ATLAS detector

The ATLAS detector [9] at the LHC covers nearly the entire solid angle around the collision point¹. It consists of an inner tracking detector surrounded by a thin superconducting solenoid, electromagnetic and hadron calorimeters, and a muon spectrometer incorporating three large superconducting air-core toroidal magnets.

The inner-detector system (ID) is immersed in a 2 T axial magnetic field and provides charged-particle tracking in the range $|\eta| < 2.5$. The high-granularity silicon pixel detector covers the vertex region and typically provides four measurements per track, the first hit normally being in the insertable B-layer (IBL) installed before Run 2 [10, 11]. It is followed by the silicon microstrip tracker (SCT), which usually provides eight measurements per track. These silicon detectors are complemented by the transition radiation tracker (TRT), which enables radially extended track reconstruction up to $|\eta| = 2.0$. The TRT also provides electron identification information based on the fraction of hits (typically 30 in total) above a higher energy-deposit threshold corresponding to transition radiation.

The calorimeter system covers the pseudorapidity range ($|\eta| < 4.9$). The solid angle coverage for $|\eta|$ between 3.2 and 4.9 is completed with copper/liquid-argon (LAr) and tungsten/LAr calorimeter modules optimised for electromagnetic and hadronic measurements, respectively. Within the region $|\eta| < 3.2$, electromagnetic calorimetry is provided by barrel and endcap high-granularity lead/LAr calorimeters, with an additional thin LAr presampler covering $|\eta| < 1.8$ to correct for energy loss in material upstream of the calorimeters. Hadron calorimetry is provided by the steel/scintillator-tile calorimeter, segmented into three barrel structures within $|\eta| < 1.7$, and two copper/LAr hadron endcap calorimeters. The solid angle coverage is completed with forward copper/LAr and tungsten/LAr calorimeter modules optimised for electromagnetic and hadronic energy measurements respectively.

The muon spectrometer (MS) comprises separate trigger and high-precision tracking chambers measuring the deflection of muons in the magnetic field generated by the superconducting air-core toroidal magnets. The field integral of the toroids ranges between 2.0 and 6.0 T m across most of the detector. Three layers of precision chambers, each consisting of layers of monitored drift tubes, cover the region $|\eta| < 2.7$, complemented by cathode-strip chambers in the forward region, where the background is highest. The muon trigger system covers the range $|\eta| < 2.4$ with resistive-plate chambers in the barrel, and thin-gap chambers in the endcap regions.

¹ ATLAS uses a right-handed coordinate system with its origin at the nominal interaction point (IP) in the centre of the detector and the z -axis along the beam pipe. The x -axis points from the IP to the centre of the LHC ring, and the y -axis points upwards. Cylindrical coordinates (r, ϕ) are used in the transverse plane, ϕ being the azimuthal angle around the z -axis. The pseudorapidity is defined in terms of the polar angle θ as $\eta = -\ln \tan(\theta/2)$. Angular distance is measured in units of $\Delta R \equiv \sqrt{(\Delta\eta)^2 + (\Delta\phi)^2}$.

Interesting events are selected by the first-level trigger system implemented in custom hardware, followed by selections made by algorithms implemented in software in the high-level trigger [12]. The first-level trigger accepts events from the 40 MHz bunch crossings at a rate below 100 kHz, which the high-level trigger further reduces in order to record events to disk at about 1 kHz.

An extensive software suite [13] is used in the reconstruction and analysis of real and simulated data, in detector operations, and in the trigger and data acquisition systems of the experiment.

3 Data and simulation samples

The dataset used for this measurement consists of the LHC proton–proton collision data recorded by the ATLAS experiment at $\sqrt{s} = 13$ TeV during the Run 2 period from 2015 to 2018. Events are selected for analysis only if they are of good quality and if all the relevant detector components are known to have been in good operating condition [14]. The total integrated luminosity of the analysed data is 138 fb^{-1} . Only events that pass relevant trigger requirements are considered in the analysis. These triggers are designed to select single electrons, single muons, or combinations of these two light leptons [15–18]. The thresholds applied to the reconstructed transverse momentum (p_T) for the single-lepton triggers were $p_T^e > 27$ (25) GeV and $p_T^\mu > 27.3$ (21) GeV for the 2016–2018 (2015) data-taking period. The p_T thresholds for the dilepton triggers were $p_T^e > 18$ GeV and $p_T^\mu > 14.7$ GeV for the entire data-taking period. The trigger selection acceptance was maximized by using the logical OR of triggers requiring one or two light leptons.

Samples of Monte Carlo (MC) simulated events are used to optimise the event selection and to model the signal and several background processes. Simulated event samples for the $VH(\tau\tau)$ signal, as well as all background samples, were produced using various MC generators, as described in Table 1. The samples were produced with the ATLAS simulation infrastructure [19] using the full detector simulation performed by the GEANT4 [20] toolkit. The POWHEG NNLOPS program [21–25] was used to model gluon-gluon fusion (ggF) Higgs boson production with next-to-next-leading-order (NNLO) accuracy. The vector boson fusion (VBF) and the VH production processes were simulated with POWHEG at next-leading-order (NLO) accuracy in QCD. The MC prediction was normalized to cross-sections calculated at NNLO in the strong coupling with NLO electroweak corrections [26–30]. The production of $t\bar{t}H$ events was simulated using POWHEGBOX [21–25] at NLO. In all signal events, the decays of the τ -leptons were modelled by PYTHIA8.235 [31]. Background samples of $V + \text{jets}$ use SHERPA 2.2.1 [32], while the diboson and triboson events were generated by SHERPA 2.2.2 [32] (including τ -lepton decays), and $t\bar{t}$ and single-top samples were generated by POWHEG+PYTHIA8.230, with PYTHIA also performing τ -lepton decays. The POWHEG+PYTHIA8 samples use EVTGEN(v1.6.0) [33] for the simulation of the b -hadron decays.

The effects of multiple interactions in the same and neighbouring bunch crossings (pile-up) were modeled by overlaying minimum-bias events to reproduce the pile-up distributions seen in the data. These minimum-bias events were simulated using the soft QCD processes of PYTHIA 8.186 [34] with the A3 [35] set of tuned parameters and the NNPDF2.3LO [36] PDF.

Table 1: Information on the Monte Carlo event samples used to produce the most relevant processes incorporated into this analysis, including the process name, names of the MC generator and the model of the underlying event with hadronisation and parton showering (UEPS), the corresponding PDF set, and the perturbative order in QCD to which the cross-section has been calculated for the normalisation of the simulated samples.

Process	MC Generator + UEPS	PDF Set	Perturbative Order
Signal			
$W \rightarrow \ell\nu, H \rightarrow \tau\tau$	POWHEG [21–25]+PYTHIA8.235 [31]	PDF4LHC15NLO [37]	NLO
$Z \rightarrow \ell\ell, H \rightarrow \tau\tau$	POWHEG+PYTHIA8.235	PDF4LHC15NLO	NLO
Background			
ggF $H \rightarrow \tau\tau$	POWHEG+PYTHIA8.235	PDF4LHC15NLO	NNLO
VBF $H \rightarrow \tau\tau$	POWHEG+PYTHIA8.235	PDF4LHC15NLO	NLO
$t\bar{t}H, H \rightarrow \tau\tau$	POWHEG+PYTHIA8.235	NNPDF30NNLO [36]	NLO
Diboson	SHERPA 2.2.2 [32]	NNPDF30NNLO	NNLO
Triboson	SHERPA 2.2.2	NNPDF30NNLO	NNLO
V + jets	SHERPA 2.2.1 [32]	NNPDF30NNLO	NNLO
Single-top	POWHEG+PYTHIA8.230	NNPDF30NLO	NLO
$t\bar{t}$	POWHEG+PYTHIA8.230	NNPDF30NLO	NLO

4 Object reconstruction and event selection

The $VH(\tau\tau)$ event selection requires the reconstruction of electrons, muons, visible products of hadronically decaying τ -leptons ($\tau_{\text{had-vis}}$), jets (along with their flavour tagging properties), and missing transverse energy ($E_{\text{T}}^{\text{miss}}$). The number of reconstructed electrons, muons and $\tau_{\text{had-vis}}$ in each event is used to separate the events into analysis channels.

4.1 Object reconstruction

Electron candidates are reconstructed from tracks in the inner detector matching calorimeter energy deposits [38]. The electron candidates must fulfill the following baseline requirements: $p_{\text{T}} > 13$ GeV, a pseudorapidity $|\eta|$ below 2.5 and not in the calorimeter crack region ($1.37 < |\eta| < 1.52$), and passing the Loose likelihood selection requirement (93% efficient) for electron identification [38]. For an electron to qualify for one of the signal-enhanced categories, it must additionally pass the Tight identification selection requirement (80% efficiency) and the Loose isolation criterion, which is defined for both calorimeter and track-based isolation [38].

Muon candidates are reconstructed from tracks in the muon spectrometer and then matched to tracks in the inner detector [39]. Baseline muon candidates included in the analysis are required to pass a minimum p_{T} threshold of 9 GeV, have an $|\eta| < 2.5$, and pass the Loose muon identification selection requirement (corresponding to over 98% efficiency). For a muon to qualify for one of the signal-enhanced categories, it must pass the Tight selection requirement (with an efficiency between 90 and 93%, depending on the p_{T} of the muon). Selected muon candidates must also pass a Tight isolation criterion that is based exclusively on tracking information. [39]

Jets are reconstructed from particle flow objects using the anti- k_t [40, 41] algorithm with a distance parameter $R = 0.4$, and calibrated as in Ref. [42]. Additional requirements on the jet-vertex-tagger (JVT) [43] are imposed to suppress jets originating from pile-up. In order to identify jets initiated by

b quarks for suppression of top quark backgrounds in $VH(\tau\tau)$ events, where V is a W boson, the DL1r b -tagging algorithm [44–47] is used on jets with $p_T > 20$ GeV and $|\eta| < 2.5$. The fixed 85% efficiency selection requirement is used.

The final states of τ -lepton hadronic decays include a neutrino and a set of visible decay products, most frequently one or three charged pions and up to two neutral pions. The reconstruction of the $\tau_{\text{had-vis}}$ is seeded by jets reconstructed via the anti- k_r algorithm, using calibrated energy clusters as inputs, with a distance parameter of $R = 0.4$ [48]. Jets seeding $\tau_{\text{had-vis}}$ candidates are additionally required to have $p_T > 10$ GeV and $|\eta| < 2.5$. To separate the $\tau_{\text{had-vis}}$ candidates initiated from hadronic τ -lepton decays from jets initiated by quarks or gluons, a Recurrent Neural Network (RNN) [49] identification method was trained on information from reconstructed charged-particle tracks and clusters of energy in the calorimeter associated to $\tau_{\text{had-vis}}$ candidates as well as high-level discriminating variables. A separate multivariate discriminant based on a Boosted Decision Tree (ϵ BDT) [50] is also used to reject backgrounds arising from electrons faking $\tau_{\text{had-vis}}$ (mainly from $Z \rightarrow ee$ +jets in this analysis). This discriminant is built using information from the calorimeter and the tracking detector. Transition radiation information from the TRT system plays a key role in the performance of this discriminant. Baseline taus are required to have 1 or 3 associated tracks, electric charge of ± 1 , $p_T > 20$ GeV and $|\eta| < 2.5$, excluding the calorimeter crack region. In addition, a dedicated muon veto criterion, designed to reject muons misreconstructed as taus (typically due to large calorimeter energy deposits), is applied. To qualify as objects at the earliest stage of the analysis event categorisation, each $\tau_{\text{had-vis}}$ must pass the Medium RNN identification selection requirement, with efficiencies of 75% for 1-prong and 60% for 3-prong taus, and the Loose ϵ BDT requirement, with an efficiency of 95%.² [50].

An overlap procedure is applied to ensure that electrons, muons, $\tau_{\text{had-vis}}$ and jets used in this analysis are built from a set of mutually exclusive tracks and calorimeter energy deposits. More details can be found in Ref. [51].

The missing transverse vector is an estimate of the imbalance in the transverse momentum in the detector. This vector is calculated as the negative vector sum of the transverse momenta of all reconstructed final-state objects (electrons, muons, taus, and jets). The magnitude of the missing transverse vector is referred to as missing transverse momentum (E_T^{miss}). Tracks not associated to any reconstructed object are also included in the calculation, and serve to estimate the contribution from low- p_T collision remnants (referred to as the *soft term* contribution). The default Tight criteria of the official ATLAS Missing Transverse Energy Tool was chosen [52].

4.2 Event categorization and selection

The analysis channels are defined by the vector boson associated with the Higgs boson production and by the decay mode (leptonic or hadronic) of the τ -leptons associated with the Higgs boson decay. This results in four different channels: $WH(\tau_{\text{lep}}\tau_{\text{had}})$, $WH(\tau_{\text{had}}\tau_{\text{had}})$, $ZH(\tau_{\text{lep}}\tau_{\text{had}})$ and $ZH(\tau_{\text{had}}\tau_{\text{had}})$. In all channels, only the final states in which the vector boson decays to light leptons are considered. In the $\tau_{\text{lep}}\tau_{\text{had}}$ channel, the leading p_T light lepton is assigned to the vector boson (V). If V is a Z boson, the sub-leading p_T light lepton assigned to the Z boson leptonic decay is required to have the same flavor and opposite charge to that of the leading p_T light lepton. If multiple opposite-sign light lepton pairs can be formed, the pair with invariant mass closest to the Z boson mass is chosen. The same invariant mass is also required to be within

² For the $WH(\tau_{\text{lep}}\tau_{\text{had}})$ category, as defined in Section 4.2, the Medium ϵ BDT requirement is used. This has an efficiency of 85%.

a given p_T range, optimized separately for each category, to suppress events with a pair of light leptons not originating from a $Z \rightarrow \ell\ell$ process. The light lepton not assigned to the V boson leptonic decay is then associated to the leptonic τ from the Higgs boson. When V is a W boson, the sub-leading p_T light lepton is assigned to the Higgs boson with no flavor or charge selection applied. For each category, the selection is organized into a PRESELECTION and SIGNAL REGION selection. The PRESELECTION is used as a starting point of shared selections from which a series of validation regions are further defined to check the modelling of specific background sources. Events in the $WH(\tau_{\text{lep}}\tau_{\text{had}})$ and $ZH(\tau_{\text{lep}}\tau_{\text{had}})$ SIGNAL REGIONS have a small light lepton parent misassignment probability of about 3% thanks to the kinematic selections applied.

The main analysis strategy uses a NN classifier as a final discriminant. As a cross-check, another version of the analysis is done using Higgs boson mass estimators as the final discriminants, as was done in the Run 1 analysis [7]. In the ZH channels, the Missing Mass Calculator (m_{MMC}) [53] is used to estimate the Higgs boson mass. The m_{MMC} method is a precise strategy for calculating a most likely parent particle mass when that parent particle decays into multiple sources of E_T^{miss} , as in most of the $H \rightarrow \tau\tau$ event topologies. For the WH channels, in which both the W and the Higgs boson decays act as sources of E_T^{miss} , the m_{MMC} assumption that the E_T^{miss} (i.e. neutrinos) originate only from the Higgs boson decay is no longer valid, so the Late-Projected transverse mass m_{2T} [54] is instead used as a discriminant³.

Table 2 summarizes the selection criteria used for each category. The event selection shown in Table 2 is identical for the cross-check analysis using the Higgs boson mass discriminants, with the exception of the Higgs boson mass window cuts. The combined signal efficiency is about 6% and 8% for the WH and ZH channels, respectively⁴. The $WH(\tau_{\text{lep}}\tau_{\text{had}})$ selection has a signal efficiency of about 7% and represents about 44% of all the $VH(\tau\tau)$ signal events across the four categories. The $WH(\tau_{\text{had}}\tau_{\text{had}})$ selection has a signal efficiency of about 5% and represents about 32% of all the $VH(\tau\tau)$ signal events across the four categories. The $ZH(\tau_{\text{lep}}\tau_{\text{had}})$ selection has a signal efficiency of about 7% and represents about 10% of all the $VH(\tau\tau)$ signal events across the four categories. The $ZH(\tau_{\text{had}}\tau_{\text{had}})$ selection has a signal efficiency of about 9% and represents about 14% of all the $VH(\tau\tau)$ signal events across the four categories.

Table 2: PRESELECTION and SIGNAL REGION selection for the four categories. ‘‘OS’’ stands for opposite-sign, ‘‘SS’’ for same-sign and ‘‘ID’’ for identification.

Selection	$WH, H \rightarrow \tau_{\text{lep}}\tau_{\text{had}}$	$WH, H \rightarrow \tau_{\text{had}}\tau_{\text{had}}$	$ZH, H \rightarrow \tau_{\text{lep}}\tau_{\text{had}}$	$ZH, H \rightarrow \tau_{\text{had}}\tau_{\text{had}}$
PRESELECTION	exactly 1 $\tau_{\text{had-vis}}$ exactly 2 ℓ b -jet veto	exactly 2 $\tau_{\text{had-vis}}$ exactly 1 ℓ b -jet veto	exactly 1 $\tau_{\text{had-vis}}$ exactly 3 ℓ same-flavour, OS ℓ pair $m_{\ell\ell} \in [81, 101]$ GeV	exactly 2 $\tau_{\text{had-vis}}$ exactly 2 ℓ same-flavour, OS ℓ pair $m_{\ell\ell} \in [71, 111]$ GeV
SIGNAL REGION	1 $\tau_{\text{had-vis}}$ and 1 τ_{lep} OS exactly 2 ℓ SS $\sum_{\ell} p_T(\ell) + p_T(\tau_{\text{had-vis}}) > 90$ GeV $m_{ee} \notin [80, 100]$ GeV	exactly 2 $\tau_{\text{had-vis}}$ OS $0.8 < \Delta R(\tau_{\text{had-vis}}, \tau_{\text{had-vis}}) < 2.8$ $\sum_{\tau_{\text{had-vis}}} p_T(\tau_{\text{had-vis}}) > 100$ GeV $m_T(\ell, E_T^{\text{miss}}) > 20$ GeV	exactly 1 $\tau_{\text{had-vis}}$ and 1 τ_{lep} OS $\sum_{\tau_{\text{had-vis}}, \tau_{\text{lep}}} p_T(\tau) > 60$ GeV	exactly 2 $\tau_{\text{had-vis}}$ OS $\sum_{\tau_{\text{had-vis}}} p_T(\tau) > 75$ GeV
HIGGS BOSON MASS WINDOW CUT (ONLY APPLIED IN THE NN-BASED ANALYSIS)	$m_{2T} \in [60, 130]$ GeV	$m_{2T} \in [80, 130]$ GeV	$m_{\text{MMC}} \in [100, 170]$ GeV	$m_{\text{MMC}} \in [100, 180]$ GeV

³ The m_{2T} variable is constructed to provide an event-by-event lower bound on the transverse mass of the heaviest parent particle – in this topology, the Higgs boson. The m_{2T} is defined as $m_{2T} = \min_{\sum \vec{q}_{iT} = \vec{p}_T^{\text{miss}}} [\max_a [m_{aT}]]$, where m_{aT} is the late-projected transverse mass of the a^{th} parent particle and $\sum \vec{q}_{iT}$ is the sum of the transverse momenta of all invisible particles.

⁴ Estimated using MC simulations and normalized to the total number of signal events from a specific process falling into the detector acceptance with no trigger requirements.

4.2.1 Selection of the $WH, H \rightarrow \tau_{\text{lep}}\tau_{\text{had}}$ events

The PRESELECTION begins with requiring exactly two light leptons and one $\tau_{\text{had-vis}}$ that pass their baseline requirements as well as additional isolation and identification criteria as described in Section 4.1. A b -jet veto is applied to suppress backgrounds from top quark production.

For the SIGNAL REGION selection, a same-sign light lepton requirement is applied to suppress Z +jets backgrounds and the $\tau_{\text{had-vis}}$ is required to have the opposite sign of the light leptons. A differentiation based on the final state light leptons is also used to further optimise the selection criteria. For the dielectron final state, the invariant mass of the two electrons m_{ee} must satisfy $m_{ee} \notin [80, 100]$ GeV to reduce the contamination of Z +jets events with $Z \rightarrow ee$ where one of the e was reconstructed with the wrong charge, thereby passing the same-sign light lepton requirement. The scalar sum of all three final state particles' p_T is required to be greater than 90 GeV to suppress events that contain one or two misidentified objects. Finally, for the main analysis strategy using a NN discriminant, the m_{2T} is required to fall within $60 < m_{2T} < 130$ GeV to improve the signal-to-background ratio.

4.2.2 Selection of the $WH, H \rightarrow \tau_{\text{had}}\tau_{\text{had}}$ events

The PRESELECTION begins with requiring exactly one light lepton and two $\tau_{\text{had-vis}}$ that pass their baseline requirements as well as additional isolation and identification criteria to qualify as analysis-level objects, as described in Section 4.1. A b -jet veto is applied to suppress backgrounds from top-quark production.

The SIGNAL REGION selection adds the following criteria. The two $\tau_{\text{had-vis}}$ are required to have opposite electric charge. A requirement on $0.8 < \Delta R(\tau_{\text{had-vis}}, \tau_{\text{had-vis}}) < 2.8$ and on the scalar sum of the p_T of the two ($\tau_{\text{had-vis}} > 100$ GeV) are imposed to suppress events that contain one or two misidentified $\tau_{\text{had-vis}}$ passing the selection. An additional cut on the transverse mass⁵ between the E_T^{miss} and the light lepton $m_T(\ell, E_T^{\text{miss}}) > 20$ GeV is applied to reduce the $Z \rightarrow \tau\tau$ background. Finally, for the main analysis strategy using a NN discriminant, the m_{2T} is required to fall within $80 < m_{2T} < 130$ GeV to improve the signal-to-background ratio.

4.2.3 Selection of the $ZH, H \rightarrow \tau_{\text{lep}}\tau_{\text{had}}$ events

The PRESELECTION begins with requiring exactly three light leptons and one $\tau_{\text{had-vis}}$ that pass their baseline requirements as well as additional isolation and identification criteria to qualify as analysis-level objects, as described in Section 4.1. Two light leptons must have the same flavour and opposite signs, as they are associated with the Z boson decay. The Missing Mass Calculator (m_{MMC}) needs to have successfully converged.

The SIGNAL REGION selection further requires that the decay products of the Higgs boson have opposite sign. The invariant mass of the light leptons $m_{\ell\ell}$ must satisfy $81 < m_{\ell\ell} < 101$ GeV. The scalar sum of p_T from the two objects associated with the Higgs boson decay is required to be greater than 60 GeV. Lastly, for the main analysis strategy using a NN discriminant, the m_{MMC} must satisfy $100 < m_{\text{MMC}} < 170$ GeV to enhance the signal-to-background ratio.

⁵ The transverse mass variable is defined by projecting the momenta to the plane perpendicular to the beam direction: $m_{\text{T}}^2 = (\sum E_{iT})^2 - (\sum \vec{p}_{iT})^2$, with $E_{iT} = \sqrt{m_i^2 + \vec{p}_{iT}^2}$.

4.2.4 Selection of the ZH , $H \rightarrow \tau_{\text{had}}\tau_{\text{had}}$ events

The PRESELECTION begins with requiring exactly two light leptons and two $\tau_{\text{had-vis}}$ that pass their baseline requirements as well as additional isolation and identification criteria to qualify as analysis-level objects, as described in Section 4.1. These two light leptons associated with the Z boson decay need to be same flavour and opposite charge. The m_{MMC} is required to have successfully converged.

For the SIGNAL REGION selection, the two $\tau_{\text{had-vis}}$ from the Higgs boson decay are required to have opposite signs. The invariant mass of the light leptons $m_{\ell\ell}$ must satisfy $71 < m_{\ell\ell} < 111$ GeV. In this case, the $m_{\ell\ell}$ acceptance window is slightly larger than the $ZH(\tau_{\text{lep}}\tau_{\text{had}})$ category due to lower background levels. To enhance the suppression of the misidentified $\tau_{\text{had-vis}}$ events, the scalar sum of the p_T of the taus is required to be greater than 75 GeV. Lastly, for the main analysis strategy using a NN discriminant, the m_{MMC} must satisfy $100 < m_{\text{MMC}} < 180$ GeV.

5 Background estimation

The main backgrounds for this analysis consist of VZ events and Z +jets events in which a jet is misidentified as a light lepton ($\ell = e, \mu$) or $\tau_{\text{had-vis}}$. The background contribution from misidentified jets is estimated using a data-driven technique. Other background components such as top quark decays, $t\bar{t}H$, and WWW triboson events are estimated using MC simulations.

In the ZH categories, the ZZ events are the main background source and are estimated using simulated events. In both ZH categories, the ZZ events form $\sim 60\%$ of the total background, while the background from misidentified jets events account for much of the remaining $\sim 40\%$. The other background sources (top-quark decays, triboson and $t\bar{t}H$ events) account for less than 1% of the total background and are estimated using simulations.

In the WH categories, background from misidentified jets events represent $\sim 70\%$ of the total background. In both WH categories, the WZ events account for $\sim 30\%$ of the total background and are estimated using simulated events. The other background sources (top quark decays, WWW triboson, and $t\bar{t}H$ events) form less than 2% of the total background and are also estimated using simulated events.

Due to the difficulties of validating the diboson background in dedicated validation regions, the analysis relies on previous measurements with higher statistics available [55, 56]. No dedicated validation region is used to extract the diboson background normalization from the data.

The background from misidentified jets is evaluated using the Fake Factor method [57, 58]. A similar background estimation was used in the previous version of this analysis [7]. A Fake Factor is defined as $f = r/(1 - r)$, where r represents the selection efficiency of misidentified objects ($\tau_{\text{had-vis}}$ or light lepton), defined as the ratio of the number of objects passing the selection requirements (as described in Section 4.1) and the number of objects that pass nearly all the selection requirements, but fail one or both of the identification and isolation requirements. For electrons and muons, at least one of the identification and isolation requirements must fail, while τ -leptons need to pass the Very-Loose identification requirement (efficiency of 99%) and fail the Medium identification requirement.

The expected number of misidentified jets in a given region is obtained using the Fake Factor to scale the number of events selected in an orthogonal region in which one or more requirements are inverted: the identification and/or isolation requirements for light leptons, and the identification for the $\tau_{\text{had-vis}}$. The Fake

Factors are measured in a dedicated Z +jets control region (CR) enriched in background from misidentified jets and are then used as extrapolation factors to estimate the number of selected fake objects in the signal region. This Z +jets CR is based on the selection of exactly two opposite-sign light leptons that are required to be consistent with a Z -boson decay, plus a third object that is assumed to originate from a jet that is misidentified either as an electron, muon or $\tau_{\text{had-vis}}$ and is used for the determination of the corresponding Fake Factors. The Fake Factors are computed in bins of lepton p_T and $|\eta|$. The $\tau_{\text{had-vis}}$ Fake Factors are also parametrized with respect to the $\tau_{\text{had-vis}}$ jet width, defined as a weighted sum of jet constituent distance from the jet axis ($\text{jetwidth} = \sum_i \Delta R^i p_T^i / \sum_i p_T^i$) separately for one- and three-track $\tau_{\text{had-vis}}$. In the $\tau_{\text{had-vis}}$ case, the jet width parametrization is particularly important because it is highly correlated with the jet quark–gluon fraction composition, and quark- vs. gluon-initiated jets exhibit different rates of faking $\tau_{\text{had-vis}}$ identification. Contributions from a jet misidentified as a light lepton that triggered the event are estimated from the simulation and found to be negligible. Diboson events can contaminate the selection at a level below a few percent, and are therefore subtracted using the MC prediction. The evaluation of the background from misidentified jets takes into account the presence of multiple misidentified objects, which can be as high as three in the ZH categories in which only one light lepton triggered the event.

In all the categories, the modelling of the background from misidentified jets is validated in a misidentified background-enriched same-sign region. For the ZH categories, the PRESELECTION criteria are applied, and the objects associated to the Higgs boson decay are required to have the same charge. For the WH categories, all the SR cuts are applied except the m_{2T} mass cut and same-sign τ -leptons selection requirement. The selected region provides sufficient statistics to minimize statistical fluctuations. The larger statistics available in the WH categories allow for verifying the good modelling of the background from misidentified jets in additional validation regions, as summarized in Table 3. The same table also shows the expected composition of the processes contributing to the background from misidentified jets in each region obtained from a pure MC study.

The uncertainties associated with the Fake Factor method have statistical and systematic components. The statistical component is estimated for each Fake Factor bin separately and consists of the statistical uncertainties from the data within the Z +jets CR propagated to the Fake Factors. For each category, a dedicated systematic uncertainty takes into account the statistical fluctuations associated with the subtracted MC component. Another dedicated systematic uncertainty accounts for the residual difference between the background from misidentified jets modelling and the data in the misidentified background-enriched same-sign region. This uncertainty is evaluated at the PRESELECTION stage, which requires the objects associated to the Higgs boson decay to have the same charge. For each category, this uncertainty is evaluated in bins of $\tau_{\text{had-vis}}$ p_T . The statistical component is negligible ($< 5\%$) compared with the systematic uncertainty, which ranges up to 23% in the high p_T region (above 60 GeV).

Figure 1 shows the distributions of some kinematic variables that demonstrate the good quality of the modelling of the background from misidentified jets in the misidentified background-enriched same-sign region in each of the four analysis categories.

6 Analysis strategy

In this analysis, the signal strength is measured by a fit to a neural network (NN) classifier score distribution. As a cross-check for this method, an alternative strategy is applied using the same mass-based analysis methods as in Run 1: m_{MMC} for the ZH channels and m_{2T} for the WH channels. The notable difference

Table 3: Validation regions, in addition to the misidentified background-enriched same-sign region, used to check the modelling of the background from misidentified jets in the WH categories. The last column shows an estimate of the major contribution to the background from misidentified jets, which was estimated using a pure MC study. The definition of the collinear mass (m_{coll}) can be found in Ref. [59].

Category	Region	Cuts	Major process contributing to the background from misidentified jets
$WH, H \rightarrow \tau_{\text{had}}\tau_{\text{had}}$	$W+\text{jets}$	PRESELECTION same-sign $\tau_{\text{had-vis}}$ $m_{\text{T}}(\ell, E_{\text{T}}^{\text{miss}}) < 60 \text{ GeV}$	$W+\text{jets} \sim 70\%$
	$Z \rightarrow \tau\tau$	PRESELECTION $m_{2\text{T}} < 60 \text{ GeV}$ $m_{\text{T}}(\ell, E_{\text{T}}^{\text{miss}}) < 40 \text{ GeV}$	$Z \rightarrow \tau\tau \sim 50\%$
	top-quark	PRESELECTION $\# b \text{ jets} > 0$	$t\bar{t} \sim 70\%$
$WH, H \rightarrow \tau_{\text{lep}}\tau_{\text{had}}$	$Z \rightarrow \tau\tau$	PRESELECTION opposite-sign light leptons $m_{\text{coll}}(\ell, \ell) \in [60, 120] \text{ GeV}$ $m_{ee} \notin [80, 100] \text{ GeV}$	$Z \rightarrow \tau\tau \sim 40\%$
	All Same Sign	PRESELECTION all objects with same-sign $m_{ee} \notin [80, 100] \text{ GeV}$	$W+\text{jets} \sim 70\%$

in significance reached with the two methods demonstrates the power of the NN to improve analysis sensitivity.

6.1 Neural network analysis

The result is extracted using a fit to the distribution of the score of a NN classifier. Six different NN classifiers are trained: one for each of the main channels and three for $WH, H \rightarrow \tau_{\text{lep}}\tau_{\text{had}}$, which has a dedicated classifier for each combination of final light lepton flavour ($e + e$, $\mu + \mu$, and $e + \mu$). The NNs are trained to distinguish simulated signal and diboson events using a combination of low-level and high-level kinematic information from the particles in the event (e.g. p_{T} , $|\eta|$, ϕ) and the overall event (e.g. $E_{\text{T}}^{\text{miss}}$ and dilepton mass). The full list of the input variables used for each NN is provided in Table 4. The mass-based observables m_{MMC} and $m_{2\text{T}}$ were not included in the list of inputs, as it was determined that they did not yield a significant improvement in sensitivity.

Each NN is implemented using KERAS [60] with a TENSORFLOW [61] backend. The networks consist of two initial transformation layers followed by three fully connected layers of 128 nodes with ReLU [62] activations. The output layer consists of a single node with a sigmoid activation function. The two initial transformation layers enforce rotation invariance in ϕ by adding a global ϕ offset during training, which is consistently applied event-by-event to all reconstructed objects.

The binning of the NN score distributions in the four categories results from an optimization process that maximized significance under the constraint that the statistical uncertainty associated with the signal and background templates is no larger than 20% in each bin.

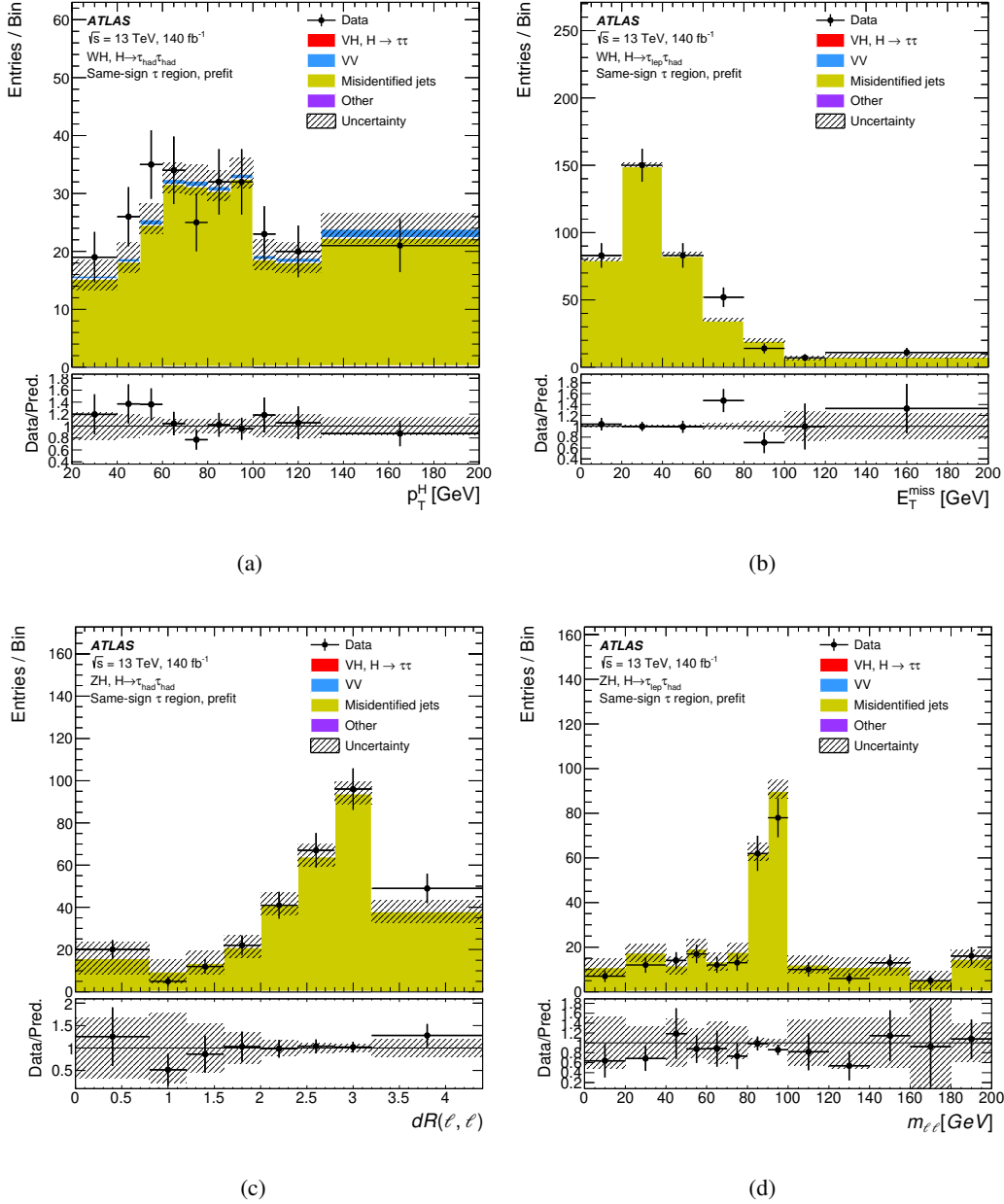


Figure 1: Distributions of representative kinematic variables in the misidentified background-enriched same-sign region: (a) the Higgs boson transverse momentum (p_T^H) in the $WH(\tau_{\text{had}}\tau_{\text{had}})$ category, (b) the missing transverse momentum (E_T^{miss}) in the $WH(\tau_{\text{lep}}\tau_{\text{had}})$ category, (c) the radial distance ($dR(\ell, \ell)$) between the two light leptons associated to the $Z \rightarrow \ell\ell$ decay process in the $ZH(\tau_{\text{had}}\tau_{\text{had}})$ category, and (d) the invariant mass ($m_{\ell\ell}$) of the two light leptons associated to the $Z \rightarrow \ell\ell$ decay in the $ZH(\tau_{\text{lep}}\tau_{\text{had}})$ category. The hatched band represents the pre-fit statistical, experimental and theoretical uncertainties. The signal contributions are considered as part of the predictions and are normalized as predicted by the Standard Model.

Table 4: Input variables for the neural networks included in all channels, and then for the specific category. The indexes “1” and “2” refer to the leading and sub-leading objects, respectively (following a p_T ordering). The symbol ℓ_τ refers to the light lepton originating from a τ -lepton decay, while ℓ (without any index) refers to a light lepton associated with the V boson decay.

All categories	$ZH, H \rightarrow \tau_{\text{had}}\tau_{\text{had}}$	$ZH, H \rightarrow \tau_{\text{lep}}\tau_{\text{had}}$	$WH, H \rightarrow \tau_{\text{had}}\tau_{\text{had}}$
N-prongs(τ_1)	N-prongs(τ_2)	$p_T(\ell_2)$	N-prongs(τ_2)
$p_T(\tau_1)$	$p_T(\tau_2)$	$\eta(\ell_2)$	$p_T(\tau_2)$
$\eta(\tau_1)$	$\eta(\tau_2)$	$\phi(\ell_2)$	$\eta(\tau_2)$
$\phi(\tau_1)$	$\phi(\tau_2)$	$p_T(H)$	$\phi(\tau_2)$
$\Delta R(\tau_1, \ell_1)$	$p_T(\ell_2)$	$\eta(\ell_\tau)$	$\sqrt{\eta(\ell_1)^2 + \phi(\ell_1)^2}$
$p_T(l_1)$	$\eta(\ell_2)$	$\phi(\ell_\tau)$	
$\eta(\ell_1)$	$\phi(\ell_2)$	$\Delta R(\ell, \ell)$	
$\phi(\ell_1)$	$m_{\ell\ell}$	$m_{\ell\ell}$	
$p_T(E_T^{\text{miss}})$	$\Delta R(\ell, \ell)$		
$\phi(E_T^{\text{miss}})$			
	$WH, W \rightarrow e\nu_e, H \rightarrow \tau_e\tau_{\text{had}}$	$WH, W \rightarrow e(\mu)\nu_{e(\mu)}, H \rightarrow \tau_{\mu(e)}\tau_{\text{had}}$	$WH, W \rightarrow \mu\nu_\mu, H \rightarrow \tau_\mu\tau_{\text{had}}$
	$p_T(\ell_\tau)$	$p_T(\ell_\tau)$	$p_T(\ell_\tau)$
	$\eta(\ell_\tau)$	$\eta(\ell_\tau)$	$\eta(\ell_\tau)$
	$\phi(\ell_\tau)$	$\phi(\ell_\tau)$	$\phi(\ell_\tau)$
	$\Delta\eta(\ell, \ell_\tau)$	$\Delta\eta(\ell, \ell_\tau)$	$\Delta\eta(\ell, \ell_\tau)$
	jet width(τ_1)	jet width(τ_1)	jet width(τ_1)
	$p_T(H)$	$m(\tau_1, \ell_\tau)$	$\Delta R(\ell, \ell_\tau)$
	$m(\tau_1, \ell_\tau)$	$\Delta R(\ell, \ell_\tau)$	$m(\tau_1, l_\tau)$
	$\Delta\eta(\tau_1, \ell_\tau)$	$\Delta\eta(\tau_1, \ell_\tau)$	$\Delta\eta(\tau_1, \ell_\tau)$
	$\Delta\phi(l_1, \ell_\tau)$	$\sum p_T(\text{all visible})$	$\Delta R(\tau_1, \ell_\tau)$
	$\Delta\phi(\tau_1, E_T^{\text{miss}})$	$\Delta\phi(\tau_1, E_T^{\text{miss}})$	$\sum p_T(\text{all visible})$
	$\Delta R(\ell, \ell_\tau)$		$\Delta\phi(\ell_1, \ell_\tau)$

6.2 Mass-based analysis

As a cross-check for the main analysis strategy, a historical approach used in the Run 1 analysis based on the mass observables (m_{MMC} for the ZH channels and the m_{2T} for the WH channels) is also adopted to extract the signal yield. The WH categories use m_{2T} instead of m_{MMC} because the presence of an additional neutrino coming from the W decay breaks an important assumption used by the m_{MMC} algorithm, as previously discussed in Section 4.2.

For the mass-based analysis, the cut on the mass observable is dropped from the SIGNAL selection criteria in all categories to better constrain the background using the sidebands in which the background contribution is dominant. As a consequence, the total number of events selected in the SIGNAL region increases up to a factor of about four due to a general increase of the background fraction from misidentified $\tau_{\text{had-vis}}$.

As shown in Table 4, the mass variables defined here (m_{MMC} and m_{2T}) are not used as inputs for the NN. However, the binning of the distributions of the mass variables follows the same optimization criteria used in the NN-based fit case discussed in the previous section.

7 Systematic uncertainties

Systematic uncertainties affect the yields in the signal and control regions as well as the shape of the fitted distribution. They can be separated into four groups: MC sample statistical uncertainties, experimental

uncertainties, theoretical uncertainties for the backgrounds, and theoretical uncertainties for the signal. The systematic uncertainties related to the estimation of misidentified objects are described in Section 5.

Experimental uncertainties pertain to the trigger as well as final-state objects: reconstruction, identification and isolation efficiency uncertainties for electrons [38], muons [63], $\tau_{\text{had-vis}}$ [64], jets [42, 65–67], b -jets [68, 69] and $E_{\text{T}}^{\text{miss}}$ [70]. The uncertainties associated with the $\tau_{\text{had-vis}}$ identification efficiency are in the range of 2% to 6%, while the eBDT efficiency uncertainty is 1% to 2%. All these uncertainties are parameterised as a function of the $\tau_{\text{had-vis}}$ p_{T} and number of associated tracks or τ -lepton decay mode (eBDT efficiency). For the $\tau_{\text{had-vis}}$ energy scale, the total uncertainty is in the range of 1% to 4%, arising from a combination of measurements: (i) a direct measurement with $Z \rightarrow \tau\tau \rightarrow \mu\tau_{\text{had-vis}} + 3\nu$ events, (ii) measurements of the calorimeter response to single particles, and (iii) comparisons between simulations using different detector geometries or GEANT4 physics lists [20]. This uncertainty is also parameterised as a function of the $\tau_{\text{had-vis}}$ p_{T} and number of associated tracks [64]. The energy scale and resolution uncertainties of final state objects are taken into account as well. Experimental uncertainties affect the shape of the distribution of the final discriminant, the background yields, and the signal cross-section through their effects on the acceptance of and migration between different analysis categories. An additional uncertainty from the measurement of the luminosity [71, 72], amounting to 0.83%, is also included.

The theoretical uncertainties for the diboson, triboson and the top quark background are estimated from simulation. These include the systematic uncertainties due to renormalisation (μ_{r}), factorisation (μ_{f}) and resummation scale (μ_{qsf}), the jet-to-parton matching scheme (CKKW) [73], the choice of α_{s} value, and the PDFs. For the diboson background, the most relevant contributions come from the systematic uncertainties due to renormalisation (μ_{r}) and factorisation (μ_{f}), which affect the shape and the global normalization with a total uncertainty that ranges from 7% to 12% in the ZZ and WZ processes respectively. For the top quark background, uncertainties related to the choice of matrix element and parton shower generators [74, 75], the initial- and final-state radiation model [76], and the PDFs are considered [77]. Their effect on the normalisation and shape of the final discriminant is considered in the statistical analysis.

The Higgs boson production cross-section uncertainties are obtained from Ref. [8]. To account for missing higher orders in QCD, additional uncertainties are estimated by varying μ_{r} , μ_{f} , μ_{qsf} , the choice of α_{s} value, and the choice of matrix element generator or parton shower and hadronisation model. For the matrix element variation, predictions by POWHEG BOX v2 are compared with those by MADGRAPH5_AMC@NLO [78]. The parton shower and hadronisation model variation replaces the nominal PYTHIA 8 simulation with HERWIG 7 [74, 75]. Additional theoretical uncertainties affecting the $t\bar{t}H$ production cross-section are also considered; more details can be found in Ref. [79].

8 Results

The statistical procedure is based on a likelihood function $\mathcal{L}(\mu, \theta)$, constructed as the product of Poisson probability terms over the bins of the input distributions. The parameter of interest, μ , is the signal strength that multiplies the SM Higgs boson production cross-section in association with a vector boson times the branching fraction into $\tau\tau$. It is extracted by maximising the likelihood. An additional statistical procedure is used to estimate two parameters of interest μ_{ZH} and μ_{WH} separately for the ZH and the WH categories, respectively. Systematic uncertainties enter the likelihood as nuisance parameters (NP), θ . Most of the uncertainties discussed in Section 7 are constrained with Gaussian or log-normal probability density functions. The systematic variations that are subject to large statistical fluctuations are smoothed, and systematic uncertainties that have a negligible impact on the final results are pruned away category

by category. Only the SIGNAL regions are considered in the fit. The normalisation of the background contributions from diboson, triboson, top processes and other small backgrounds are taken from the simulation. The probability that the background-only hypothesis is compatible with the observed data is determined using the q_0 test statistic constructed from the profile-likelihood ratio with the asymptotic approximation [80].

8.1 Results of the neural network analysis

For a Higgs boson mass of 125 GeV, when the ZH and WH categories are combined under the constraint that $\mu_{VH}^{\tau\tau} = \mu_{ZH}^{\tau\tau} = \mu_{WH}^{\tau\tau}$, the NN-based fit shows an observed significance of 4.2 standard deviations from the background-only hypothesis, compared with an expectation of 3.6 standard deviations. The fitted value of the signal strength is:

$$\mu_{VH}^{\tau\tau} = 1.28^{+0.39}_{-0.36} = 1.28^{+0.30}_{-0.29} \text{ (stat.) }^{+0.25}_{-0.21} \text{ (syst.)}.$$

Using a predicted cross-section of (6.59 ± 0.03) fb from the Standard Model [8], this corresponds to a measured cross-section of $8.5^{+2.6}_{-2.4}$ fb.

The total statistical uncertainty is defined as the uncertainty in $\mu_{VH}^{\tau\tau}$ when all the NPs are fixed to their best-fit values. The total systematic uncertainty is then defined as the difference in quadrature between the total uncertainty in $\mu_{VH}^{\tau\tau}$ and the total statistical uncertainty. The result obtained is limited by the data sample size, as shown by the breakdown of the statistical and systematic uncertainties.

The relative effects of systematic uncertainties on the measurement of $\mu_{VH}^{\tau\tau}$ are shown in Table 5. The impact of a category of systematic uncertainties is defined as the difference in quadrature between the uncertainty in $\mu_{VH}^{\tau\tau}$ computed when all NPs are fitted and that when the NPs in the category are fixed to their best-fit values. As shown in Table 5, the systematic uncertainties associated to the $\tau_{\text{had-vis}}$ reconstruction (including its identification and calibration) and the systematic uncertainties associated to the background sample size play a dominant role, followed by the modelling of the background from misidentified jets.

Figure 2 shows the post-fit distributions of the NN scores. The background prediction in all post-fit distributions is obtained by setting the nuisance parameters according to their best-fit values.

Figure 3 shows the data, background and signal yields, where final-discriminant bins in all regions are combined into bins of $\log_{10}(S/B)$. Here, S and B are the fitted signal and background yields in each analysis bin. Table 6 shows the good agreement obtained in the resulting yields in the four categories.

A combined fit is also performed with floating signal strengths separately for the WH and ZH production processes. The results of this fit are shown in Figure 4. The probability that the signal strengths measured in the two production processes are compatible is 56%⁶.

⁶ The compatibility between fits differing only in their number of parameters of interest is evaluated in the asymptotic regime, where the difference between their maximum likelihoods follows a χ^2 distribution with a number of degrees of freedom equal to the difference between the numbers of parameters of interest.

Table 5: Summary of the different sources of uncertainty affecting the observed $\mu_{VH}^{\tau\tau}$ and their impact as computed by the NN-based fit described in Section 6.1. Experimental uncertainties for reconstructed objects combine efficiency and energy/momentum scale and resolution uncertainties. ‘Background sample size’ includes the bin-by-bin statistical uncertainties in the simulated backgrounds as well as statistical uncertainties in misidentified jets backgrounds, which are estimated using data.

Source of uncertainty	$\delta\mu/\mu_{VH}^{\tau\tau}$ [%]
Hadronic τ -lepton decay	9
Simulated background sample size	9
Misidentified jets	4
Jet and E_T^{miss}	4
Theoretical uncertainty in signal	4
Theoretical uncertainty in top-quark, VV and VVV processes	4
Electrons and muons	2
Luminosity	1
Flavour tagging	< 1
Total systematic uncertainty	16
Total statistical uncertainty	24
Total	30

Table 6: Post-fit yields from the NN-based fit performed with $\mu_{VH}^{\tau\tau} = \mu_{ZH}^{\tau\tau} = \mu_{WH}^{\tau\tau}$. The symbol “-” is used when no events or $< 10^{-2}$ events are present.

	$ZH(\tau_{\text{had}}\tau_{\text{had}})$	$ZH(\tau_{\text{lep}}\tau_{\text{had}})$	$WH(\tau_{\text{had}}\tau_{\text{had}})$	$WH(\tau_{\text{lep}}\tau_{\text{had}})$
ZH	14 ± 4	10 ± 3	-	-
WH	-	-	31 ± 9	40 ± 12
Misidentified jets	17 ± 2	12 ± 1	160 ± 7	677 ± 31
top-quark	0.35 ± 0.06	2.3 ± 0.4	0.64 ± 0.11	3.2 ± 1.6
VVV	0.09 ± 0.02	0.43 ± 0.07	0.46 ± 0.07	6 ± 1
ZZ	27 ± 3	17 ± 2	-	0.06 ± 0.04
$t\bar{t}H$	0.51 ± 0.07	0.44 ± 0.07	2.49 ± 0.77	3.86 ± 1.19
WZ	-	-	76 ± 10	273 ± 26
Total	59 ± 5	42 ± 4	272 ± 12	1003 ± 28
Data	59	38	262	1020

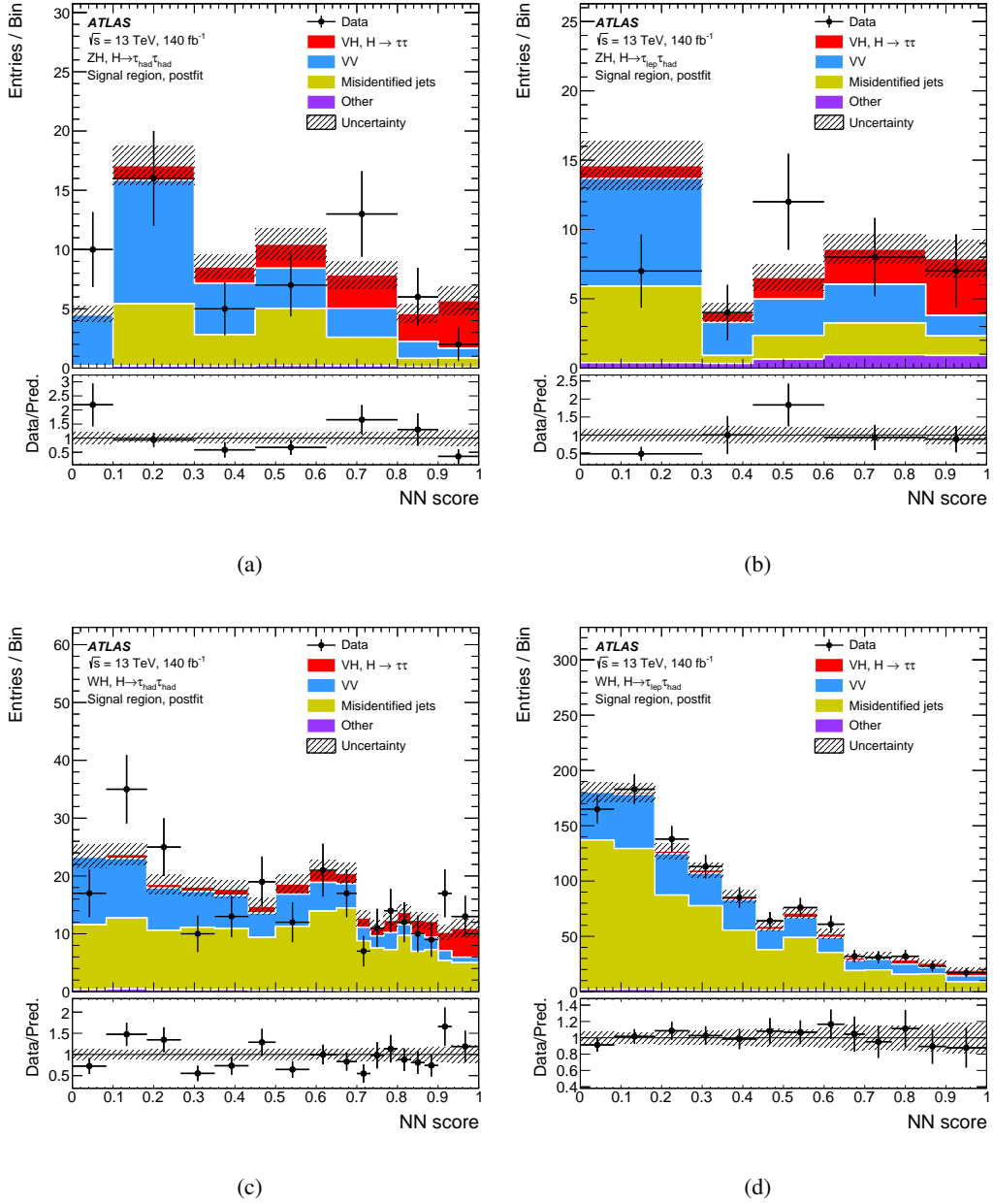


Figure 2: Post-fit distributions for NN-based analysis of the NN-scores in the $ZH(\tau_{\text{had}}\tau_{\text{had}})$ (a), $ZH(\tau_{\text{lep}}\tau_{\text{had}})$ (b), $WH(\tau_{\text{had}}\tau_{\text{had}})$ (c) and $WH(\tau_{\text{lep}}\tau_{\text{had}})$ (d) categories. The hatched band indicates the total post-fit uncertainty of the total predicted yields. The post-fit signal contributions are considered as part of the predictions.

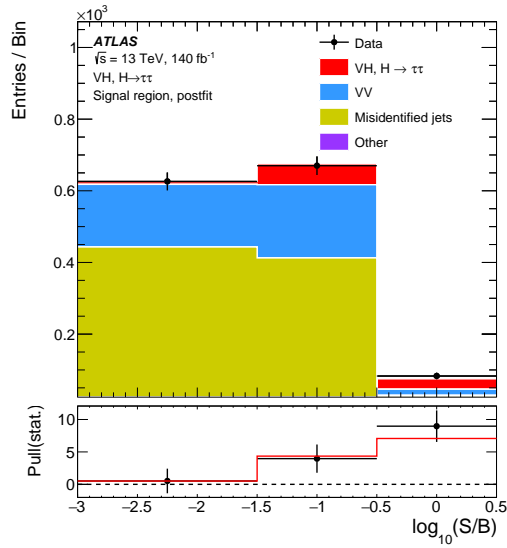


Figure 3: Event yields as a function of $\log_{10}(S/B)$ for data, background and a Higgs boson signal with $m_H = 125$ GeV. Final-discriminant bins in all regions are combined into bins of $\log_{10}(S/B)$, with S being the fitted signal and B the fitted background yields from the NN-based fit. The Higgs boson signal contribution is shown after re-scaling the SM cross-section according to the value of the signal strength extracted from data ($\mu = 1.28$). In the lower panel, the pull of the data relative to the background (the statistical significance of the difference between data and fitted background) is shown with statistical uncertainties only. The solid line shows the expected pull in each bin for the best-fit signal value.

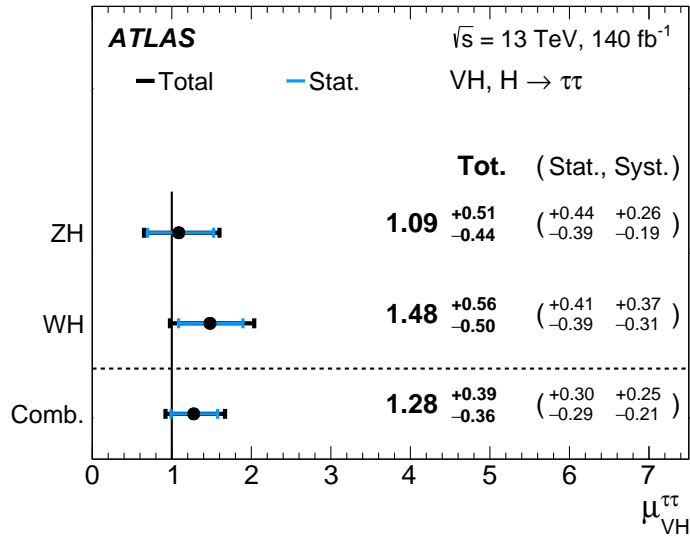


Figure 4: The fitted values of the Higgs boson signal strength $\mu_{VH}^{\tau\tau}$ for $m_H = 125$ GeV for the WH and ZH processes and their combination from the NN-based fit. The individual $\mu_{VH}^{\tau\tau}$ values for the $(W/Z)H$ processes are obtained from a simultaneous fit with the signal strength for each of the WH and ZH processes floating independently. The probability of compatibility of the individual signal strengths is 56%.

8.2 Results of the mass-based analysis

For all channels combined, the fitted value of the signal strength is:

$$\mu_{VH}^{\tau\tau} = 1.40^{+0.49}_{-0.45} = 1.40^{+0.36}_{-0.35} \text{ (stat.) }^{+0.33}_{-0.28} \text{ (syst.)}$$

in good agreement with the result of the NN-based analysis discussed in the previous section. The observed excess in the mass analysis has a significance of 3.5 standard deviations, compared to an expectation of 2.6 standard deviations. The relative effects of systematic uncertainties on the measurement of $\mu_{VH}^{\tau\tau}$ in this case are quite similar to the results discussed in Section 8.1.

Figure 5 shows the post-fit distributions of the observables used in the mass-based analysis: m_{MMC} for the ZH categories and m_{2T} for the WH ones. The background prediction in all post-fit distributions is obtained by setting the nuisance parameters according to the results of the combined ZH and WH fit.

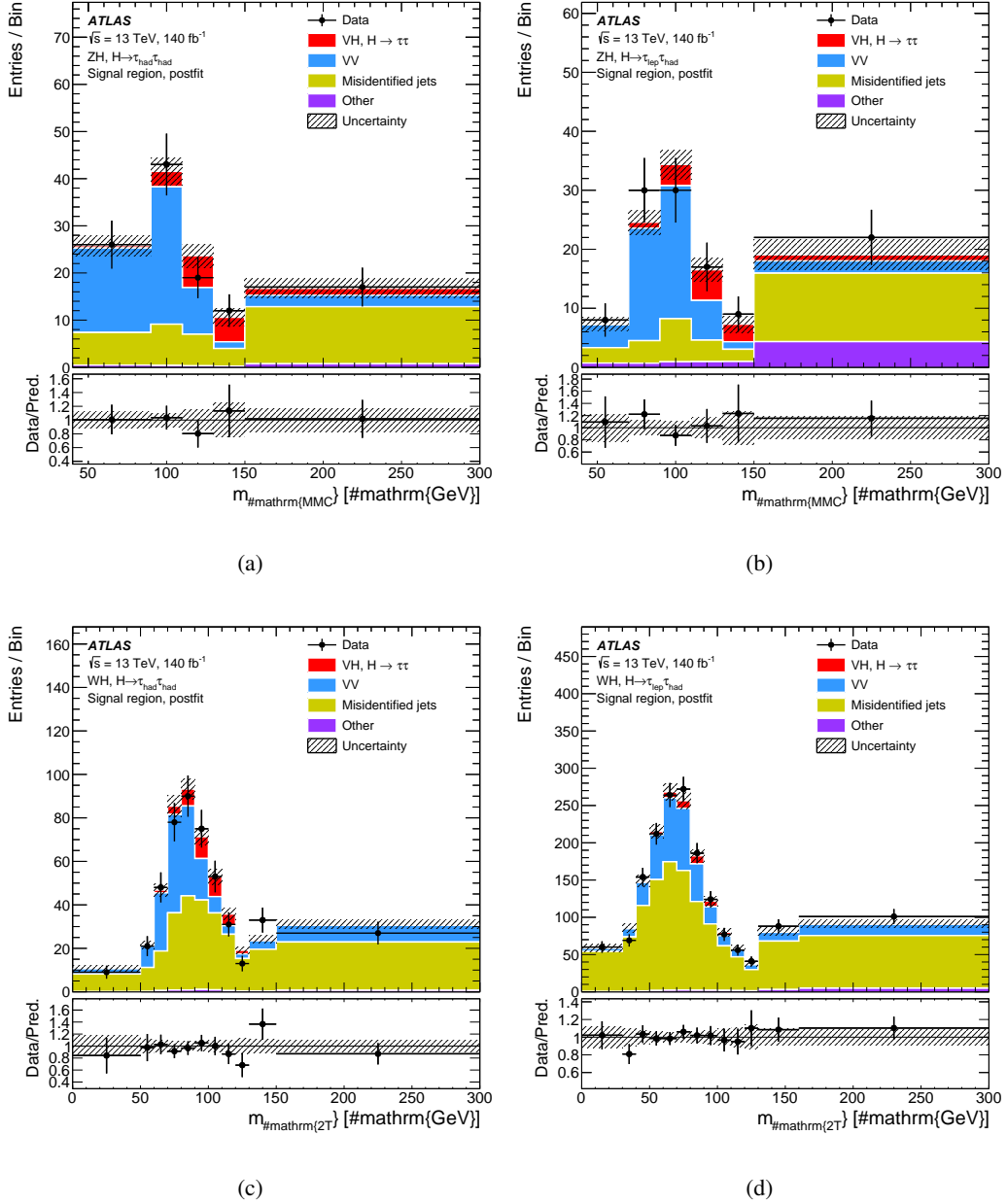


Figure 5: Post-fit distributions for mass-based analysis for m_{MMC} in the (a) $ZH(\tau_{\text{had}}\tau_{\text{had}})$, (b) $ZH(\tau_{\text{lep}}\tau_{\text{had}})$, and for m_{2T} in the (c) $WH(\tau_{\text{had}}\tau_{\text{had}})$ and (d) $WH(\tau_{\text{lep}}\tau_{\text{had}})$ categories. The hatched band indicates the total post-fit uncertainty of the total predicted yields. The post-fit signal contributions are considered as part of the predictions.

9 Conclusion

A search for the Standard Model Higgs boson decaying into a $\tau\tau$ pair and produced in association with a leptonically-decaying W or Z boson is presented, using data collected by the ATLAS experiment in proton–proton collisions from Run 2 of the LHC. The data correspond to an integrated luminosity of 140 fb^{-1} collected at a centre-of-mass energy of $\sqrt{s} = 13 \text{ TeV}$.

In addition to the approximately seven times larger dataset, the main sources of improvement with respect to the Run 1 result are the more sophisticated analysis methodologies. These include the introduction of a neural network discriminator for rejecting the diboson background and better $\tau_{\text{had-vis}}$ identification algorithms.

An excess over the expected background is observed with a significance of 4.2 standard deviations compared with an expectation of 3.6. The measured signal strength relative to the SM prediction for $m_H = 125$ GeV is found to be $\mu_{\text{VH}} = 1.28^{+0.30}_{-0.29}$ (stat.) $^{+0.25}_{-0.21}$ (syst.). This measurement provides evidence for the associated production of the Higgs boson and a leptonically-decaying vector boson in events where the Higgs boson decays into a pair of τ -leptons.

Acknowledgements

We thank CERN for the very successful operation of the LHC, as well as the support staff from our institutions without whom ATLAS could not be operated efficiently.

We acknowledge the support of ANPCyT, Argentina; YerPhI, Armenia; ARC, Australia; BMWFW and FWF, Austria; ANAS, Azerbaijan; CNPq and FAPESP, Brazil; NSERC, NRC and CFI, Canada; CERN; ANID, Chile; CAS, MOST and NSFC, China; Minciencias, Colombia; MEYS CR, Czech Republic; DNRF and DNSRC, Denmark; IN2P3-CNRS and CEA-DRF/IRFU, France; SRNSFG, Georgia; BMBF, HGF and MPG, Germany; GSRI, Greece; RGC and Hong Kong SAR, China; ISF and Benozziyo Center, Israel; INFN, Italy; MEXT and JSPS, Japan; CNRST, Morocco; NWO, Netherlands; RCN, Norway; MEiN, Poland; FCT, Portugal; MNE/IFA, Romania; MESTD, Serbia; MSSR, Slovakia; ARRS and MIZŠ, Slovenia; DSI/NRF, South Africa; MICINN, Spain; SRC and Wallenberg Foundation, Sweden; SERI, SNSF and Cantons of Bern and Geneva, Switzerland; MOST, Taiwan; TENMAK, Türkiye; STFC, United Kingdom; DOE and NSF, United States of America. In addition, individual groups and members have received support from BCKDF, CANARIE, Compute Canada and CRC, Canada; PRIMUS 21/SCI/017 and UNCE SCI/013, Czech Republic; COST, ERC, ERDF, Horizon 2020, ICSC-NextGenerationEU and Marie Skłodowska-Curie Actions, European Union; Investissements d’Avenir Labex, Investissements d’Avenir IDEX and ANR, France; DFG and AvH Foundation, Germany; Herakleitos, Thales and Aristeia programmes co-financed by EU-ESF and the Greek NSRF, Greece; BSF-NSF and MINERVA, Israel; Norwegian Financial Mechanism 2014-2021, Norway; NCN and NAWA, Poland; La Caixa Banking Foundation, CERCA Programme Generalitat de Catalunya and PROMETEO and GenT Programmes Generalitat Valenciana, Spain; Göran Gustafssons Stiftelse, Sweden; The Royal Society and Leverhulme Trust, United Kingdom.

The crucial computing support from all WLCG partners is acknowledged gratefully, in particular from CERN, the ATLAS Tier-1 facilities at TRIUMF (Canada), NDGF (Denmark, Norway, Sweden), CC-IN2P3 (France), KIT/GridKA (Germany), INFN-CNAF (Italy), NL-T1 (Netherlands), PIC (Spain), ASGC (Taiwan), RAL (UK) and BNL (USA), the Tier-2 facilities worldwide and large non-WLCG resource providers. Major contributors of computing resources are listed in Ref. [81].

References

- [1] ATLAS Collaboration, *Measurement of the production cross section for a Higgs boson in association with a vector boson in the $H \rightarrow WW^* \rightarrow \ell\nu\ell\nu$ channel in pp collisions at $\sqrt{s} = 13$ TeV with the ATLAS detector*, *Phys. Lett. B* **798** (2019) 134949, arXiv: [1903.10052 \[hep-ex\]](#).
- [2] ATLAS Collaboration, *Observation of $H \rightarrow b\bar{b}$ decays and VH production with the ATLAS detector*, *Phys. Lett. B* **786** (2018) 59, arXiv: [1808.08238 \[hep-ex\]](#).
- [3] CMS Collaboration, *Observation of Higgs Boson Decay to Bottom Quarks*, *Phys. Rev. Lett.* **121** (2018) 121801, arXiv: [1808.08242 \[hep-ex\]](#).
- [4] ATLAS Collaboration, *Cross-section measurements of the Higgs boson decaying into a pair of τ -leptons in proton–proton collisions at $\sqrt{s} = 13$ TeV with the ATLAS detector*, *Phys. Rev. D* **99** (2019) 072001, arXiv: [1811.08856 \[hep-ex\]](#).
- [5] CMS Collaboration, *Observation of the Higgs boson decay to a pair of τ leptons with the CMS detector*, *Phys. Lett. B* **779** (2018) 283, arXiv: [1708.00373 \[hep-ex\]](#).
- [6] CMS Collaboration, *Measurements of Higgs boson production in the decay channel with a pair of τ leptons in proton–proton collisions at $\sqrt{s} = 13$ TeV*, (2023), arXiv: [2204.12957 \[hep-ex\]](#).
- [7] ATLAS Collaboration, *Search for the standard model Higgs boson produced in association with a vector boson and decaying into a tau pair in pp collisions at $\sqrt{s} = 8$ TeV with the ATLAS detector*, *Phys. Rev. D* **93** (2016) 092005, arXiv: [1511.08352 \[hep-ex\]](#).
- [8] D. de Florian et al., *Handbook of LHC Higgs Cross Sections: 4. Deciphering the Nature of the Higgs Sector*, (2017), arXiv: [1610.07922 \[hep-ph\]](#).
- [9] ATLAS Collaboration, *The ATLAS Experiment at the CERN Large Hadron Collider*, *JINST* **3** (2008) S08003.
- [10] ATLAS Collaboration, *ATLAS Insertable B-Layer: Technical Design Report*, ATLAS-TDR-19; CERN-LHCC-2010-013, 2010, URL: <https://cds.cern.ch/record/1291633>, Addendum: ATLAS-TDR-19-ADD-1; CERN-LHCC-2012-009, 2012, URL: <https://cds.cern.ch/record/1451888>.
- [11] B. Abbott et al., *Production and integration of the ATLAS Insertable B-Layer*, *JINST* **13** (2018) T05008, arXiv: [1803.00844 \[physics.ins-det\]](#).
- [12] ATLAS Collaboration, *Performance of the ATLAS trigger system in 2015*, *Eur. Phys. J. C* **77** (2017) 317, arXiv: [1611.09661 \[hep-ex\]](#).
- [13] ATLAS Collaboration, *The ATLAS Collaboration Software and Firmware*, ATL-SOFT-PUB-2021-001, 2021, URL: <https://cds.cern.ch/record/2767187>.
- [14] ATLAS Collaboration, *ATLAS data quality operations and performance for 2015–2018 data-taking*, *JINST* **15** (2020) P04003, arXiv: [1911.04632 \[physics.ins-det\]](#).
- [15] ATLAS Collaboration, *Performance of electron and photon triggers in ATLAS during LHC Run 2*, *Eur. Phys. J. C* **80** (2020) 47, arXiv: [1909.00761 \[hep-ex\]](#).
- [16] ATLAS Collaboration, *Performance of the ATLAS muon triggers in Run 2*, *JINST* **15** (2020) P09015, arXiv: [2004.13447 \[physics.ins-det\]](#).

- [17] ATLAS Collaboration, *The ATLAS Inner Detector Trigger performance in pp collisions at 13 TeV during LHC Run 2*, *Eur. Phys. J. C* **82** (2022) 206, arXiv: [2107.02485 \[hep-ex\]](#).
- [18] ATLAS Collaboration, *Performance of the ATLAS Level-1 topological trigger in Run 2*, *Eur. Phys. J. C* **82** (2022) 7, arXiv: [2105.01416 \[hep-ex\]](#).
- [19] ATLAS Collaboration, *The ATLAS Simulation Infrastructure*, *Eur. Phys. J. C* **70** (2010) 823, arXiv: [1005.4568 \[physics.ins-det\]](#).
- [20] S. Agostinelli et al., *GEANT4 – a simulation toolkit*, *Nucl. Instrum. Meth. A* **506** (2003) 250.
- [21] S. Frixione, G. Ridolfi and P. Nason, *A positive-weight next-to-leading-order Monte Carlo for heavy flavour hadroproduction*, *JHEP* **09** (2007) 126, arXiv: [0707.3088 \[hep-ph\]](#).
- [22] P. Nason, *A new method for combining NLO QCD with shower Monte Carlo algorithms*, *JHEP* **11** (2004) 040, arXiv: [hep-ph/0409146](#).
- [23] S. Frixione, P. Nason and C. Oleari, *Matching NLO QCD computations with parton shower simulations: the POWHEG method*, *JHEP* **11** (2007) 070, arXiv: [0709.2092 \[hep-ph\]](#).
- [24] S. Alioli, P. Nason, C. Oleari and E. Re, *A general framework for implementing NLO calculations in shower Monte Carlo programs: the POWHEG BOX*, *JHEP* **06** (2010) 043, arXiv: [1002.2581 \[hep-ph\]](#).
- [25] H. B. Hartanto, B. Jäger, L. Reina and D. Wackerroth, *Higgs boson production in association with top quarks in the POWHEG BOX*, *Phys. Rev. D* **91** (2015) 094003, arXiv: [1501.04498 \[hep-ph\]](#).
- [26] M. L. Ciccolini, S. Dittmaier and M. Krämer, *Electroweak radiative corrections to associated WH and ZH production at hadron colliders*, *Phys. Rev. D* **68** (2003) 073003, arXiv: [hep-ph/0306234 \[hep-ph\]](#).
- [27] O. Brein, A. Djouadi and R. Harlander, *NNLO QCD corrections to the Higgs-strahlung processes at hadron colliders*, *Phys. Lett. B* **579** (2004) 149, arXiv: [hep-ph/0307206](#).
- [28] O. Brein, R. V. Harlander, M. Wiesemann and T. Zirke, *Top-quark mediated effects in hadronic Higgs-Strahlung*, *Eur. Phys. J. C* **72** (2012) 1868, arXiv: [1111.0761 \[hep-ph\]](#).
- [29] A. Denner, S. Dittmaier, S. Kallweit and A. Mück, *HAWK 2.0: A Monte Carlo program for Higgs production in vector-boson fusion and Higgs strahlung at hadron colliders*, *Comput. Phys. Commun.* **195** (2015) 161, arXiv: [1412.5390 \[hep-ph\]](#).
- [30] O. Brein, R. V. Harlander and T. J. E. Zirke, *vh@nnlo – Higgs Strahlung at hadron colliders*, *Comput. Phys. Commun.* **184** (2013) 998, arXiv: [1210.5347 \[hep-ph\]](#).
- [31] T. Sjöstrand et al., *An introduction to PYTHIA 8.2*, *Comput. Phys. Commun.* **191** (2015) 159, arXiv: [1410.3012 \[hep-ph\]](#).
- [32] E. Bothmann et al., *Event generation with Sherpa 2.2*, *SciPost Phys.* **7** (2019) 034, arXiv: [1905.09127 \[hep-ph\]](#).
- [33] D. J. Lange, *The EvtGen particle decay simulation package*, *Nucl. Instrum. Meth. A* **462** (2001) 152.

- [34] T. Sjöstrand, S. Mrenna and P. Skands, *A Brief Introduction to PYTHIA 8.1*, *Comput. Phys. Commun.* **178** (2008) 852, arXiv: [0710.3820 \[hep-ph\]](#).
- [35] ATLAS Collaboration, *The Pythia 8 A3 tune description of ATLAS minimum bias and inelastic measurements incorporating the Donnachie–Landshoff diffractive model*, ATL-PHYS-PUB-2016-017, 2016, URL: <https://cds.cern.ch/record/2206965>.
- [36] NNPDF Collaboration, *Parton distributions with LHC data*, *Nucl. Phys. B* **867** (2013) 244, arXiv: [1207.1303 \[hep-ph\]](#).
- [37] J. Butterworth et al., *PDF4LHC recommendations for LHC Run II*, *J. Phys. G* **43** (2016) 023001, arXiv: [1510.03865 \[hep-ph\]](#).
- [38] ATLAS Collaboration, *Electron and photon efficiencies in LHC Run 2 with the ATLAS experiment*, (2023), arXiv: [2308.13362 \[hep-ex\]](#).
- [39] ATLAS Collaboration, *Muon reconstruction and identification efficiency in ATLAS using the full Run 2 pp collision data set at $\sqrt{s} = 13$ TeV*, *Eur. Phys. J. C* **81** (2021) 578, arXiv: [2012.00578 \[hep-ex\]](#).
- [40] M. Cacciari, G. P. Salam and G. Soyez, *The anti- k_t jet clustering algorithm*, *JHEP* **04** (2008) 063, arXiv: [0802.1189 \[hep-ph\]](#).
- [41] M. Cacciari, G. P. Salam and G. Soyez, *FastJet user manual*, *Eur. Phys. J. C* **72** (2012) 1896, arXiv: [1111.6097 \[hep-ph\]](#).
- [42] ATLAS Collaboration, *Jet energy scale and resolution measured in proton–proton collisions at $\sqrt{s} = 13$ TeV with the ATLAS detector*, *Eur. Phys. J. C* **81** (2021) 689, arXiv: [2007.02645 \[hep-ex\]](#).
- [43] ATLAS Collaboration, *Performance of pile-up mitigation techniques for jets in pp collisions at $\sqrt{s} = 8$ TeV using the ATLAS detector*, *Eur. Phys. J. C* **76** (2016) 581, arXiv: [1510.03823 \[hep-ex\]](#).
- [44] ATLAS Collaboration, *Calibration of the ATLAS b-tagging algorithm in $t\bar{t}$ semileptonic events*, ATL-CONF-2018-045, 2018, URL: <https://cds.cern.ch/record/2638455>.
- [45] ATLAS Collaboration, *ATLAS b-jet identification performance and efficiency measurement with $t\bar{t}$ events in pp collisions at $\sqrt{s} = 13$ TeV*, *Eur. Phys. J. C* **79** (2019) 970, arXiv: [1907.05120 \[hep-ex\]](#).
- [46] ATLAS Collaboration, *Optimisation and performance studies of the ATLAS b-tagging algorithms for the 2017-18 LHC run*, ATL-PHYS-PUB-2017-013, 2017, URL: <https://cds.cern.ch/record/2273281>.
- [47] ATLAS Collaboration, *ATLAS flavour-tagging algorithms for the LHC Run 2 pp collision dataset*, *Eur. Phys. J. C* **83** (2023) 681, arXiv: [2211.16345 \[physics.data-an\]](#).
- [48] ATLAS Collaboration, *Reconstruction, Energy Calibration, and Identification of Hadronically Decaying Tau Leptons in the ATLAS Experiment for Run-2 of the LHC*, ATL-PHYS-PUB-2015-045, 2015, URL: <https://cds.cern.ch/record/2064383>.
- [49] ATLAS Collaboration, *Identification of hadronic tau lepton decays using neural networks in the ATLAS experiment*, ATL-PHYS-PUB-2019-033, 2019, URL: <https://cds.cern.ch/record/2688062>.

- [50] ATLAS Collaboration, *Reconstruction, Identification, and Calibration of hadronically decaying tau leptons with the ATLAS detector for the LHC Run 3 and reprocessed Run 2 data*, ATL-PHYS-PUB-2022-044, 2022, URL: <https://cds.cern.ch/record/2827111>.
- [51] ATLAS Collaboration, *Measurements of Higgs boson production cross-sections in the $H \rightarrow \tau^+\tau^-$ decay channel in pp collisions at $\sqrt{s} = 13$ TeV with the ATLAS detector*, *JHEP* **08** (2022) 175, arXiv: [2201.08269](https://arxiv.org/abs/2201.08269) [[hep-ex](#)].
- [52] ATLAS Collaboration, *E_T^{miss} performance in the ATLAS detector using 2015–2016 LHC pp collisions*, ATLAS-CONF-2018-023, 2018, URL: <https://cds.cern.ch/record/2625233>.
- [53] A. Elagin, P. Murat, A. Pranko and A. Safonov, *A new mass reconstruction technique for resonances decaying to $\tau\tau$* , *Nucl. Instrum. Meth. A* **654** (2011) 481, arXiv: [1012.4686](https://arxiv.org/abs/1012.4686) [[hep-ex](#)].
- [54] A. J. Barr et al., *Guide to transverse projections and mass-constraining variables*, *Phys. Rev. D* **84** (2011), arXiv: [1105.2977](https://arxiv.org/abs/1105.2977) [[hep-ex](#)].
- [55] ATLAS Collaboration, *Measurement of $W^\pm Z$ production cross sections and gauge boson polarisation in pp collisions at $\sqrt{s} = 13$ TeV with the ATLAS detector*, *Eur. Phys. J. C* **79** (2019) 535, arXiv: [1902.05759](https://arxiv.org/abs/1902.05759) [[hep-ex](#)].
- [56] ATLAS Collaboration, *$ZZ \rightarrow \ell^+\ell^-\ell'^+\ell'^-$ cross-section measurements and search for anomalous triple gauge couplings in 13 TeV pp collisions with the ATLAS detector*, *Phys. Rev. D* **97** (2018) 032005, arXiv: [1709.07703](https://arxiv.org/abs/1709.07703) [[hep-ex](#)].
- [57] ATLAS Collaboration, *Evidence for the Higgs-boson Yukawa coupling to tau leptons with the ATLAS detector*, *JHEP* **04** (2015) 117, arXiv: [1501.04943](https://arxiv.org/abs/1501.04943) [[hep-ex](#)].
- [58] ATLAS Collaboration, *Measurements of Higgs boson production and couplings in the four-lepton channel in pp collisions at center-of-mass energies of 7 and 8 TeV with the ATLAS detector*, *Phys. Rev. D* **91** (2015) 012006, arXiv: [1408.5191](https://arxiv.org/abs/1408.5191) [[hep-ex](#)].
- [59] R. K. Ellis, I. Hinchliffe, M. Soldate and J. J. van der Bij, *Higgs decay to $\tau^+\tau^-$ A possible signature of intermediate mass Higgs bosons at high energy hadron colliders*, *Nucl. Phys. B* **297** (1988) 221.
- [60] F. Chollet et al., *Keras*, 2015, URL: <https://github.com/fchollet/keras>.
- [61] Martín Abadi et al., *TensorFlow: A system for large-scale machine learning*, 12th USENIX Symposium on Operating Systems Design and Implementation (OSDI'16) (2016) 265.
- [62] A. F. Agarap, *Deep learning using rectified linear units (relu)*, (2018), arXiv: [1605.08695](https://arxiv.org/abs/1605.08695) [[hep-ex](#)].
- [63] ATLAS Collaboration, *Muon reconstruction performance of the ATLAS detector in proton–proton collision data at $\sqrt{s} = 13$ TeV*, *Eur. Phys. J. C* **76** (2016) 292, arXiv: [1603.05598](https://arxiv.org/abs/1603.05598) [[hep-ex](#)].
- [64] ATLAS Collaboration, *Measurement of the tau lepton reconstruction and identification performance in the ATLAS experiment using pp collisions at $\sqrt{s} = 13$ TeV*, ATLAS-CONF-2017-029, 2017, URL: <https://cds.cern.ch/record/2261772>.
- [65] ATLAS Collaboration, *Jet energy scale measurements and their systematic uncertainties in proton–proton collisions at $\sqrt{s} = 13$ TeV with the ATLAS detector*, *Phys. Rev. D* **96** (2017) 072002, arXiv: [1703.09665](https://arxiv.org/abs/1703.09665) [[hep-ex](#)].

- [66] ATLAS Collaboration, *Tagging and suppression of pileup jets with the ATLAS detector*, ATLAS-CONF-2014-018, 2014, URL: <https://cds.cern.ch/record/1700870>.
- [67] ATLAS Collaboration, *Identification and rejection of pile-up jets at high pseudorapidity with the ATLAS detector*, *Eur. Phys. J. C* **77** (2017) 580, arXiv: [1705.02211](https://arxiv.org/abs/1705.02211) [hep-ex], Erratum: *Eur. Phys. J. C* **77** (2017) 712.
- [68] ATLAS Collaboration, *Measurements of b -jet tagging efficiency with the ATLAS detector using $t\bar{t}$ events at $\sqrt{s} = 13$ TeV*, *JHEP* **08** (2018) 089, arXiv: [1805.01845](https://arxiv.org/abs/1805.01845) [hep-ex].
- [69] ATLAS Collaboration, *Calibration of the light-flavour jet mistagging efficiency of the b -tagging algorithms with Z +jets events using 139 fb^{-1} of ATLAS proton–proton collision data at $\sqrt{s} = 13$ TeV*, *Eur. Phys. J. C* **83** (2023) 728, arXiv: [2301.06319](https://arxiv.org/abs/2301.06319) [hep-ex].
- [70] ATLAS Collaboration, *Performance of missing transverse momentum reconstruction with the ATLAS detector using proton–proton collisions at $\sqrt{s} = 13$ TeV*, *Eur. Phys. J. C* **78** (2018) 903, arXiv: [1802.08168](https://arxiv.org/abs/1802.08168) [hep-ex].
- [71] ATLAS Collaboration, *Luminosity determination in pp collisions at $\sqrt{s} = 13$ TeV using the ATLAS detector at the LHC*, *Eur. Phys. J. C* **10** (2023) 982, arXiv: [2212.09379](https://arxiv.org/abs/2212.09379) [hep-ex].
- [72] G. Avoni et al., *The new LUCID-2 detector for luminosity measurement and monitoring in ATLAS*, *JINST* **13** (2018) P07017.
- [73] L. Lönnblad and S. Prestel, *Matching tree-level matrix elements with interleaved showers*, *JHEP* **03** (2012) 019, arXiv: [1109.4829](https://arxiv.org/abs/1109.4829) [hep-ph].
- [74] M. Bähr et al., *Herwig++ physics and manual*, *Eur. Phys. J. C* **58** (2008) 639, arXiv: [0803.0883](https://arxiv.org/abs/0803.0883) [hep-ph].
- [75] J. Bellm et al., *Herwig 7.0/Herwig++ 3.0 release note*, *Eur. Phys. J. C* **76** (2016) 196, arXiv: [1512.01178](https://arxiv.org/abs/1512.01178) [hep-ph].
- [76] ATLAS Collaboration, *Studies on top-quark Monte Carlo modelling with Sherpa and MG5_aMC@NLO*, ATLAS-CONF-2017-007, 2017, URL: <https://cds.cern.ch/record/2261938>.
- [77] L. A. Harland-Lang, A. D. Martin, P. Motylinski and R. S. Thorne, *Parton distributions in the LHC era: MMHT 2014 PDFs*, *Eur. Phys. J. C* **75** (2015) 204, arXiv: [1412.3989](https://arxiv.org/abs/1412.3989) [hep-ph].
- [78] J. Alwall et al., *The automated computation of tree-level and next-to-leading order differential cross sections, and their matching to parton shower simulations*, *JHEP* **07** (2014) 079, arXiv: [1405.0301](https://arxiv.org/abs/1405.0301) [hep-ph].
- [79] ATLAS Collaboration, *Measurements of Higgs boson production cross-sections in the $H \rightarrow \tau^+\tau^-$ decay channel in pp collisions at $\sqrt{s} = 13$ TeV with the ATLAS detector*, *JHEP* **08** (2022) 175, arXiv: [2201.08269](https://arxiv.org/abs/2201.08269) [hep-ex].
- [80] G. Cowan, K. Cranmer, E. Gross and O. Vitells, *Asymptotic formulae for likelihood-based tests of new physics*, *Eur. Phys. J. C* **71** (2011) 1554, arXiv: [1007.1727](https://arxiv.org/abs/1007.1727) [physics.data-an], Erratum: *Eur. Phys. J. C* **73** (2013) 2501.

The ATLAS Collaboration

G. Aad ¹⁰³, E. Aakvaag ¹⁶, B. Abbott ¹²¹, K. Abeling ⁵⁵, N.J. Abicht ⁴⁹, S.H. Abidi ²⁹,
A. Aboulhorma ^{35e}, H. Abramowicz ¹⁵², H. Abreu ¹⁵¹, Y. Abulaiti ¹¹⁸, B.S. Acharya ^{69a,69b,m},
C. Adam Bourdarios ⁴, L. Adamczyk ^{86a}, S.V. Addepalli ²⁶, M.J. Addison ¹⁰², J. Adelman ¹¹⁶,
A. Adiguzel ^{21c}, T. Adye ¹³⁵, A.A. Affolder ¹³⁷, Y. Afik ³⁹, M.N. Agaras ¹³, J. Agarwala ^{73a,73b},
A. Aggarwal ¹⁰¹, C. Agheorghiesei ^{27c}, A. Ahmad ³⁶, F. Ahmadov ^{38,z}, W.S. Ahmed ¹⁰⁵,
S. Ahuja ⁹⁶, X. Ai ^{62e}, G. Aielli ^{76a,76b}, A. Aikot ¹⁶⁴, M. Ait Tamlhat ^{35e}, B. Aitbenchikh ^{35a},
I. Aizenberg ¹⁷⁰, M. Akbiyik ¹⁰¹, T.P.A. Åkesson ⁹⁹, A.V. Akimov ³⁷, D. Akiyama ¹⁶⁹,
N.N. Akolkar ²⁴, S. Aktas ^{21a}, K. Al Houry ⁴¹, G.L. Alberghi ^{23b}, J. Albert ¹⁶⁶,
P. Albicocco ⁵³, G.L. Albouy ⁶⁰, S. Alderweireldt ⁵², Z.L. Alegria ¹²², M. Aleksa ³⁶,
I.N. Aleksandrov ³⁸, C. Alexa ^{27b}, T. Alexopoulos ¹⁰, F. Alfonsi ^{23b}, M. Algren ⁵⁶,
M. Alhroob ¹⁴², B. Ali ¹³³, H.M.J. Ali ⁹², S. Ali ¹⁴⁹, S.W. Alibocus ⁹³, M. Aliev ^{33c},
G. Alimonti ^{71a}, W. Alkakh ⁵⁵, C. Allaire ⁶⁶, B.M.M. Allbrooke ¹⁴⁷, J.F. Allen ⁵²,
C.A. Allendes Flores ^{138f}, P.P. Allport ²⁰, A. Aloisio ^{72a,72b}, F. Alonso ⁹¹, C. Alpigiani ¹³⁹,
M. Alvarez Estevez ¹⁰⁰, A. Alvarez Fernandez ¹⁰¹, M. Alves Cardoso ⁵⁶, M.G. Alviggi ^{72a,72b},
M. Aly ¹⁰², Y. Amaral Coutinho ^{83b}, A. Ambler ¹⁰⁵, C. Amelung ³⁶, M. Amerl ¹⁰²,
C.G. Ames ¹¹⁰, D. Amidei ¹⁰⁷, K.J. Amirie ¹⁵⁶, S.P. Amor Dos Santos ^{131a}, K.R. Amos ¹⁶⁴,
V. Ananiev ¹²⁶, C. Anastopoulos ¹⁴⁰, T. Andeen ¹¹, J.K. Anders ³⁶, S.Y. Andrean ^{47a,47b},
A. Andreazza ^{71a,71b}, S. Angelidakis ⁹, A. Angerami ^{41,ab}, A.V. Anisenkov ³⁷, A. Annovi ^{74a},
C. Antel ⁵⁶, M.T. Anthony ¹⁴⁰, E. Antipov ¹⁴⁶, M. Antonelli ⁵³, F. Anulli ^{75a}, M. Aoki ⁸⁴,
T. Aoki ¹⁵⁴, J.A. Aparisi Pozo ¹⁶⁴, M.A. Aparo ¹⁴⁷, L. Aperio Bella ⁴⁸, C. Appelt ¹⁸,
A. Apyan ²⁶, S.J. Arbiol Val ⁸⁷, C. Arcangeletti ⁵³, A.T.H. Arce ⁵¹, E. Arena ⁹³, J-F. Arguin ¹⁰⁹,
S. Argyropoulos ⁵⁴, J.-H. Arling ⁴⁸, O. Arnaez ⁴, H. Arnold ¹¹⁵, G. Artoni ^{75a,75b}, H. Asada ¹¹²,
K. Asai ¹¹⁹, S. Asai ¹⁵⁴, N.A. Asbah ³⁶, K. Assamagan ²⁹, R. Astalos ^{28a}, S. Atashi ¹⁶⁰,
R.J. Atkin ^{33a}, M. Atkinson ¹⁶³, H. Atmani ^{35f}, P.A. Atmasiddha ¹²⁹, K. Augsten ¹³³,
S. Auricchio ^{72a,72b}, A.D. Auriol ²⁰, V.A. Austrup ¹⁰², G. Avolio ³⁶, K. Axiotis ⁵⁶,
G. Azuelos ^{109,af}, D. Babal ^{28b}, H. Bachacou ¹³⁶, K. Bachas ^{153,q}, A. Bachiu ³⁴,
F. Backman ^{47a,47b}, A. Badea ³⁹, T.M. Baer ¹⁰⁷, P. Bagnaia ^{75a,75b}, M. Bahmani ¹⁸,
D. Bahner ⁵⁴, K. Bai ¹²⁴, A.J. Bailey ¹⁶⁴, J.T. Baines ¹³⁵, L. Baines ⁹⁵, O.K. Baker ¹⁷³,
E. Bakos ¹⁵, D. Bakshi Gupta ⁸, V. Balakrishnan ¹²¹, R. Balasubramanian ¹¹⁵, E.M. Baldin ³⁷,
P. Balek ^{86a}, E. Ballabene ^{23b,23a}, F. Balli ¹³⁶, L.M. Baltes ^{63a}, W.K. Balunas ³², J. Balz ¹⁰¹,
E. Banas ⁸⁷, M. Bandieramonte ¹³⁰, A. Bandyopadhyay ²⁴, S. Bansal ²⁴, L. Barak ¹⁵²,
M. Barakat ⁴⁸, E.L. Barberio ¹⁰⁶, D. Barberis ^{57b,57a}, M. Barbero ¹⁰³, M.Z. Barel ¹¹⁵,
K.N. Barends ^{33a}, T. Barillari ¹¹¹, M-S. Barisits ³⁶, T. Barklow ¹⁴⁴, P. Baron ¹²³,
D.A. Baron Moreno ¹⁰², A. Baroncelli ^{62a}, G. Barone ²⁹, A.J. Barr ¹²⁷, J.D. Barr ⁹⁷,
F. Barreiro ¹⁰⁰, J. Barreiro Guimarães da Costa ^{14a}, U. Barron ¹⁵², M.G. Barros Teixeira ^{131a},
S. Barsov ³⁷, F. Bartels ^{63a}, R. Bartoldus ¹⁴⁴, A.E. Barton ⁹², P. Bartos ^{28a}, A. Basan ¹⁰¹,
M. Baselga ⁴⁹, A. Bassalat ^{66,b}, M.J. Basso ^{157a}, C.R. Basson ¹⁰², R.L. Bates ⁵⁹, S. Batlamous ^{35e},
B. Batool ¹⁴², M. Battaglia ¹³⁷, D. Battulga ¹⁸, M. Bause ^{75a,75b}, M. Bauer ³⁶, P. Bauer ²⁴,
L.T. Bazzano Hurrell ³⁰, J.B. Beacham ⁵¹, T. Beau ¹²⁸, J.Y. Beaucamp ⁹¹, P.H. Beauchemin ¹⁵⁹,
P. Bechtle ²⁴, H.P. Beck ^{19,p}, K. Becker ¹⁶⁸, A.J. Beddall ⁸², V.A. Bednyakov ³⁸, C.P. Bee ¹⁴⁶,
L.J. Beemster ¹⁵, T.A. Beermann ³⁶, M. Begalli ^{83d}, M. Biegel ²⁹, A. Behera ¹⁴⁶, J.K. Behr ⁴⁸,

J.F. Beirer ³⁶, F. Beisiegel ²⁴, M. Belfkir ^{117b}, G. Bella ¹⁵², L. Bellagamba ^{23b}, A. Bellerive ³⁴,
 P. Bellos ²⁰, K. Beloborodov ³⁷, D. Benchekroun ^{35a}, F. Bendebba ^{35a}, Y. Benhammou ¹⁵²,
 K.C. Benkendorfer ⁶¹, L. Beresford ⁴⁸, M. Beretta ⁵³, E. Bergeaas Kuutmann ¹⁶², N. Berger ⁴,
 B. Bergmann ¹³³, J. Beringer ^{17a}, G. Bernardi ⁵, C. Bernius ¹⁴⁴, F.U. Bernlochner ²⁴,
 F. Bernon ^{36,103}, A. Berrocal Guardia ¹³, T. Berry ⁹⁶, P. Berta ¹³⁴, A. Berthold ⁵⁰, S. Bethke ¹¹¹,
 A. Betti ^{75a,75b}, A.J. Bevan ⁹⁵, N.K. Bhalla ⁵⁴, M. Bhamjee ^{33c}, S. Bhatta ¹⁴⁶,
 D.S. Bhattacharya ¹⁶⁷, P. Bhattarai ¹⁴⁴, K.D. Bhide ⁵⁴, V.S. Bhopatkar ¹²², R.M. Bianchi ¹³⁰,
 G. Bianco ^{23b,23a}, O. Biebel ¹¹⁰, R. Bielski ¹²⁴, M. Biglietti ^{77a}, C.S. Billingsley ⁴⁴, M. Bindi ⁵⁵,
 A. Bingul ^{21b}, C. Bini ^{75a,75b}, A. Biondini ⁹³, C.J. Birch-sykes ¹⁰², G.A. Bird ³², M. Birman ¹⁷⁰,
 M. Biroš ¹³⁴, S. Biryukov ¹⁴⁷, T. Bisanz ⁴⁹, E. Bisceglie ^{43b,43a}, J.P. Biswal ¹³⁵, D. Biswas ¹⁴²,
 K. Bjørke ¹²⁶, I. Bloch ⁴⁸, A. Blue ⁵⁹, U. Blumenschein ⁹⁵, J. Blumenthal ¹⁰¹,
 V.S. Bobrovnikov ³⁷, M. Boehler ⁵⁴, B. Boehm ¹⁶⁷, D. Bogavac ³⁶, A.G. Bogdanchikov ³⁷,
 C. Bohm ^{47a}, V. Boisvert ⁹⁶, P. Bokan ³⁶, T. Bold ^{86a}, M. Bomben ⁵, M. Bona ⁹⁵,
 M. Boonekamp ¹³⁶, C.D. Booth ⁹⁶, A.G. Borbély ⁵⁹, I.S. Bordulev ³⁷, H.M. Borecka-Bielska ¹⁰⁹,
 G. Borissov ⁹², D. Bortoletto ¹²⁷, D. Boscherini ^{23b}, M. Bosman ¹³, J.D. Bossio Sola ³⁶,
 K. Bouaouda ^{35a}, N. Bouchhar ¹⁶⁴, J. Boudreau ¹³⁰, E.V. Bouhova-Thacker ⁹², D. Boumediene ⁴⁰,
 R. Bouquet ^{57b,57a}, A. Boveia ¹²⁰, J. Boyd ³⁶, D. Boye ²⁹, I.R. Boyko ³⁸, J. Bracinik ²⁰,
 N. Brahimi ⁴, G. Brandt ¹⁷², O. Brandt ³², F. Braren ⁴⁸, B. Brau ¹⁰⁴, J.E. Brau ¹²⁴,
 R. Brenner ¹⁷⁰, L. Brenner ¹¹⁵, R. Brenner ¹⁶², S. Bressler ¹⁷⁰, D. Britton ⁵⁹, D. Britzger ¹¹¹,
 I. Brock ²⁴, G. Brooijmans ⁴¹, E. Brost ²⁹, L.M. Brown ¹⁶⁶, L.E. Bruce ⁶¹, T.L. Bruckler ¹²⁷,
 P.A. Bruckman de Renstrom ⁸⁷, B. Brüers ⁴⁸, A. Bruni ^{23b}, G. Bruni ^{23b}, M. Bruschi ^{23b},
 N. Bruscano ^{75a,75b}, T. Buanes ¹⁶, Q. Buat ¹³⁹, D. Buchin ¹¹¹, A.G. Buckley ⁵⁹, O. Bulekov ³⁷,
 B.A. Bullard ¹⁴⁴, S. Burdin ⁹³, C.D. Burgard ⁴⁹, A.M. Burger ³⁶, B. Burghgrave ⁸,
 O. Burlayenko ⁵⁴, J.T.P. Burr ³², C.D. Burton ¹¹, J.C. Burzynski ¹⁴³, E.L. Busch ⁴¹,
 V. Büscher ¹⁰¹, P.J. Bussey ⁵⁹, J.M. Butler ²⁵, C.M. Buttar ⁵⁹, J.M. Butterworth ⁹⁷,
 W. Buttinger ¹³⁵, C.J. Buxo Vazquez ¹⁰⁸, A.R. Buzykaev ³⁷, S. Cabrera Urbán ¹⁶⁴,
 L. Cadamuro ⁶⁶, D. Caforio ⁵⁸, H. Cai ¹³⁰, Y. Cai ^{14a,14e}, Y. Cai ^{14c}, V.M.M. Cairo ³⁶,
 O. Cakir ^{3a}, N. Calace ³⁶, P. Calafiura ^{17a}, G. Calderini ¹²⁸, P. Calfayan ⁶⁸, G. Callea ⁵⁹,
 L.P. Caloba ^{83b}, D. Calvet ⁴⁰, S. Calvet ⁴⁰, M. Calvetti ^{74a,74b}, R. Camacho Toro ¹²⁸,
 S. Camarda ³⁶, D. Camarero Munoz ²⁶, P. Camarri ^{76a,76b}, M.T. Camerlingo ^{72a,72b},
 D. Cameron ³⁶, C. Camincher ¹⁶⁶, M. Campanelli ⁹⁷, A. Camplani ⁴², V. Canale ^{72a,72b},
 A.C. Canbay ^{3a}, J. Cantero ¹⁶⁴, Y. Cao ¹⁶³, F. Capocasa ²⁶, M. Capua ^{43b,43a}, A. Carbone ^{71a,71b},
 R. Cardarelli ^{76a}, J.C.J. Cardenas ⁸, F. Cardillo ¹⁶⁴, G. Carducci ^{43b,43a}, T. Carli ³⁶,
 G. Carlino ^{72a}, J.I. Carlotto ¹³, B.T. Carlson ^{130,r}, E.M. Carlson ^{166,157a}, L. Carminati ^{71a,71b},
 A. Carnelli ¹³⁶, M. Carnesale ^{75a,75b}, S. Caron ¹¹⁴, E. Carquin ^{138f}, S. Carrá ^{71a,71b},
 G. Carratta ^{23b,23a}, A.M. Carroll ¹²⁴, T.M. Carter ⁵², M.P. Casado ^{13,i}, M. Caspar ⁴⁸,
 F.L. Castillo ⁴, L. Castillo Garcia ¹³, V. Castillo Gimenez ¹⁶⁴, N.F. Castro ^{131a,131e},
 A. Catinaccio ³⁶, J.R. Catmore ¹²⁶, T. Cavaliere ⁴, V. Cavaliere ²⁹, N. Cavalli ^{23b,23a},
 Y.C. Cekmecelioglu ⁴⁸, E. Celebi ^{21a}, F. Celli ¹²⁷, M.S. Centonze ^{70a,70b}, V. Cepaitis ⁵⁶,
 K. Cerny ¹²³, A.S. Cerqueira ^{83a}, A. Cerri ¹⁴⁷, L. Cerrito ^{76a,76b}, F. Cerutti ^{17a}, B. Cervato ¹⁴²,
 A. Cervelli ^{23b}, G. Cesarini ⁵³, S.A. Cetin ⁸², D. Chakraborty ¹¹⁶, J. Chan ¹⁷¹, W.Y. Chan ¹⁵⁴,
 J.D. Chapman ³², E. Chapon ¹³⁶, B. Chargeishvili ^{150b}, D.G. Charlton ²⁰, M. Chatterjee ¹⁹,
 C. Chauhan ¹³⁴, Y. Che ^{14c}, S. Chekanov ⁶, S.V. Chekulaev ^{157a}, G.A. Chelkov ^{38,a},
 A. Chen ¹⁰⁷, B. Chen ¹⁵², B. Chen ¹⁶⁶, H. Chen ^{14c}, H. Chen ²⁹, J. Chen ^{62c}, J. Chen ¹⁴³,
 M. Chen ¹²⁷, S. Chen ¹⁵⁴, S.J. Chen ^{14c}, X. Chen ^{62c,136}, X. Chen ^{14b,ae}, Y. Chen ^{62a},
 C.L. Cheng ¹⁷¹, H.C. Cheng ^{64a}, S. Cheong ¹⁴⁴, A. Cheplakov ³⁸, E. Cheremushkina ⁴⁸,
 E. Cherepanova ¹¹⁵, R. Cherkaoui El Moursli ^{35e}, E. Cheu ⁷, K. Cheung ⁶⁵, L. Chevalier ¹³⁶,

V. Chiarella ^{id53}, G. Chiarelli ^{id74a}, N. Chiedde ^{id103}, G. Chiodini ^{id70a}, A.S. Chisholm ^{id20},
A. Chitan ^{id27b}, M. Chitishvili ^{id164}, M.V. Chizhov ^{id38}, K. Choi ^{id11}, Y. Chou ^{id139}, E.Y.S. Chow ^{id114},
K.L. Chu ^{id170}, M.C. Chu ^{id64a}, X. Chu ^{id14a,14e}, J. Chudoba ^{id132}, J.J. Chwastowski ^{id87}, D. Cieri ^{id111},
K.M. Ciesla ^{id86a}, V. Cindro ^{id94}, A. Ciocio ^{id17a}, F. Cirotto ^{id72a,72b}, Z.H. Citron ^{id170,k}, M. Citterio ^{id71a},
D.A. Ciubotaru ^{id27b}, A. Clark ^{id56}, P.J. Clark ^{id52}, C. Clarry ^{id156}, J.M. Clavijo Columbie ^{id48},
S.E. Clawson ^{id48}, C. Clement ^{id47a,47b}, J. Clercx ^{id48}, Y. Coadou ^{id103}, M. Cobal ^{id69a,69c},
A. Coccaro ^{id57b}, R.F. Coelho Barrue ^{id131a}, R. Coelho Lopes De Sa ^{id104}, S. Coelli ^{id71a}, B. Cole ^{id41},
J. Collot ^{id60}, P. Conde Muiño ^{id131a,131g}, M.P. Connell ^{id33c}, S.H. Connell ^{id33c}, E.I. Conroy ^{id127},
F. Conventi ^{id72a,ag}, H.G. Cooke ^{id20}, A.M. Cooper-Sarkar ^{id127}, A. Cordeiro Oudot Choi ^{id128},
L.D. Corpe ^{id40}, M. Corradi ^{id75a,75b}, F. Corriveau ^{id105,x}, A. Cortes-Gonzalez ^{id18}, M.J. Costa ^{id164},
F. Costanza ^{id4}, D. Costanzo ^{id140}, B.M. Cote ^{id120}, G. Cowan ^{id96}, K. Cranmer ^{id171},
D. Cremonini ^{id23b,23a}, S. Crépe-Renaudin ^{id60}, F. Crescioli ^{id128}, M. Cristinziani ^{id142},
M. Cristoforetti ^{id78a,78b}, V. Croft ^{id115}, J.E. Crosby ^{id122}, G. Crosetti ^{id43b,43a}, A. Cueto ^{id100},
T. Cuhadar Donszelmann ^{id160}, H. Cui ^{id14a,14e}, Z. Cui ^{id7}, W.R. Cunningham ^{id59}, F. Curcio ^{id43b,43a},
J.R. Curran ^{id52}, P. Czodrowski ^{id36}, M.M. Czurylo ^{id63b}, M.J. Da Cunha Sargedas De Sousa ^{id57b,57a},
J.V. Da Fonseca Pinto ^{id83b}, C. Da Via ^{id102}, W. Dabrowski ^{id86a}, T. Dado ^{id49}, S. Dahbi ^{id149},
T. Dai ^{id107}, D. Dal Santo ^{id19}, C. Dallapiccola ^{id104}, M. Dam ^{id42}, G. D'amen ^{id29}, V. D'Amico ^{id110},
J. Damp ^{id101}, J.R. Dandoy ^{id34}, M. Danninger ^{id143}, V. Dao ^{id36}, G. Darbo ^{id57b}, S. Darmora ^{id6},
S.J. Das ^{id29,ah}, S. D'Auria ^{id71a,71b}, A. D'Avanzo ^{id131a}, C. David ^{id33a}, T. Davidek ^{id134},
B. Davis-Purcell ^{id34}, I. Dawson ^{id95}, H.A. Day-hall ^{id133}, K. De ^{id8}, R. De Asmundis ^{id72a},
N. De Biase ^{id48}, S. De Castro ^{id23b,23a}, N. De Groot ^{id114}, P. de Jong ^{id115}, H. De la Torre ^{id116},
A. De Maria ^{id14c}, A. De Salvo ^{id75a}, U. De Sanctis ^{id76a,76b}, F. De Santis ^{id70a,70b}, A. De Santo ^{id147},
J.B. De Vivie De Regie ^{id60}, D.V. Dedovich ^{id38}, J. Degens ^{id115}, A.M. Deiana ^{id44}, F. Del Corso ^{id23b,23a},
J. Del Peso ^{id100}, F. Del Rio ^{id63a}, L. Delagrangé ^{id128}, F. Deliot ^{id136}, C.M. Delitzsch ^{id49},
M. Della Pietra ^{id72a,72b}, D. Della Volpe ^{id56}, A. Dell'Acqua ^{id36}, L. Dell'Asta ^{id71a,71b}, M. Delmastro ^{id4},
P.A. Delsart ^{id60}, S. Demers ^{id173}, M. Demichev ^{id38}, S.P. Denisov ^{id37}, L. D'Eramo ^{id40},
D. Derendarz ^{id87}, F. Derue ^{id128}, P. Dervan ^{id93}, K. Desch ^{id24}, C. Deutsch ^{id24}, F.A. Di Bello ^{id57b,57a},
A. Di Ciaccio ^{id76a,76b}, L. Di Ciaccio ^{id4}, A. Di Domenico ^{id75a,75b}, C. Di Donato ^{id72a,72b},
A. Di Girolamo ^{id36}, G. Di Gregorio ^{id36}, A. Di Luca ^{id78a,78b}, B. Di Micco ^{id77a,77b}, R. Di Nardo ^{id77a,77b},
M. Diamantopoulou ^{id34}, F.A. Dias ^{id115}, T. Dias Do Vale ^{id143}, M.A. Diaz ^{id138a,138b},
F.G. Diaz Capriles ^{id24}, M. Didenko ^{id164}, E.B. Diehl ^{id107}, S. Díez Cornell ^{id48}, C. Diez Pardos ^{id142},
C. Dimitriadi ^{id162,24}, A. Dimitrievska ^{id17a}, J. Dingfelder ^{id24}, I-M. Dinu ^{id27b}, S.J. Dittmeier ^{id63b},
F. Dittus ^{id36}, F. Djama ^{id103}, T. Djobava ^{id150b}, C. Doglioni ^{id102,99}, A. Dohnalova ^{id28a}, J. Dolejsi ^{id134},
Z. Dolezal ^{id134}, K.M. Dona ^{id39}, M. Donadelli ^{id83c}, B. Dong ^{id108}, J. Donini ^{id40}, A. D'Onofrio ^{id72a,72b},
M. D'Onofrio ^{id93}, J. Dopke ^{id135}, A. Doria ^{id72a}, N. Dos Santos Fernandes ^{id131a}, P. Dougan ^{id102},
M.T. Dova ^{id91}, A.T. Doyle ^{id59}, M.A. Dragnet ^{id127}, E. Dreyer ^{id170}, I. Drivas-koulouris ^{id10},
M. Drnevich ^{id118}, M. Drozdova ^{id56}, D. Du ^{id62a}, T.A. du Pree ^{id115}, F. Dubinin ^{id37}, M. Dubovsky ^{id28a},
E. Duchovni ^{id170}, G. Duckeck ^{id110}, O.A. Ducu ^{id27b}, D. Duda ^{id52}, A. Dudarev ^{id36}, E.R. Duden ^{id26},
M. D'uffizi ^{id102}, L. Dufлот ^{id66}, M. Dührssen ^{id36}, A.E. Dumitriu ^{id27b}, M. Dunford ^{id63a}, S. Dungs ^{id49},
K. Dunne ^{id47a,47b}, A. Duperrin ^{id103}, H. Duran Yildiz ^{id3a}, M. Düren ^{id58}, A. Durglishvili ^{id150b},
B.L. Dwyer ^{id116}, G.I. Dyckes ^{id17a}, M. Dyndal ^{id86a}, B.S. Dziedzic ^{id87}, Z.O. Earnshaw ^{id147},
G.H. Eberwein ^{id127}, B. Eckerova ^{id28a}, S. Eggebrecht ^{id55}, E. Egidio Purcino De Souza ^{id128},
L.F. Ehrke ^{id56}, G. Eigen ^{id16}, K. Einsweiler ^{id17a}, T. Ekelof ^{id162}, P.A. Ekman ^{id99}, S. El Farkh ^{id35b},
Y. El Ghazali ^{id35b}, H. El Jarrari ^{id36}, A. El Moussaouy ^{id109}, V. Ellajosyula ^{id162}, M. Ellert ^{id162},
F. Ellinghaus ^{id172}, N. Ellis ^{id36}, J. Elmsheuser ^{id29}, M. Elsing ^{id36}, D. Emelianov ^{id135}, Y. Enari ^{id154},
I. Ene ^{id17a}, S. Epari ^{id13}, P.A. Erland ^{id87}, M. Errenst ^{id172}, M. Escalier ^{id66}, C. Escobar ^{id164},
E. Etzion ^{id152}, G. Evans ^{id131a}, H. Evans ^{id68}, L.S. Evans ^{id96}, A. Ezhilov ^{id37}, S. Ezzarqtouni ^{id35a},

F. Fabbri [ID23b,23a](#), L. Fabbri [ID23b,23a](#), G. Facini [ID97](#), V. Fadeyev [ID137](#), R.M. Fakhruddinov [ID37](#), D. Fakoudis [ID101](#), S. Falciano [ID75a](#), L.F. Falda Ulhoa Coelho [ID36](#), P.J. Falke [ID24](#), J. Faltova [ID134](#), C. Fan [ID163](#), Y. Fan [ID14a](#), Y. Fang [ID14a,14e](#), M. Fanti [ID71a,71b](#), M. Faraj [ID69a,69b](#), Z. Farazpay [ID98](#), A. Farbin [ID8](#), A. Farilla [ID77a](#), T. Farooque [ID108](#), S.M. Farrington [ID52](#), F. Fassi [ID35e](#), D. Fassouliotis [ID9](#), M. Faucci Giannelli [ID76a,76b](#), W.J. Fawcett [ID32](#), L. Fayard [ID66](#), P. Federic [ID134](#), P. Federicova [ID132](#), O.L. Fedin [ID37,a](#), M. Feickert [ID171](#), L. Feligioni [ID103](#), D.E. Fellers [ID124](#), C. Feng [ID62b](#), M. Feng [ID14b](#), Z. Feng [ID115](#), M.J. Fenton [ID160](#), L. Ferencz [ID48](#), R.A.M. Ferguson [ID92](#), S.I. Fernandez Luengo [ID138f](#), P. Fernandez Martinez [ID13](#), M.J.V. Fernoux [ID103](#), J. Ferrando [ID92](#), A. Ferrari [ID162](#), P. Ferrari [ID115,114](#), R. Ferrari [ID73a](#), D. Ferrere [ID56](#), C. Ferretti [ID107](#), F. Fiedler [ID101](#), P. Fiedler [ID133](#), A. Filipčič [ID94](#), E.K. Filmer [ID1](#), F. Filthaut [ID114](#), M.C.N. Fiolhais [ID131a,131c,c](#), L. Fiorini [ID164](#), W.C. Fisher [ID108](#), T. Fitschen [ID102](#), P.M. Fitzhugh [ID136](#), I. Fleck [ID142](#), P. Fleischmann [ID107](#), T. Flick [ID172](#), M. Flores [ID33d,ac](#), L.R. Flores Castillo [ID64a](#), L. Flores Sanz De Acedo [ID36](#), F.M. Follega [ID78a,78b](#), N. Fomin [ID16](#), J.H. Foo [ID156](#), A. Formica [ID136](#), A.C. Forti [ID102](#), E. Fortin [ID36](#), A.W. Fortman [ID17a](#), M.G. Foti [ID17a](#), L. Fountas [ID9j](#), D. Fournier [ID66](#), H. Fox [ID92](#), P. Francavilla [ID74a,74b](#), S. Francescato [ID61](#), S. Franchellucci [ID56](#), M. Franchini [ID23b,23a](#), S. Franchino [ID63a](#), D. Francis [ID36](#), L. Franco [ID114](#), V. Franco Lima [ID36](#), L. Franconi [ID48](#), M. Franklin [ID61](#), G. Frattari [ID26](#), W.S. Freund [ID83b](#), Y.Y. Frid [ID152](#), J. Friend [ID59](#), N. Fritzsche [ID50](#), A. Froch [ID54](#), D. Froidevaux [ID36](#), J.A. Frost [ID127](#), Y. Fu [ID62a](#), S. Fuenzalida Garrido [ID138f](#), M. Fujimoto [ID103](#), K.Y. Fung [ID64a](#), E. Furtado De Simas Filho [ID83b](#), M. Furukawa [ID154](#), J. Fuster [ID164](#), A. Gabrielli [ID23b,23a](#), A. Gabrielli [ID156](#), P. Gadow [ID36](#), G. Gagliardi [ID57b,57a](#), L.G. Gagnon [ID17a](#), S. Galantzan [ID152](#), E.J. Gallas [ID127](#), B.J. Gallop [ID135](#), K.K. Gan [ID120](#), S. Ganguly [ID154](#), Y. Gao [ID52](#), F.M. Garay Walls [ID138a,138b](#), B. Garcia [ID29](#), C. García [ID164](#), A. Garcia Alonso [ID115](#), A.G. Garcia Caffaro [ID173](#), J.E. García Navarro [ID164](#), M. Garcia-Sciveres [ID17a](#), G.L. Gardner [ID129](#), R.W. Gardner [ID39](#), N. Garelli [ID159](#), D. Garg [ID80](#), R.B. Garg [ID144,n](#), J.M. Gargan [ID52](#), C.A. Garner [ID156](#), C.M. Garvey [ID33a](#), P. Gaspar [ID83b](#), V.K. Gassmann [ID159](#), G. Gaudio [ID73a](#), V. Gautam [ID13](#), P. Gauzzi [ID75a,75b](#), I.L. Gavrilenko [ID37](#), A. Gavrilyuk [ID37](#), C. Gay [ID165](#), G. Gaycken [ID48](#), E.N. Gazis [ID10](#), A.A. Geanta [ID27b](#), C.M. Gee [ID137](#), A. Gekow [ID120](#), C. Gemme [ID57b](#), M.H. Genest [ID60](#), A.D. Gentry [ID113](#), S. George [ID96](#), W.F. George [ID20](#), T. Geralis [ID46](#), P. Gessinger-Befurt [ID36](#), M.E. Geyik [ID172](#), M. Ghani [ID168](#), M. Ghneimat [ID142](#), K. Ghorbanian [ID95](#), A. Ghosal [ID142](#), A. Ghosh [ID160](#), A. Ghosh [ID7](#), B. Giacobbe [ID23b](#), S. Giagu [ID75a,75b](#), T. Giani [ID115](#), P. Giannetti [ID74a](#), A. Giannini [ID62a](#), S.M. Gibson [ID96](#), M. Gignac [ID137](#), D.T. Gil [ID86b](#), A.K. Gilbert [ID86a](#), B.J. Gilbert [ID41](#), D. Gillberg [ID34](#), G. Gilles [ID115](#), L. Ginabat [ID128](#), D.M. Gingrich [ID2,af](#), M.P. Giordani [ID69a,69c](#), P.F. Giraud [ID136](#), G. Giugliarelli [ID69a,69c](#), D. Giugni [ID71a](#), F. Giuli [ID36](#), I. Gkialas [ID9j](#), L.K. Gladilin [ID37](#), C. Glasman [ID100](#), G.R. Gledhill [ID124](#), G. Glemža [ID48](#), M. Glisic [ID124](#), I. Gnesi [ID43b,f](#), Y. Go [ID29](#), M. Goblirsch-Kolb [ID36](#), B. Gocke [ID49](#), D. Godin [ID109](#), B. Gokturk [ID21a](#), S. Goldfarb [ID106](#), T. Golling [ID56](#), M.G.D. Gololo [ID33g](#), D. Golubkov [ID37](#), J.P. Gombas [ID108](#), A. Gomes [ID131a,131b](#), G. Gomes Da Silva [ID142](#), A.J. Gomez Delegido [ID164](#), R. Gonçalves [ID131a,131c](#), L. Gonella [ID20](#), A. Gongadze [ID150c](#), F. Gonnella [ID20](#), J.L. Gonski [ID144](#), R.Y. González Andana [ID52](#), S. González de la Hoz [ID164](#), R. Gonzalez Lopez [ID93](#), C. Gonzalez Renteria [ID17a](#), M.V. Gonzalez Rodrigues [ID48](#), R. Gonzalez Suarez [ID162](#), S. Gonzalez-Sevilla [ID56](#), G.R. Gonzalvo Rodriguez [ID164](#), L. Goossens [ID36](#), B. Gorini [ID36](#), E. Gorini [ID70a,70b](#), A. Gorišek [ID94](#), T.C. Gosart [ID129](#), A.T. Goshaw [ID51](#), M.I. Gostkin [ID38](#), S. Goswami [ID122](#), C.A. Gottardo [ID36](#), S.A. Gotz [ID110](#), M. Gouighri [ID35b](#), V. Goumarre [ID48](#), A.G. Goussiou [ID139](#), N. Govender [ID33c](#), I. Grabowska-Bold [ID86a](#), K. Graham [ID34](#), E. Gramstad [ID126](#), S. Grancagnolo [ID70a,70b](#), C.M. Grant [ID1,136](#), P.M. Gravila [ID27f](#), F.G. Gravili [ID70a,70b](#), H.M. Gray [ID17a](#), M. Greco [ID70a,70b](#), C. Grefe [ID24](#), I.M. Gregor [ID48](#), P. Grenier [ID144](#), S.G. Grewe [ID111](#), A.A. Grillo [ID137](#), K. Grimm [ID31](#), S. Grinstein [ID13,t](#), J.-F. Grivaz [ID66](#), E. Gross [ID170](#), J. Grosse-Knetter [ID55](#), J.C. Grundy [ID127](#), L. Guan [ID107](#), C. Gubbels [ID165](#), J.G.R. Guerrero Rojas [ID164](#), G. Guerrieri [ID69a,69c](#), F. Guescini [ID111](#), R. Gugel [ID101](#), J.A.M. Guhit [ID107](#), A. Guida [ID18](#), E. Guilloton [ID168](#), S. Guindon [ID36](#),

F. Guo ^{14a,14e}, J. Guo ^{62c}, L. Guo ⁴⁸, Y. Guo ¹⁰⁷, R. Gupta ⁴⁸, R. Gupta ¹³⁰, S. Gurbuz ²⁴,
 S.S. Gurdasani ⁵⁴, G. Gustavino ³⁶, M. Guth ⁵⁶, P. Gutierrez ¹²¹, L.F. Gutierrez Zagazeta ¹²⁹,
 M. Gutsche ⁵⁰, C. Gutschow ⁹⁷, C. Gwenlan ¹²⁷, C.B. Gwilliam ⁹³, E.S. Haaland ¹²⁶,
 A. Haas ¹¹⁸, M. Habedank ⁴⁸, C. Haber ^{17a}, H.K. Hadavand ⁸, A. Hadeef ⁵⁰, S. Hadzic ¹¹¹,
 A.I. Hagan ⁹², J.J. Hahn ¹⁴², E.H. Haines ⁹⁷, M. Haleem ¹⁶⁷, J. Haley ¹²², J.J. Hall ¹⁴⁰,
 G.D. Hallewell ¹⁰³, L. Halser ¹⁹, K. Hamano ¹⁶⁶, M. Hamer ²⁴, G.N. Hamity ⁵²,
 E.J. Hampshire ⁹⁶, J. Han ^{62b}, K. Han ^{62a}, L. Han ^{14c}, L. Han ^{62a}, S. Han ^{17a}, Y.F. Han ¹⁵⁶,
 K. Hanagaki ⁸⁴, M. Hance ¹³⁷, D.A. Hangal ⁴¹, H. Hanif ¹⁴³, M.D. Hank ¹²⁹, J.B. Hansen ⁴²,
 P.H. Hansen ⁴², K. Hara ¹⁵⁸, D. Harada ⁵⁶, T. Harenberg ¹⁷², S. Harkusha ³⁷, M.L. Harris ¹⁰⁴,
 Y.T. Harris ¹²⁷, J. Harrison ¹³, N.M. Harrison ¹²⁰, P.F. Harrison ¹⁶⁸, N.M. Hartman ¹¹¹,
 N.M. Hartmann ¹¹⁰, Y. Hasegawa ¹⁴¹, R. Hauser ¹⁰⁸, C.M. Hawkes ²⁰, R.J. Hawkings ³⁶,
 Y. Hayashi ¹⁵⁴, S. Hayashida ¹¹², D. Hayden ¹⁰⁸, C. Hayes ¹⁰⁷, R.L. Hayes ¹¹⁵, C.P. Hays ¹²⁷,
 J.M. Hays ⁹⁵, H.S. Hayward ⁹³, F. He ^{62a}, M. He ^{14a,14e}, Y. He ¹⁵⁵, Y. He ⁴⁸, Y. He ⁹⁷,
 N.B. Heatley ⁹⁵, V. Hedberg ⁹⁹, A.L. Heggelund ¹²⁶, N.D. Hehir ⁹⁵, C. Heidegger ⁵⁴,
 K.K. Heidegger ⁵⁴, W.D. Heidorn ⁸¹, J. Heilman ³⁴, S. Heim ⁴⁸, T. Heim ^{17a}, J.G. Heinlein ¹²⁹,
 J.J. Heinrich ¹²⁴, L. Heinrich ^{111,ad}, J. Hejbal ¹³², A. Held ¹⁷¹, S. Hellesund ¹⁶,
 C.M. Helling ¹⁶⁵, S. Hellman ^{47a,47b}, R.C.W. Henderson ⁹², L. Henkelmann ³²,
 A.M. Henriques Correia ³⁶, H. Herde ⁹⁹, Y. Hernández Jiménez ¹⁴⁶, L.M. Herrmann ²⁴,
 T. Herrmann ⁵⁰, G. Herten ⁵⁴, R. Hertenberger ¹¹⁰, L. Hervas ³⁶, M.E. Hespang ¹⁰¹,
 N.P. Hesse ^{157a}, E. Hill ¹⁵⁶, S.J. Hillier ²⁰, J.R. Hinds ¹⁰⁸, F. Hinterkeuser ²⁴, M. Hirose ¹²⁵,
 S. Hirose ¹⁵⁸, D. Hirschbuehl ¹⁷², T.G. Hitchings ¹⁰², B. Hiti ⁹⁴, J. Hobbs ¹⁴⁶, R. Hobincu ^{27e},
 N. Hod ¹⁷⁰, M.C. Hodgkinson ¹⁴⁰, B.H. Hodgkinson ¹²⁷, A. Hoecker ³⁶, D.D. Hofer ¹⁰⁷,
 J. Hofer ⁴⁸, T. Holm ²⁴, M. Holzbock ¹¹¹, L.B.A.H. Hommels ³², B.P. Honan ¹⁰², J. Hong ^{62c},
 T.M. Hong ¹³⁰, B.H. Hooberman ¹⁶³, W.H. Hopkins ⁶, Y. Horii ¹¹², S. Hou ¹⁴⁹, A.S. Howard ⁹⁴,
 J. Howarth ⁵⁹, J. Hoya ⁶, M. Hrabovsky ¹²³, A. Hrynevich ⁴⁸, T. Hryn'ova ⁴, P.J. Hsu ⁶⁵,
 S.-C. Hsu ¹³⁹, Q. Hu ^{62a}, S. Huang ^{64b}, X. Huang ^{14c}, X. Huang ^{14a,14e}, Y. Huang ¹⁴⁰,
 Y. Huang ^{14a}, Z. Huang ¹⁰², Z. Hubacek ¹³³, M. Huebner ²⁴, F. Huegging ²⁴, T.B. Huffman ¹²⁷,
 C.A. Hugli ⁴⁸, M. Huhtinen ³⁶, S.K. Huiberts ¹⁶, R. Hulsken ¹⁰⁵, N. Huseynov ¹², J. Huston ¹⁰⁸,
 J. Huth ⁶¹, R. Hyneman ¹⁴⁴, G. Iacobucci ⁵⁶, G. Iakovidis ²⁹, I. Ibragimov ¹⁴²,
 L. Iconomidou-Fayard ⁶⁶, J.P. Iddon ³⁶, P. Iengo ^{72a,72b}, R. Iguchi ¹⁵⁴, T. Iizawa ¹²⁷,
 Y. Ikegami ⁸⁴, N. Ilic ¹⁵⁶, H. Imam ^{35a}, M. Ince Lezki ⁵⁶, T. Ingebretsen Carlson ^{47a,47b},
 G. Introzzi ^{73a,73b}, M. Iodice ^{77a}, V. Ippolito ^{75a,75b}, R.K. Irwin ⁹³, M. Ishino ¹⁵⁴, W. Islam ¹⁷¹,
 C. Issever ^{18,48}, S. Istin ^{21a,aj}, H. Ito ¹⁶⁹, R. Iuppa ^{78a,78b}, A. Ivina ¹⁷⁰, J.M. Izen ⁴⁵, V. Izzo ^{72a},
 P. Jacka ^{132,133}, P. Jackson ¹, B.P. Jaeger ¹⁴³, C.S. Jagfeld ¹¹⁰, G. Jain ^{157a}, P. Jain ⁵⁴,
 K. Jakobs ⁵⁴, T. Jakoubek ¹⁷⁰, J. Jamieson ⁵⁹, K.W. Janas ^{86a}, M. Javurkova ¹⁰⁴, L. Jeanty ¹²⁴,
 J. Jejelava ^{150a,aa}, P. Jenni ^{54,g}, C.E. Jessiman ³⁴, C. Jia ^{62b}, J. Jia ¹⁴⁶, X. Jia ⁶¹, X. Jia ^{14a,14e},
 Z. Jia ^{14c}, S. Jiggins ⁴⁸, J. Jimenez Pena ¹³, S. Jin ^{14c}, A. Jinaru ^{27b}, O. Jinnouchi ¹⁵⁵,
 P. Johansson ¹⁴⁰, K.A. Johns ⁷, J.W. Johnson ¹³⁷, D.M. Jones ³², E. Jones ⁴⁸, P. Jones ³²,
 R.W.L. Jones ⁹², T.J. Jones ⁹³, H.L. Joos ^{55,36}, R. Joshi ¹²⁰, J. Jovicevic ¹⁵, X. Ju ^{17a},
 J.J. Junggeburth ¹⁰⁴, T. Junkermann ^{63a}, A. Juste Rozas ^{13,t}, M.K. Juzek ⁸⁷, S. Kabana ^{138e},
 A. Kaczmarska ⁸⁷, M. Kado ¹¹¹, H. Kagan ¹²⁰, M. Kagan ¹⁴⁴, A. Kahn ⁴¹, A. Kahn ¹²⁹,
 C. Kahra ¹⁰¹, T. Kaji ¹⁵⁴, E. Kajomovitz ¹⁵¹, N. Kakati ¹⁷⁰, I. Kalaitzidou ⁵⁴, C.W. Kalderon ²⁹,
 N.J. Kang ¹³⁷, D. Kar ^{33g}, K. Karava ¹²⁷, M.J. Kareem ^{157b}, E. Karentzos ⁵⁴, I. Karkanas ¹⁵³,
 O. Karkout ¹¹⁵, S.N. Karpov ³⁸, Z.M. Karpova ³⁸, V. Kartvelishvili ⁹², A.N. Karyukhin ³⁷,
 E. Kasimi ¹⁵³, J. Katzy ⁴⁸, S. Kaur ³⁴, K. Kawade ¹⁴¹, M.P. Kawale ¹²¹, C. Kawamoto ⁸⁸,
 T. Kawamoto ^{62a}, E.F. Kay ³⁶, F.I. Kaya ¹⁵⁹, S. Kazakos ¹⁰⁸, V.F. Kazanin ³⁷, Y. Ke ¹⁴⁶,
 J.M. Keaveney ^{33a}, R. Keeler ¹⁶⁶, G.V. Kehris ⁶¹, J.S. Keller ³⁴, A.S. Kelly ⁹⁷, J.J. Kempster ¹⁴⁷,

P.D. Kennedy [ID101](#), O. Kepka [ID132](#), B.P. Kerridge [ID135](#), S. Kersten [ID172](#), B.P. Kerševan [ID94](#),
 S. Keshri [ID66](#), L. Keszeghova [ID28a](#), S. Ketabchi Haghghat [ID156](#), R.A. Khan [ID130](#), A. Khanov [ID122](#),
 A.G. Kharlamov [ID37](#), T. Kharlamova [ID37](#), E.E. Khoda [ID139](#), M. Kholodenko [ID37](#), T.J. Khoo [ID18](#),
 G. Khorauli [ID167](#), J. Khubua [ID150b](#), Y.A.R. Khwaira [ID66](#), B. Kibirige [ID33g](#), A. Kilgallon [ID124](#),
 D.W. Kim [ID47a,47b](#), Y.K. Kim [ID39](#), N. Kimura [ID97](#), M.K. Kingston [ID55](#), A. Kirchhoff [ID55](#), C. Kirfel [ID24](#),
 F. Kirfel [ID24](#), J. Kirk [ID135](#), A.E. Kiryunin [ID111](#), C. Kitsaki [ID10](#), O. Kivernyk [ID24](#), M. Klassen [ID63a](#),
 C. Klein [ID34](#), L. Klein [ID167](#), M.H. Klein [ID44](#), S.B. Klein [ID56](#), U. Klein [ID93](#), P. Klimek [ID36](#),
 A. Klimentov [ID29](#), T. Klioutchnikova [ID36](#), P. Kluit [ID115](#), S. Kluth [ID111](#), E. Kneringer [ID79](#),
 T.M. Knight [ID156](#), A. Knue [ID49](#), R. Kobayashi [ID88](#), D. Kobylanski [ID170](#), S.F. Koch [ID127](#),
 M. Kocian [ID144](#), P. Kodyš [ID134](#), D.M. Koeck [ID124](#), P.T. Koenig [ID24](#), T. Koffas [ID34](#), O. Kolay [ID50](#),
 I. Koletsou [ID4](#), T. Komarek [ID123](#), K. Köneke [ID54](#), A.X.Y. Kong [ID1](#), T. Kono [ID119](#), N. Konstantinidis [ID97](#),
 P. Kontaxakis [ID56](#), B. Konya [ID99](#), R. Kopeliansky [ID68](#), S. Koperny [ID86a](#), K. Korcyl [ID87](#), K. Kordas [ID153,e](#),
 A. Korn [ID97](#), S. Korn [ID55](#), I. Korolkov [ID13](#), N. Korotkova [ID37](#), B. Kortman [ID115](#), O. Kortner [ID111](#),
 S. Kortner [ID111](#), W.H. Kostecka [ID116](#), V.V. Kostyukhin [ID142](#), A. Kotsokechagia [ID136](#), A. Kotwal [ID51](#),
 A. Koulouris [ID36](#), A. Kourkoumeli-Charalampidi [ID73a,73b](#), C. Kourkoumelis [ID9](#), E. Kourlitis [ID111,ad](#),
 O. Kovanda [ID124](#), R. Kowalewski [ID166](#), W. Kozanecki [ID136](#), A.S. Kozhin [ID37](#), V.A. Kramarenko [ID37](#),
 G. Kramberger [ID94](#), P. Kramer [ID101](#), M.W. Krasny [ID128](#), A. Krasznahorkay [ID36](#), J.W. Kraus [ID172](#),
 J.A. Kremer [ID48](#), T. Kresse [ID50](#), J. Kretschmar [ID93](#), K. Kreul [ID18](#), P. Krieger [ID156](#),
 S. Krishnamurthy [ID104](#), M. Krivos [ID134](#), K. Krizka [ID20](#), K. Kroeninger [ID49](#), H. Kroha [ID111](#), J. Kroll [ID132](#),
 J. Kroll [ID129](#), K.S. Krowpman [ID108](#), U. Kruchonak [ID38](#), H. Krüger [ID24](#), N. Krumnack [ID81](#), M.C. Kruse [ID51](#),
 O. Kuchinskaia [ID37](#), S. Kудay [ID3a](#), S. Kuehn [ID36](#), R. Kuesters [ID54](#), T. Kuhl [ID48](#), V. Kukhtin [ID38](#),
 Y. Kulchitsky [ID37,a](#), S. Kuleshov [ID138d,138b](#), M. Kumar [ID33g](#), N. Kumari [ID48](#), P. Kumari [ID157b](#),
 A. Kupco [ID132](#), T. Kupfer [ID49](#), A. Kupich [ID37](#), O. Kuprash [ID54](#), H. Kurashige [ID85](#), L.L. Kurchaninov [ID157a](#),
 O. Kurdysh [ID66](#), Y.A. Kurochkin [ID37](#), A. Kurova [ID37](#), M. Kuze [ID155](#), A.K. Kvam [ID104](#), J. Kvita [ID123](#),
 T. Kwan [ID105](#), N.G. Kyriacou [ID107](#), L.A.O. Laatu [ID103](#), C. Lacasta [ID164](#), F. Lacava [ID75a,75b](#),
 H. Lacker [ID18](#), D. Lacour [ID128](#), N.N. Lad [ID97](#), E. Ladygin [ID38](#), B. Laforge [ID128](#), T. Lagouri [ID27b](#),
 F.Z. Lahbabi [ID35a](#), S. Lai [ID55](#), I.K. Lakomic [ID86a](#), N. Lalloue [ID60](#), J.E. Lambert [ID166](#), S. Lammers [ID68](#),
 W. Lampl [ID7](#), C. Lampoudis [ID153,e](#), G. Lamprinoudis [ID101](#), A.N. Lancaster [ID116](#), E. Lançon [ID29](#),
 U. Landgraf [ID54](#), M.P.J. Landon [ID95](#), V.S. Lang [ID54](#), O.K.B. Langrekken [ID126](#), A.J. Lankford [ID160](#),
 F. Lanni [ID36](#), K. Lantzsch [ID24](#), A. Lanza [ID73a](#), A. Lapertosa [ID57b,57a](#), J.F. Laporte [ID136](#), T. Lari [ID71a](#),
 F. Lasagni Manghi [ID23b](#), M. Lassnig [ID36](#), V. Latonova [ID132](#), A. Laudrain [ID101](#), A. Laurier [ID151](#),
 S.D. Lawlor [ID140](#), Z. Lawrence [ID102](#), R. Lazaridou [ID168](#), M. Lazzaroni [ID71a,71b](#), B. Le [ID102](#),
 E.M. Le Boulicaut [ID51](#), B. Leban [ID94](#), A. Lebedev [ID81](#), M. LeBlanc [ID102](#), F. Ledroit-Guillon [ID60](#),
 A.C.A. Lee [ID97](#), S.C. Lee [ID149](#), S. Lee [ID47a,47b](#), T.F. Lee [ID93](#), L.L. Leeuw [ID33c](#), H.P. Lefebvre [ID96](#),
 M. Lefebvre [ID166](#), C. Leggett [ID17a](#), G. Lehmann Miotto [ID36](#), M. Leigh [ID56](#), W.A. Leight [ID104](#),
 W. Leinonen [ID114](#), A. Leisos [ID153,s](#), M.A.L. Leite [ID83c](#), C.E. Leitgeb [ID18](#), R. Leitner [ID134](#),
 K.J.C. Leney [ID44](#), T. Lenz [ID24](#), S. Leone [ID74a](#), C. Leonidopoulos [ID52](#), A. Leopold [ID145](#), C. Leroy [ID109](#),
 R. Les [ID108](#), C.G. Lester [ID32](#), M. Levchenko [ID37](#), J. Levêque [ID4](#), L.J. Levinson [ID170](#), G. Levrini [ID23b,23a](#),
 M.P. Lewicki [ID87](#), D.J. Lewis [ID4](#), A. Li [ID5](#), B. Li [ID62b](#), C. Li [ID62a](#), C-Q. Li [ID111](#), H. Li [ID62a](#), H. Li [ID62b](#),
 H. Li [ID14c](#), H. Li [ID14b](#), H. Li [ID62b](#), J. Li [ID62c](#), K. Li [ID139](#), L. Li [ID62c](#), M. Li [ID14a,14e](#), Q.Y. Li [ID62a](#),
 S. Li [ID14a,14e](#), S. Li [ID62d,62c,d](#), T. Li [ID5](#), X. Li [ID105](#), Z. Li [ID127](#), Z. Li [ID105](#), Z. Li [ID14a,14e](#), S. Liang [ID14a,14e](#),
 Z. Liang [ID14a](#), M. Liberatore [ID136](#), B. Liberti [ID76a](#), K. Lie [ID64c](#), J. Lieber Marin [ID83b](#), H. Lien [ID68](#),
 K. Lin [ID108](#), R.E. Lindley [ID7](#), J.H. Lindon [ID2](#), E. Lipeles [ID129](#), A. Lipniacka [ID16](#), A. Lister [ID165](#),
 J.D. Little [ID4](#), B. Liu [ID14a](#), B.X. Liu [ID143](#), D. Liu [ID62d,62c](#), E.H.L. Liu [ID20](#), J.B. Liu [ID62a](#), J.K.K. Liu [ID32](#),
 K. Liu [ID62d](#), K. Liu [ID62d,62c](#), M. Liu [ID62a](#), M.Y. Liu [ID62a](#), P. Liu [ID14a](#), Q. Liu [ID62d,139,62c](#), X. Liu [ID62a](#),
 X. Liu [ID62b](#), Y. Liu [ID14d,14e](#), Y.L. Liu [ID62b](#), Y.W. Liu [ID62a](#), J. Llorente Merino [ID143](#), S.L. Lloyd [ID95](#),
 E.M. Lobodzinska [ID48](#), P. Loch [ID7](#), T. Lohse [ID18](#), K. Lohwasser [ID140](#), E. Loiacono [ID48](#),

M. Lokajicek [id](#)^{132,*}, J.D. Lomas [id](#)²⁰, J.D. Long [id](#)¹⁶³, I. Longarini [id](#)¹⁶⁰, L. Longo [id](#)^{70a,70b},
R. Longo [id](#)¹⁶³, I. Lopez Paz [id](#)⁶⁷, A. Lopez Solis [id](#)⁴⁸, N. Lorenzo Martinez [id](#)⁴, A.M. Lory [id](#)¹¹⁰,
G. Löschke Centeno [id](#)¹⁴⁷, O. Loseva [id](#)³⁷, X. Lou [id](#)^{47a,47b}, X. Lou [id](#)^{14a,14e}, A. Lounis [id](#)⁶⁶,
P.A. Love [id](#)⁹², G. Lu [id](#)^{14a,14e}, M. Lu [id](#)⁸⁰, S. Lu [id](#)¹²⁹, Y.J. Lu [id](#)⁶⁵, H.J. Lubatti [id](#)¹³⁹, C. Luci [id](#)^{75a,75b},
F.L. Lucio Alves [id](#)^{14c}, F. Luehring [id](#)⁶⁸, I. Luise [id](#)¹⁴⁶, O. Lukianchuk [id](#)⁶⁶, O. Lundberg [id](#)¹⁴⁵,
B. Lund-Jensen [id](#)¹⁴⁵, N.A. Luongo [id](#)⁶, M.S. Lutz [id](#)³⁶, A.B. Lux [id](#)²⁵, D. Lynn [id](#)²⁹, R. Lysak [id](#)¹³²,
E. Lytken [id](#)⁹⁹, V. Lyubushkin [id](#)³⁸, T. Lyubushkina [id](#)³⁸, M.M. Lyukova [id](#)¹⁴⁶, H. Ma [id](#)²⁹, K. Ma [id](#)^{62a},
L.L. Ma [id](#)^{62b}, W. Ma [id](#)^{62a}, Y. Ma [id](#)¹²², D.M. Mac Donell [id](#)¹⁶⁶, G. Maccarrone [id](#)⁵³,
J.C. MacDonald [id](#)¹⁰¹, P.C. Machado De Abreu Farias [id](#)^{83b}, R. Madar [id](#)⁴⁰, W.F. Mader [id](#)⁵⁰,
T. Madula [id](#)⁹⁷, J. Maeda [id](#)⁸⁵, T. Maeno [id](#)²⁹, H. Maguire [id](#)¹⁴⁰, V. Maiboroda [id](#)¹³⁶,
A. Maio [id](#)^{131a,131b,131d}, K. Maj [id](#)^{86a}, O. Majersky [id](#)⁴⁸, S. Majewski [id](#)¹²⁴, N. Makovec [id](#)⁶⁶,
V. Maksimovic [id](#)¹⁵, B. Malaescu [id](#)¹²⁸, Pa. Malecki [id](#)⁸⁷, V.P. Maleev [id](#)³⁷, F. Malek [id](#)^{60,o}, M. Mali [id](#)⁹⁴,
D. Malito [id](#)⁹⁶, U. Mallik [id](#)⁸⁰, S. Maltezos¹⁰, S. Malyukov³⁸, J. Mamuzic [id](#)¹³, G. Mancini [id](#)⁵³,
M.N. Mancini [id](#)²⁶, G. Manco [id](#)^{73a,73b}, J.P. Mandalia [id](#)⁹⁵, I. Mandić [id](#)⁹⁴,
L. Manhaes de Andrade Filho [id](#)^{83a}, I.M. Maniatis [id](#)¹⁷⁰, J. Manjarres Ramos [id](#)⁹⁰, D.C. Mankad [id](#)¹⁷⁰,
A. Mann [id](#)¹¹⁰, S. Manzoni [id](#)³⁶, L. Mao [id](#)^{62c}, X. Mapekula [id](#)^{33c}, A. Marantis [id](#)^{153,s}, G. Marchiori [id](#)⁵,
M. Marcisovsky [id](#)¹³², C. Marcon [id](#)^{71a,71b}, M. Marinescu [id](#)²⁰, S. Marium [id](#)⁴⁸, M. Marjanovic [id](#)¹²¹,
M. Markovitch [id](#)⁶⁶, E.J. Marshall [id](#)⁹², Z. Marshall [id](#)^{17a}, S. Marti-Garcia [id](#)¹⁶⁴, T.A. Martin [id](#)¹⁶⁸,
V.J. Martin [id](#)⁵², B. Martin dit Latour [id](#)¹⁶, L. Martinelli [id](#)^{75a,75b}, M. Martinez [id](#)^{13,t},
P. Martinez Agullo [id](#)¹⁶⁴, V.I. Martinez Outschoorn [id](#)¹⁰⁴, P. Martinez Suarez [id](#)¹³, S. Martin-Haugh [id](#)¹³⁵,
G. Martinovicova [id](#)¹³⁴, V.S. Martoiu [id](#)^{27b}, A.C. Martyniuk [id](#)⁹⁷, A. Marzin [id](#)³⁶, D. Mascione [id](#)^{78a,78b},
L. Masetti [id](#)¹⁰¹, T. Mashimo [id](#)¹⁵⁴, J. Masik [id](#)¹⁰², A.L. Maslennikov [id](#)³⁷, P. Massarotti [id](#)^{72a,72b},
P. Mastrandrea [id](#)^{74a,74b}, A. Mastroberardino [id](#)^{43b,43a}, T. Masubuchi [id](#)¹⁵⁴, T. Mathisen [id](#)¹⁶²,
J. Matousek [id](#)¹³⁴, N. Matsuzawa¹⁵⁴, J. Maurer [id](#)^{27b}, A.J. Maury [id](#)⁶⁶, B. Maček [id](#)⁹⁴, D.A. Maximov [id](#)³⁷,
R. Mazini [id](#)¹⁴⁹, I. Maznas [id](#)¹¹⁶, M. Mazza [id](#)¹⁰⁸, S.M. Mazza [id](#)¹³⁷, E. Mazzeo [id](#)^{71a,71b}, C. Mc Ginn [id](#)²⁹,
J.P. Mc Gowan [id](#)¹⁰⁵, S.P. Mc Kee [id](#)¹⁰⁷, C.C. McCracken [id](#)¹⁶⁵, E.F. McDonald [id](#)¹⁰⁶,
A.E. McDougall [id](#)¹¹⁵, J.A. Mcfayden [id](#)¹⁴⁷, R.P. McGovern [id](#)¹²⁹, G. Mchedlidze [id](#)^{150b},
R.P. Mckenzie [id](#)^{33g}, T.C. Mclachlan [id](#)⁴⁸, D.J. Mclaughlin [id](#)⁹⁷, S.J. McMahan [id](#)¹³⁵,
C.M. Mccpartland [id](#)⁹³, R.A. McPherson [id](#)^{166,x}, S. Mehlhase [id](#)¹¹⁰, A. Mehta [id](#)⁹³, D. Melini [id](#)¹⁶⁴,
B.R. Mellado Garcia [id](#)^{33g}, A.H. Melo [id](#)⁵⁵, F. Meloni [id](#)⁴⁸, A.M. Mendes Jacques Da Costa [id](#)¹⁰²,
H.Y. Meng [id](#)¹⁵⁶, L. Meng [id](#)⁹², S. Menke [id](#)¹¹¹, M. Mentink [id](#)³⁶, E. Meoni [id](#)^{43b,43a}, G. Mercado [id](#)¹¹⁶,
C. Merlassino [id](#)^{69a,69c}, L. Merola [id](#)^{72a,72b}, C. Meroni [id](#)^{71a,71b}, J. Metcalfe [id](#)⁶, A.S. Mete [id](#)⁶,
C. Meyer [id](#)⁶⁸, J-P. Meyer [id](#)¹³⁶, R.P. Middleton [id](#)¹³⁵, L. Mijović [id](#)⁵², G. Mikenberg [id](#)¹⁷⁰,
M. Mikestikova [id](#)¹³², M. Mikuž [id](#)⁹⁴, H. Mildner [id](#)¹⁰¹, A. Milic [id](#)³⁶, D.W. Miller [id](#)³⁹, E.H. Miller [id](#)¹⁴⁴,
L.S. Miller [id](#)³⁴, A. Milov [id](#)¹⁷⁰, D.A. Milstead^{47a,47b}, T. Min^{14c}, A.A. Minaenko [id](#)³⁷,
I.A. Minashvili [id](#)^{150b}, L. Mince [id](#)⁵⁹, A.I. Mincer [id](#)¹¹⁸, B. Mindur [id](#)^{86a}, M. Mineev [id](#)³⁸, Y. Mino [id](#)⁸⁸,
L.M. Mir [id](#)¹³, M. Miralles Lopez [id](#)⁵⁹, M. Mironova [id](#)^{17a}, A. Mishima¹⁵⁴, M.C. Missio [id](#)¹¹⁴,
A. Mitra [id](#)¹⁶⁸, V.A. Mitsou [id](#)¹⁶⁴, Y. Mitsumori [id](#)¹¹², O. Miu [id](#)¹⁵⁶, P.S. Miyagawa [id](#)⁹⁵,
T. Mkrtychyan [id](#)^{63a}, M. Mlinarevic [id](#)⁹⁷, T. Mlinarevic [id](#)⁹⁷, M. Mlynarikova [id](#)³⁶, S. Mobius [id](#)¹⁹,
P. Mogg [id](#)¹¹⁰, M.H. Mohamed Farook [id](#)¹¹³, A.F. Mohammed [id](#)^{14a,14e}, S. Mohapatra [id](#)⁴¹,
G. Mokgatitswane [id](#)^{33g}, L. Moleri [id](#)¹⁷⁰, B. Mondal [id](#)¹⁴², S. Mondal [id](#)¹³³, K. Mönig [id](#)⁴⁸,
E. Monnier [id](#)¹⁰³, L. Monsonis Romero¹⁶⁴, J. Montejo Berlingen [id](#)¹³, M. Montella [id](#)¹²⁰,
F. Montekali [id](#)^{77a,77b}, F. Monticelli [id](#)⁹¹, S. Monzani [id](#)^{69a,69c}, N. Morange [id](#)⁶⁶,
A.L. Moreira De Carvalho [id](#)^{131a}, M. Moreno Llácer [id](#)¹⁶⁴, C. Moreno Martinez [id](#)⁵⁶, P. Morettini [id](#)^{57b},
S. Morgenstern [id](#)³⁶, M. Morii [id](#)⁶¹, M. Morinaga [id](#)¹⁵⁴, F. Morodei [id](#)^{75a,75b}, L. Morvaj [id](#)³⁶,
P. Moschovakos [id](#)³⁶, B. Moser [id](#)³⁶, M. Mosidze^{150b}, T. Moskalets [id](#)⁵⁴, P. Moskvitina [id](#)¹¹⁴, J. Moss [id](#)^{31,1},
A. Moussa [id](#)^{35d}, E.J.W. Moyse [id](#)¹⁰⁴, O. Mtintsilana [id](#)^{33g}, S. Muanza [id](#)¹⁰³, J. Mueller [id](#)¹³⁰,

D. Muenstermann ¹⁹², R. Müller ¹⁹, G.A. Mullier ¹⁶², A.J. Mullin ³², J.J. Mullin ¹²⁹, D.P. Mungo ¹⁵⁶,
 D. Munoz Perez ¹⁶⁴, F.J. Munoz Sanchez ¹⁰², M. Murin ¹⁰², W.J. Murray ^{168,135}, M. Muškinja ⁹⁴,
 C. Mwewa ²⁹, A.G. Myagkov ^{37,a}, A.J. Myers ⁸, G. Myers ¹⁰⁷, M. Myska ¹³³,
 B.P. Nachman ^{17a}, O. Nackenhorst ⁴⁹, K. Nagai ¹²⁷, K. Nagano ⁸⁴, J.L. Nagle ^{29,ah}, E. Nagy ¹⁰³,
 A.M. Nairz ³⁶, Y. Nakahama ⁸⁴, K. Nakamura ⁸⁴, K. Nakkalil ⁵, H. Nanjo ¹²⁵, R. Narayan ⁴⁴,
 E.A. Narayanan ¹¹³, I. Naryshkin ³⁷, M. Naseri ³⁴, S. Nasri ^{117b}, C. Nass ²⁴, G. Navarro ^{22a},
 J. Navarro-Gonzalez ¹⁶⁴, R. Nayak ¹⁵², A. Nayaz ¹⁸, P.Y. Nechaeva ³⁷, F. Nechansky ⁴⁸,
 L. Nedic ¹²⁷, T.J. Neep ²⁰, A. Negri ^{73a,73b}, M. Negrini ^{23b}, C. Nellist ¹¹⁵, C. Nelson ¹⁰⁵,
 K. Nelson ¹⁰⁷, S. Nemecek ¹³², M. Nessi ^{36,h}, M.S. Neubauer ¹⁶³, F. Neuhaus ¹⁰¹,
 J. Neundorf ⁴⁸, R. Newhouse ¹⁶⁵, P.R. Newman ²⁰, C.W. Ng ¹³⁰, Y.W.Y. Ng ⁴⁸, B. Ngair ^{117a},
 H.D.N. Nguyen ¹⁰⁹, R.B. Nickerson ¹²⁷, R. Nicolaidou ¹³⁶, J. Nielsen ¹³⁷, M. Niemeyer ⁵⁵,
 J. Niermann ⁵⁵, N. Nikiforou ³⁶, V. Nikolaenko ^{37,a}, I. Nikolic-Audit ¹²⁸, K. Nikolopoulos ²⁰,
 P. Nilsson ²⁹, I. Ninca ⁴⁸, H.R. Nindhito ⁵⁶, G. Ninio ¹⁵², A. Nisati ^{75a}, N. Nishu ²,
 R. Nisius ¹¹¹, J-E. Nitschke ⁵⁰, E.K. Nkadimeng ^{33g}, T. Nobe ¹⁵⁴, D.L. Noel ³²,
 T. Nommensen ¹⁴⁸, M.B. Norfolk ¹⁴⁰, R.R.B. Norisam ⁹⁷, B.J. Norman ³⁴, M. Noury ^{35a},
 J. Novak ⁹⁴, T. Novak ⁴⁸, L. Novotny ¹³³, R. Novotny ¹¹³, L. Nozka ¹²³, K. Ntekas ¹⁶⁰,
 N.M.J. Nunes De Moura Junior ^{83b}, J. Ocariz ¹²⁸, A. Ochi ⁸⁵, I. Ochoa ^{131a}, S. Oerdek ⁴⁸,
 J.T. Offermann ³⁹, A. Ogrodnik ¹³⁴, A. Oh ¹⁰², C.C. Ohm ¹⁴⁵, H. Oide ⁸⁴, R. Oishi ¹⁵⁴,
 M.L. Ojeda ⁴⁸, Y. Okumura ¹⁵⁴, L.F. Oleiro Seabra ^{131a}, S.A. Olivares Pino ^{138d},
 D. Oliveira Damazio ²⁹, D. Oliveira Goncalves ^{83a}, J.L. Oliver ¹⁶⁰, Ö.O. Öncel ⁵⁴,
 A.P. O'Neill ¹⁹, A. Onofre ^{131a,131e}, P.U.E. Onyisi ¹¹, M.J. Oreglia ³⁹, G.E. Orellana ⁹¹,
 D. Orestano ^{77a,77b}, N. Orlando ¹³, R.S. Orr ¹⁵⁶, V. O'Shea ⁵⁹, L.M. Osojnak ¹²⁹,
 R. Ospanov ^{62a}, G. Otero y Garzon ³⁰, H. Otono ⁸⁹, P.S. Ott ^{63a}, G.J. Ottino ^{17a}, M. Ouchrif ^{35d},
 F. Ould-Saada ¹²⁶, T. Ovsiannikova ¹³⁹, M. Owen ⁵⁹, R.E. Owen ¹³⁵, K.Y. Oyulmaz ^{21a},
 V.E. Ozcan ^{21a}, F. Ozturk ⁸⁷, N. Ozturk ⁸, S. Ozturk ⁸², H.A. Pacey ¹²⁷, A. Pacheco Pages ¹³,
 C. Padilla Aranda ¹³, G. Padovano ^{75a,75b}, S. Pagan Griso ^{17a}, G. Palacino ⁶⁸, A. Palazzo ^{70a,70b},
 J. Pampel ²⁴, J. Pan ¹⁷³, T. Pan ^{64a}, D.K. Panchal ¹¹, C.E. Pandini ¹¹⁵, J.G. Panduro Vazquez ⁹⁶,
 H.D. Pandya ¹, H. Pang ^{14b}, P. Pani ⁴⁸, G. Panizzo ^{69a,69c}, L. Panwar ¹²⁸, L. Paolozzi ⁵⁶,
 S. Parajuli ¹⁶³, A. Paramonov ⁶, C. Paraskevopoulos ⁵³, D. Paredes Hernandez ^{64b},
 A. Pareti ^{73a,73b}, K.R. Park ⁴¹, T.H. Park ¹⁵⁶, M.A. Parker ³², F. Parodi ^{57b,57a}, E.W. Parrish ¹¹⁶,
 V.A. Parrish ⁵², J.A. Parsons ⁴¹, U. Parzefall ⁵⁴, B. Pascual Dias ¹⁰⁹, L. Pascual Dominguez ¹⁵²,
 E. Pasqualucci ^{75a}, S. Passaggio ^{57b}, F. Pastore ⁹⁶, P. Patel ⁸⁷, U.M. Patel ⁵¹, J.R. Pater ¹⁰²,
 T. Pauly ³⁶, C.I. Pazos ¹⁵⁹, J. Pearkes ¹⁴⁴, M. Pedersen ¹²⁶, R. Pedro ^{131a}, S.V. Peleganchuk ³⁷,
 O. Penc ³⁶, E.A. Pender ⁵², G.D. Penn ¹⁷³, K.E. Penski ¹¹⁰, M. Penzin ³⁷, B.S. Peralva ^{83d},
 A.P. Pereira Peixoto ¹³⁹, L. Pereira Sanchez ¹⁴⁴, D.V. Perepelitsa ^{29,ah}, E. Perez Codina ^{157a},
 M. Perganti ¹⁰, H. Pernegger ³⁶, O. Perrin ⁴⁰, K. Peters ⁴⁸, R.F.Y. Peters ¹⁰², B.A. Petersen ³⁶,
 T.C. Petersen ⁴², E. Petit ¹⁰³, V. Petousis ¹³³, C. Petridou ^{153,e}, T. Petru ¹³⁴, A. Petrukhin ¹⁴²,
 M. Pettee ^{17a}, N.E. Pettersson ³⁶, A. Petukhov ³⁷, K. Petukhova ¹³⁴, R. Pezoa ^{138f},
 L. Pezzotti ³⁶, G. Pezzullo ¹⁷³, T.M. Pham ¹⁷¹, T. Pham ¹⁰⁶, P.W. Phillips ¹³⁵, G. Piacquadio ¹⁴⁶,
 E. Pianori ^{17a}, F. Piazza ¹²⁴, R. Piegai ³⁰, D. Pietreanu ^{27b}, A.D. Pilkington ¹⁰²,
 M. Pinamonti ^{69a,69c}, J.L. Pinfeld ², B.C. Pinheiro Pereira ^{131a}, A.E. Pinto Pinoargote ^{101,136},
 L. Pintucci ^{69a,69c}, K.M. Piper ¹⁴⁷, A. Pirttikoski ⁵⁶, D.A. Pizzi ³⁴, L. Pizzimento ^{64b},
 A. Pizzini ¹¹⁵, M.-A. Pleier ²⁹, V. Plesanovs ⁵⁴, V. Pleskot ¹³⁴, E. Plotnikova ³⁸, G. Poddar ⁴,
 R. Poettgen ⁹⁹, L. Poggioli ¹²⁸, I. Pokharel ⁵⁵, S. Polacek ¹³⁴, G. Polesello ^{73a}, A. Poley ^{143,157a},
 A. Polini ^{23b}, C.S. Pollard ¹⁶⁸, Z.B. Pollock ¹²⁰, E. Pompa Pacchi ^{75a,75b}, D. Ponomarenko ¹¹⁴,
 L. Pontecorvo ³⁶, S. Popa ^{27a}, G.A. Popeneciu ^{27d}, A. Poreba ³⁶, D.M. Portillo Quintero ^{157a},
 S. Pospisil ¹³³, M.A. Postill ¹⁴⁰, P. Postolache ^{27c}, K. Potamianos ¹⁶⁸, P.A. Potepa ^{86a},

I.N. Potrap ³⁸, C.J. Potter ³², H. Potti ¹, T. Poulsen ⁴⁸, J. Poveda ¹⁶⁴, M.E. Pozo Astigarraga ³⁶,
 A. Prades Ibanez ¹⁶⁴, J. Pretel ⁵⁴, D. Price ¹⁰², M. Primavera ^{70a}, M.A. Principe Martin ¹⁰⁰,
 R. Privara ¹²³, T. Procter ⁵⁹, M.L. Proffitt ¹³⁹, N. Proklova ¹²⁹, K. Prokofiev ^{64c}, G. Proto ¹¹¹,
 J. Proudfoot ⁶, M. Przybycien ^{36a}, W.W. Przygoda ^{86b}, A. Psallidas ⁴⁶, J.E. Puddefoot ¹⁴⁰,
 D. Pudzha ³⁷, D. Pyatiizbyantseva ³⁷, J. Qian ¹⁰⁷, D. Qichen ¹⁰², Y. Qin ¹³, T. Qiu ⁵²,
 A. Quadt ⁵⁵, M. Queitsch-Maitland ¹⁰², G. Quetant ⁵⁶, R.P. Quinn ¹⁶⁵, G. Rabanal Bolanos ⁶¹,
 D. Rafanoharana ⁵⁴, F. Ragusa ^{71a,71b}, J.L. Rainbolt ³⁹, J.A. Raine ⁵⁶, S. Rajagopalan ²⁹,
 E. Ramakoti ³⁷, I.A. Ramirez-Berend ³⁴, K. Ran ^{48,14e}, N.P. Rapheeha ^{33g}, H. Rasheed ^{27b},
 V. Raskina ¹²⁸, D.F. Rassloff ^{63a}, A. Rastogi ^{17a}, S. Rave ¹⁰¹, B. Ravina ⁵⁵, I. Ravinovich ¹⁷⁰,
 M. Raymond ³⁶, A.L. Read ¹²⁶, N.P. Readioff ¹⁴⁰, D.M. Rebutzi ^{73a,73b}, G. Redlinger ²⁹,
 A.S. Reed ¹¹¹, K. Reeves ²⁶, J.A. Reidelsturz ¹⁷², D. Reikher ¹⁵², A. Rej ⁴⁹, C. Rembser ³⁶,
 M. Renda ^{27b}, M.B. Rendel ¹¹¹, F. Renner ⁴⁸, A.G. Rennie ¹⁶⁰, A.L. Rescia ⁴⁸, S. Resconi ^{71a},
 M. Ressegotti ^{57b,57a}, S. Rettie ³⁶, J.G. Reyes Rivera ¹⁰⁸, E. Reynolds ^{17a}, O.L. Rezanova ³⁷,
 P. Reznicek ¹³⁴, H. Riani ^{35d}, N. Ribaric ⁹², E. Ricci ^{78a,78b}, R. Richter ¹¹¹, S. Richter ^{47a,47b},
 E. Richter-Was ^{86b}, M. Ridel ¹²⁸, S. Ridouani ^{35d}, P. Rieck ¹¹⁸, P. Riedler ³⁶, E.M. Riefel ^{47a,47b},
 J.O. Rieger ¹¹⁵, M. Rijssenbeek ¹⁴⁶, M. Rimoldi ³⁶, L. Rinaldi ^{23b,23a}, T.T. Rinn ²⁹,
 M.P. Rinnagel ¹¹⁰, G. Ripellino ¹⁶², I. Riu ¹³, J.C. Rivera Vergara ¹⁶⁶, F. Rizatdinova ¹²²,
 E. Rizvi ⁹⁵, B.R. Roberts ^{17a}, S.H. Robertson ^{105,x}, D. Robinson ³², C.M. Robles Gajardo ^{138f},
 M. Robles Manzano ¹⁰¹, A. Robson ⁵⁹, A. Rocchi ^{76a,76b}, C. Roda ^{74a,74b}, S. Rodriguez Bosca ³⁶,
 Y. Rodriguez Garcia ^{22a}, A. Rodriguez Rodriguez ⁵⁴, A.M. Rodriguez Vera ^{157b}, S. Roe ³⁶,
 J.T. Roemer ¹⁶⁰, A.R. Roepe-Gier ¹³⁷, J. Roggel ¹⁷², O. Røhne ¹²⁶, R.A. Rojas ¹⁰⁴,
 C.P.A. Roland ¹²⁸, J. Roloff ²⁹, A. Romaniouk ³⁷, E. Romano ^{73a,73b}, M. Romano ^{23b},
 A.C. Romero Hernandez ¹⁶³, N. Rompotis ⁹³, L. Roos ¹²⁸, S. Rosati ^{75a}, B.J. Rosser ³⁹,
 E. Rossi ¹²⁷, E. Rossi ^{72a,72b}, L.P. Rossi ⁶¹, L. Rossini ⁵⁴, R. Rosten ¹²⁰, M. Rotaru ^{27b},
 B. Rottler ⁵⁴, C. Rougier ⁹⁰, D. Rousseau ⁶⁶, D. Rousoo ³², A. Roy ¹⁶³, S. Roy-Garand ¹⁵⁶,
 A. Rozanov ¹⁰³, Z.M.A. Rozario ⁵⁹, Y. Rozen ¹⁵¹, A. Rubio Jimenez ¹⁶⁴, A.J. Ruby ⁹³,
 V.H. Ruelas Rivera ¹⁸, T.A. Ruggeri ¹, A. Ruggiero ¹²⁷, A. Ruiz-Martinez ¹⁶⁴, A. Rummler ³⁶,
 Z. Rurikova ⁵⁴, N.A. Rusakovich ³⁸, H.L. Russell ¹⁶⁶, G. Russo ^{75a,75b}, J.P. Rutherford ⁷,
 S. Rutherford Colmenares ³², K. Rybacki ⁹², M. Rybar ¹³⁴, E.B. Rye ¹²⁶, A. Ryzhov ⁴⁴,
 J.A. Sabater Iglesias ⁵⁶, P. Sabatini ¹⁶⁴, H.F.W. Sadrozinski ¹³⁷, F. Safai Tehrani ^{75a},
 B. Safarzadeh Samani ¹³⁵, M. Safdari ¹⁴⁴, S. Saha ¹, M. Sahinsoy ¹¹¹, A. Saibel ¹⁶⁴,
 M. Saimpert ¹³⁶, M. Saito ¹⁵⁴, T. Saito ¹⁵⁴, D. Salamani ³⁶, A. Salnikov ¹⁴⁴, J. Salt ¹⁶⁴,
 A. Salvador Salas ¹⁵², D. Salvatore ^{43b,43a}, F. Salvatore ¹⁴⁷, A. Salzburger ³⁶, D. Sammel ⁵⁴,
 E. Sampson ⁹², D. Sampsonidis ^{153,e}, D. Sampsonidou ¹²⁴, J. Sánchez ¹⁶⁴,
 V. Sanchez Sebastian ¹⁶⁴, H. Sandaker ¹²⁶, C.O. Sander ⁴⁸, J.A. Sandesara ¹⁰⁴, M. Sandhoff ¹⁷²,
 C. Sandoval ^{22b}, D.P.C. Sankey ¹³⁵, T. Sano ⁸⁸, A. Sansoni ⁵³, L. Santi ^{75a,75b}, C. Santoni ⁴⁰,
 H. Santos ^{131a,131b}, A. Santra ¹⁷⁰, K.A. Saoucha ¹⁶¹, J.G. Saraiva ^{131a,131d}, J. Sardain ⁷,
 O. Sasaki ⁸⁴, K. Sato ¹⁵⁸, C. Sauer ^{63b}, F. Sauerburger ⁵⁴, E. Sauvan ⁴, P. Savard ^{156,af},
 R. Sawada ¹⁵⁴, C. Sawyer ¹³⁵, L. Sawyer ⁹⁸, I. Sayago Galvan ¹⁶⁴, C. Sbarra ^{23b}, A. Sbrizzi ^{23b,23a},
 T. Scanlon ⁹⁷, J. Schaarschmidt ¹³⁹, U. Schäfer ¹⁰¹, A.C. Schaffer ^{66,44}, D. Schaile ¹¹⁰,
 R.D. Schamberger ¹⁴⁶, C. Scharf ¹⁸, M.M. Schefer ¹⁹, V.A. Schegelsky ³⁷, D. Scheirich ¹³⁴,
 F. Schenck ¹⁸, M. Schernau ¹⁶⁰, C. Scheulen ⁵⁵, C. Schiavi ^{57b,57a}, M. Schioppa ^{43b,43a},
 B. Schlag ^{144,n}, K.E. Schleicher ⁵⁴, S. Schlenker ³⁶, J. Schmeing ¹⁷², M.A. Schmidt ¹⁷²,
 K. Schmieden ¹⁰¹, C. Schmitt ¹⁰¹, N. Schmitt ¹⁰¹, S. Schmitt ⁴⁸, L. Schoeffel ¹³⁶,
 A. Schoening ^{63b}, P.G. Scholer ³⁴, E. Schopf ¹²⁷, M. Schott ¹⁰¹, J. Schovancova ³⁶,
 S. Schramm ⁵⁶, T. Schroer ⁵⁶, H-C. Schultz-Coulon ^{63a}, M. Schumacher ⁵⁴, B.A. Schumm ¹³⁷,
 Ph. Schune ¹³⁶, A.J. Schuy ¹³⁹, H.R. Schwartz ¹³⁷, A. Schwartzman ¹⁴⁴, T.A. Schwarz ¹⁰⁷,

Ph. Schwemling ¹³⁶, R. Schwienhorst ¹⁰⁸, A. Sciandra ¹³⁷, G. Sciolla ²⁶, F. Scuri ^{74a},
 C.D. Sebastiani ⁹³, K. Sedlaczek ¹¹⁶, P. Seema ¹⁸, S.C. Seidel ¹¹³, A. Seiden ¹³⁷,
 B.D. Seidlitz ⁴¹, C. Seitz ⁴⁸, J.M. Seixas ^{83b}, G. Sekhniadze ^{72a}, L. Selem ⁶⁰,
 N. Semprini-Cesari ^{23b,23a}, D. Sengupta ⁵⁶, V. Senthilkumar ¹⁶⁴, L. Serin ⁶⁶, L. Serkin ^{69a,69b},
 M. Sessa ^{76a,76b}, H. Severini ¹²¹, F. Sforza ^{57b,57a}, A. Sfyrla ⁵⁶, Q. Sha ^{14a}, E. Shabalina ⁵⁵,
 R. Shaheen ¹⁴⁵, J.D. Shahinian ¹²⁹, D. Shaked Renous ¹⁷⁰, L.Y. Shan ^{14a}, M. Shapiro ^{17a},
 A. Sharma ³⁶, A.S. Sharma ¹⁶⁵, P. Sharma ⁸⁰, P.B. Shatalov ³⁷, K. Shaw ¹⁴⁷, S.M. Shaw ¹⁰²,
 A. Shcherbakova ³⁷, Q. Shen ^{62c,5}, D.J. Sheppard ¹⁴³, P. Sherwood ⁹⁷, L. Shi ⁹⁷, X. Shi ^{14a},
 C.O. Shimmin ¹⁷³, J.D. Shinner ⁹⁶, I.P.J. Shipsey ¹²⁷, S. Shirabe ⁸⁹, M. Shiyakova ^{38,v},
 J. Shlomi ¹⁷⁰, M.J. Shochet ³⁹, J. Shojaii ¹⁰⁶, D.R. Shope ¹²⁶, B. Shrestha ¹²¹, S. Shrestha ^{120,ai},
 E.M. Shrif ^{33g}, M.J. Shroff ¹⁶⁶, P. Sicho ¹³², A.M. Sickles ¹⁶³, E. Sideras Haddad ^{33g},
 A. Sidoti ^{23b}, F. Siegert ⁵⁰, Dj. Sijacki ¹⁵, F. Sili ⁹¹, J.M. Silva ⁵², M.V. Silva Oliveira ²⁹,
 S.B. Silverstein ^{47a}, S. Simion ⁶⁶, R. Simoniello ³⁶, E.L. Simpson ⁵⁹, H. Simpson ¹⁴⁷,
 L.R. Simpson ¹⁰⁷, N.D. Simpson ⁹⁹, S. Simsek ⁸², S. Sindhu ⁵⁵, P. Sinervo ¹⁵⁶, S. Singh ¹⁵⁶,
 S. Sinha ⁴⁸, S. Sinha ¹⁰², M. Sioli ^{23b,23a}, I. Siral ³⁶, E. Sitnikova ⁴⁸, J. Sjölin ^{47a,47b},
 A. Skaf ⁵⁵, E. Skorda ²⁰, P. Skubic ¹²¹, M. Slawinska ⁸⁷, V. Smakhtin ¹⁷⁰, B.H. Smart ¹³⁵,
 S.Yu. Smirnov ³⁷, Y. Smirnov ³⁷, L.N. Smirnova ^{37,a}, O. Smirnova ⁹⁹, A.C. Smith ⁴¹,
 E.A. Smith ³⁹, H.A. Smith ¹²⁷, J.L. Smith ⁹³, R. Smith ¹⁴⁴, M. Smizanska ⁹², K. Smolek ¹³³,
 A.A. Snesarev ³⁷, S.R. Snider ¹⁵⁶, H.L. Snoek ¹¹⁵, S. Snyder ²⁹, R. Sobie ^{166,x}, A. Soffer ¹⁵²,
 C.A. Solans Sanchez ³⁶, E.Yu. Soldatov ³⁷, U. Soldevila ¹⁶⁴, A.A. Solodkov ³⁷, S. Solomon ²⁶,
 A. Soloshenko ³⁸, K. Solovieva ⁵⁴, O.V. Solovyanov ⁴⁰, V. Solovyev ³⁷, P. Sommer ³⁶,
 A. Sonay ¹³, W.Y. Song ^{157b}, A. Sopczak ¹³³, A.L. Soppio ⁹⁷, F. Sopkova ^{28b}, J.D. Sorenson ¹¹³,
 I.R. Sotarriva Alvarez ¹⁵⁵, V. Sothilingam ^{63a}, O.J. Soto Sandoval ^{138c,138b}, S. Sottocornola ⁶⁸,
 R. Soualah ¹⁶¹, Z. Soumami ^{35e}, D. South ⁴⁸, N. Soybelman ¹⁷⁰, S. Spagnolo ^{70a,70b},
 M. Spalla ¹¹¹, D. Sperlich ⁵⁴, G. Spigo ³⁶, S. Spinali ⁹², D.P. Spiteri ⁵⁹, M. Spousta ¹³⁴,
 E.J. Staats ³⁴, R. Stamen ^{63a}, A. Stampekis ²⁰, M. Standke ²⁴, E. Stanecka ⁸⁷, M.V. Stange ⁵⁰,
 B. Stanislaus ^{17a}, M.M. Stanitzki ⁴⁸, B. Stapf ⁴⁸, E.A. Starchenko ³⁷, G.H. Stark ¹³⁷, J. Stark ⁹⁰,
 P. Staroba ¹³², P. Starovoitov ^{63a}, S. Stärz ¹⁰⁵, R. Staszewski ⁸⁷, G. Stavropoulos ⁴⁶,
 J. Steentoft ¹⁶², P. Steinberg ²⁹, B. Stelzer ^{143,157a}, H.J. Stelzer ¹³⁰, O. Stelzer-Chilton ^{157a},
 H. Stenzel ⁵⁸, T.J. Stevenson ¹⁴⁷, G.A. Stewart ³⁶, J.R. Stewart ¹²², M.C. Stockton ³⁶,
 G. Stoicea ^{27b}, M. Stolarski ^{131a}, S. Stonjek ¹¹¹, A. Straessner ⁵⁰, J. Strandberg ¹⁴⁵,
 S. Strandberg ^{47a,47b}, M. Stratmann ¹⁷², M. Strauss ¹²¹, T. Strebler ¹⁰³, P. Strizenec ^{28b},
 R. Ströhmer ¹⁶⁷, D.M. Strom ¹²⁴, R. Stroynowski ⁴⁴, A. Strubig ^{47a,47b}, S.A. Stucci ²⁹,
 B. Stugu ¹⁶, J. Stupak ¹²¹, N.A. Styles ⁴⁸, D. Su ¹⁴⁴, S. Su ^{62a}, W. Su ^{62d}, X. Su ^{62a},
 D. Suchy ^{28a}, K. Sugizaki ¹⁵⁴, V.V. Sulim ³⁷, M.J. Sullivan ⁹³, D.M.S. Sultan ¹²⁷,
 L. Sultanaliyeva ³⁷, S. Sultansoy ^{3b}, T. Sumida ⁸⁸, S. Sun ¹⁰⁷, S. Sun ¹⁷¹,
 O. Sunneborn Gudnadottir ¹⁶², N. Sur ¹⁰³, M.R. Sutton ¹⁴⁷, H. Suzuki ¹⁵⁸, M. Svatos ¹³²,
 M. Swiatlowski ^{157a}, T. Swirski ¹⁶⁷, I. Sykora ^{28a}, M. Sykora ¹³⁴, T. Sykora ¹³⁴, D. Ta ¹⁰¹,
 K. Tackmann ^{48,u}, A. Taffard ¹⁶⁰, R. Tafirout ^{157a}, J.S. Tafoya Vargas ⁶⁶, Y. Takubo ⁸⁴,
 M. Talby ¹⁰³, A.A. Talyshev ³⁷, K.C. Tam ^{64b}, N.M. Tamir ¹⁵², A. Tanaka ¹⁵⁴, J. Tanaka ¹⁵⁴,
 R. Tanaka ⁶⁶, M. Tanasini ^{57b,57a}, Z. Tao ¹⁶⁵, S. Tapia Araya ^{138f}, S. Tapprogge ¹⁰¹,
 A. Tarek Abouelfadl Mohamed ¹⁰⁸, S. Tarem ¹⁵¹, K. Tariq ^{14a}, G. Tarna ^{103,27b}, G.F. Tartarelli ^{71a},
 P. Tas ¹³⁴, M. Tasevsky ¹³², E. Tassi ^{43b,43a}, A.C. Tate ¹⁶³, G. Tateno ¹⁵⁴, Y. Tayalati ^{35e,w},
 G.N. Taylor ¹⁰⁶, W. Taylor ^{157b}, A.S. Tee ¹⁷¹, R. Teixeira De Lima ¹⁴⁴, P. Teixeira-Dias ⁹⁶,
 J.J. Teoh ¹⁵⁶, K. Terashi ¹⁵⁴, J. Terron ¹⁰⁰, S. Terzo ¹³, M. Testa ⁵³, R.J. Teuscher ^{156,x},
 A. Thaler ⁷⁹, O. Theiner ⁵⁶, N. Themistokleous ⁵², T. Thevenaux-Pelzer ¹⁰³, O. Thielmann ¹⁷²,
 D.W. Thomas ⁹⁶, J.P. Thomas ²⁰, E.A. Thompson ^{17a}, P.D. Thompson ²⁰, E. Thomson ¹²⁹,

R.E. Thornberry⁴⁴, Y. Tian⁵⁵, V. Tikhomirov^{37,a}, Yu.A. Tikhonov³⁷, S. Timoshenko³⁷, D. Timoshyn¹³⁴, E.X.L. Ting¹, P. Tipton¹⁷³, S.H. Tlou^{33g}, A. Tnourji⁴⁰, K. Todome¹⁵⁵, S. Todorova-Nova¹³⁴, S. Todt⁵⁰, M. Togawa⁸⁴, J. Tojo⁸⁹, S. Tokár^{28a}, K. Tokushuku⁸⁴, O. Toldaiev⁶⁸, R. Tombs³², M. Tomoto^{84,112}, L. Tompkins^{144,n}, K.W. Topolnicki^{86b}, E. Torrence¹²⁴, H. Torres⁹⁰, E. Torró Pastor¹⁶⁴, M. Toscani³⁰, C. Tosciri³⁹, M. Tost¹¹, D.R. Tovey¹⁴⁰, A. Traeet¹⁶, I.S. Trandafir^{27b}, T. Trefzger¹⁶⁷, A. Tricoli²⁹, I.M. Trigger^{157a}, S. Trincaz-Duvoid¹²⁸, D.A. Trischuk²⁶, B. Trocmé⁶⁰, L. Truong^{33c}, M. Trzebinski⁸⁷, A. Trzupek⁸⁷, F. Tsai¹⁴⁶, M. Tsai¹⁰⁷, A. Tsiamis^{153,e}, P.V. Tsiareshka³⁷, S. Tsigaridas^{157a}, A. Tsirigotis^{153,s}, V. Tsiskaridze¹⁵⁶, E.G. Tskhadadze^{150a}, M. Tsopoulou¹⁵³, Y. Tsujikawa⁸⁸, I.I. Tsukerman³⁷, V. Tsulaia^{17a}, S. Tsuno⁸⁴, K. Tsuru¹¹⁹, D. Tsybychev¹⁴⁶, Y. Tu^{64b}, A. Tudorache^{27b}, V. Tudorache^{27b}, A.N. Tuna⁶¹, S. Turchikhin^{57b,57a}, I. Turk Cakir^{3a}, R. Turra^{71a}, T. Turtuvshin^{38,y}, P.M. Tuts⁴¹, S. Tzamarias^{153,e}, P. Tzanis¹⁰, E. Tzovara¹⁰¹, F. Ukegawa¹⁵⁸, P.A. Ulloa Poblete^{138c,138b}, E.N. Umaka²⁹, G. Unal³⁶, M. Unal¹¹, A. Undrus²⁹, G. Unel¹⁶⁰, J. Urban^{28b}, P. Urquijo¹⁰⁶, P. Urrejola^{138a}, G. Usai⁸, R. Ushioda¹⁵⁵, M. Usman¹⁰⁹, Z. Uysal⁸², V. Vacek¹³³, B. Vachon¹⁰⁵, K.O.H. Vadla¹²⁶, T. Vafeiadis³⁶, A. Vaitkus⁹⁷, C. Valderanis¹¹⁰, E. Valdes Santurio^{47a,47b}, M. Valente^{157a}, S. Valentinetti^{23b,23a}, A. Valero¹⁶⁴, E. Valiente Moreno¹⁶⁴, A. Vallier⁹⁰, J.A. Valls Ferrer¹⁶⁴, D.R. Van Arneman¹¹⁵, T.R. Van Daalen¹³⁹, A. Van Der Graaf⁴⁹, P. Van Gemmeren⁶, M. Van Rijnbach¹²⁶, S. Van Stroud⁹⁷, I. Van Vulpen¹¹⁵, P. Vana¹³⁴, M. Vanadia^{76a,76b}, W. Vandelli³⁶, E.R. Vandewall¹²², D. Vannicola¹⁵², L. Vannoli^{57b,57a}, R. Vari^{75a}, E.W. Varnes⁷, C. Varni^{17b}, T. Varol¹⁴⁹, D. Varouchas⁶⁶, L. Varriale¹⁶⁴, K.E. Varvell¹⁴⁸, M.E. Vasile^{27b}, L. Vaslin⁸⁴, G.A. Vasquez¹⁶⁶, A. Vasyukov³⁸, R. Vavricka¹⁰¹, F. Vazeille⁴⁰, T. Vazquez Schroeder³⁶, J. Veatch³¹, V. Vecchio¹⁰², M.J. Veen¹⁰⁴, I. Veliscek²⁹, L.M. Veloce¹⁵⁶, F. Veloso^{131a,131c}, S. Veneziano^{75a}, A. Ventura^{70a,70b}, S. Ventura Gonzalez¹³⁶, A. Verbytskyi¹¹¹, M. Verducci^{74a,74b}, C. Vergis²⁴, M. Verissimo De Araujo^{83b}, W. Verkerke¹¹⁵, J.C. Vermeulen¹¹⁵, C. Vernieri¹⁴⁴, M. Vessella¹⁰⁴, M.C. Vetterli^{143,af}, A. Vgenopoulos^{153,e}, N. Viaux Maira^{138f}, T. Vickey¹⁴⁰, O.E. Vickey Boeriu¹⁴⁰, G.H.A. Viehhauser¹²⁷, L. Vigani^{63b}, M. Villa^{23b,23a}, M. Villaplana Perez¹⁶⁴, E.M. Villhauer⁵², E. Vilucchi⁵³, M.G. Vincter³⁴, G.S. Virdee²⁰, A. Vishwakarma⁵², A. Visibile¹¹⁵, C. Vittori³⁶, I. Vivarelli^{23b,23a}, E. Voevodina¹¹¹, F. Vogel¹¹⁰, J.C. Voigt⁵⁰, P. Vokac¹³³, Yu. Volkotrub^{86a}, J. Von Ahnen⁴⁸, E. Von Toerne²⁴, B. Vormwald³⁶, V. Vorobel¹³⁴, K. Vorobev³⁷, M. Vos¹⁶⁴, K. Voss¹⁴², M. Vozak¹¹⁵, L. Vozdecky¹²¹, N. Vranjes¹⁵, M. Vranjes Milosavljevic¹⁵, M. Vreeswijk¹¹⁵, N.K. Vu^{62d,62c}, R. Vuillermet³⁶, O. Vujanovic¹⁰¹, I. Vukotic³⁹, S. Wada¹⁵⁸, C. Wagner¹⁰⁴, J.M. Wagner^{17a}, W. Wagner¹⁷², S. Wahdan¹⁷², H. Wahlberg⁹¹, M. Wakida¹¹², J. Walder¹³⁵, R. Walker¹¹⁰, W. Walkowiak¹⁴², A. Wall¹²⁹, E.J. Wallin⁹⁹, T. Wamorkar⁶, A.Z. Wang¹³⁷, C. Wang¹⁰¹, C. Wang¹¹, H. Wang^{17a}, J. Wang^{64c}, R.-J. Wang¹⁰¹, R. Wang⁶¹, R. Wang⁶, S.M. Wang¹⁴⁹, S. Wang^{62b}, T. Wang^{62a}, W.T. Wang⁸⁰, W. Wang^{14a}, X. Wang^{14c}, X. Wang¹⁶³, X. Wang^{62c}, Y. Wang^{62d}, Y. Wang^{14c}, Z. Wang¹⁰⁷, Z. Wang^{62d,51,62c}, Z. Wang¹⁰⁷, A. Warburton¹⁰⁵, R.J. Ward²⁰, N. Warrack⁵⁹, S. Waterhouse⁹⁶, A.T. Watson²⁰, H. Watson⁵⁹, M.F. Watson²⁰, E. Watton^{59,135}, G. Watts¹³⁹, B.M. Waugh⁹⁷, C. Weber²⁹, H.A. Weber¹⁸, M.S. Weber¹⁹, S.M. Weber^{63a}, C. Wei^{62a}, Y. Wei¹²⁷, A.R. Weidberg¹²⁷, E.J. Weik¹¹⁸, J. Weingarten⁴⁹, M. Weirich¹⁰¹, C. Weiser⁵⁴, C.J. Wells⁴⁸, T. Wenaus²⁹, B. Wendland⁴⁹, T. Wengler³⁶, N.S. Wenke¹¹¹, N. Wermes²⁴, M. Wessels^{63a}, A.M. Wharton⁹², A.S. White⁶¹, A. White⁸, M.J. White¹, D. Whiteson¹⁶⁰, L. Wickremasinghe¹²⁵, W. Wiedenmann¹⁷¹, M. Wielers¹³⁵, C. Wiglesworth⁴², D.J. Wilbern¹²¹, H.G. Wilkens³⁶, D.M. Williams⁴¹, H.H. Williams¹²⁹, S. Williams³², S. Willocq¹⁰⁴, B.J. Wilson¹⁰², P.J. Windischhofer³⁹, F.I. Winkel³⁰,

F. Winklmeier ¹²⁴, B.T. Winter ⁵⁴, J.K. Winter ¹⁰², M. Wittgen ¹⁴⁴, M. Wobisch ⁹⁸, Z. Wolffs ¹¹⁵, J. Wollrath ¹⁶⁰, M.W. Wolter ⁸⁷, H. Wolters ^{131a,131c}, M.C. Wong ¹³⁷, E.L. Woodward ⁴¹, S.D. Worm ⁴⁸, B.K. Wosiek ⁸⁷, K.W. Woźniak ⁸⁷, S. Wozniowski ⁵⁵, K. Wraight ⁵⁹, C. Wu ²⁰, M. Wu ^{14d}, M. Wu ¹¹⁴, S.L. Wu ¹⁷¹, X. Wu ⁵⁶, Y. Wu ^{62a}, Z. Wu ¹³⁶, J. Wuerzinger ^{111,ad}, T.R. Wyatt ¹⁰², B.M. Wynne ⁵², S. Xella ⁴², L. Xia ^{14c}, M. Xia ^{14b}, J. Xiang ^{64c}, M. Xie ^{62a}, X. Xie ^{62a}, S. Xin ^{14a,14e}, A. Xiong ¹²⁴, J. Xiong ^{17a}, D. Xu ^{14a}, H. Xu ^{62a}, L. Xu ^{62a}, R. Xu ¹²⁹, T. Xu ¹⁰⁷, Y. Xu ^{14b}, Z. Xu ⁵², Z. Xu ^{14c}, B. Yabsley ¹⁴⁸, S. Yacoob ^{33a}, Y. Yamaguchi ¹⁵⁵, E. Yamashita ¹⁵⁴, H. Yamauchi ¹⁵⁸, T. Yamazaki ^{17a}, Y. Yamazaki ⁸⁵, J. Yan ^{62c}, S. Yan ⁵⁹, Z. Yan ¹⁰⁴, H.J. Yang ^{62c,62d}, H.T. Yang ^{62a}, S. Yang ^{62a}, T. Yang ^{64c}, X. Yang ³⁶, X. Yang ^{14a}, Y. Yang ⁴⁴, Y. Yang ^{62a}, Z. Yang ^{62a}, W-M. Yao ^{17a}, H. Ye ^{14c}, H. Ye ⁵⁵, J. Ye ^{14a}, S. Ye ²⁹, X. Ye ^{62a}, Y. Yeh ⁹⁷, I. Yeletsikh ³⁸, B.K. Yeo ^{17b}, M.R. Yexley ⁹⁷, P. Yin ⁴¹, K. Yorita ¹⁶⁹, S. Younas ^{27b}, C.J.S. Young ³⁶, C. Young ¹⁴⁴, C. Yu ^{14a,14e}, Y. Yu ^{62a}, M. Yuan ¹⁰⁷, R. Yuan ^{62b}, L. Yue ⁹⁷, M. Zaazoua ^{62a}, B. Zabinski ⁸⁷, E. Zaid ⁵², Z.K. Zak ⁸⁷, T. Zakareishvili ¹⁶⁴, N. Zakharchuk ³⁴, S. Zambito ⁵⁶, J.A. Zamora Saa ^{138d,138b}, J. Zang ¹⁵⁴, D. Zanzi ⁵⁴, O. Zaplatilek ¹³³, C. Zeitnitz ¹⁷², H. Zeng ^{14a}, J.C. Zeng ¹⁶³, D.T. Zenger Jr ²⁶, O. Zenin ³⁷, T. Ženiš ^{28a}, S. Zenz ⁹⁵, S. Zerradi ^{35a}, D. Zerwas ⁶⁶, M. Zhai ^{14a,14e}, D.F. Zhang ¹⁴⁰, J. Zhang ^{62b}, J. Zhang ⁶, K. Zhang ^{14a,14e}, L. Zhang ^{14c}, P. Zhang ^{14a,14e}, R. Zhang ¹⁷¹, S. Zhang ¹⁰⁷, S. Zhang ⁴⁴, T. Zhang ¹⁵⁴, X. Zhang ^{62c}, X. Zhang ^{62b}, Y. Zhang ^{62c,5}, Y. Zhang ⁹⁷, Y. Zhang ^{14c}, Z. Zhang ^{17a}, Z. Zhang ⁶⁶, H. Zhao ¹³⁹, T. Zhao ^{62b}, Y. Zhao ¹³⁷, Z. Zhao ^{62a}, A. Zhemchugov ³⁸, J. Zheng ^{14c}, K. Zheng ¹⁶³, X. Zheng ^{62a}, Z. Zheng ¹⁴⁴, D. Zhong ¹⁶³, B. Zhou ¹⁰⁷, H. Zhou ⁷, N. Zhou ^{62c}, Y. Zhou ^{14c}, Y. Zhou ⁷, C.G. Zhu ^{62b}, J. Zhu ¹⁰⁷, Y. Zhu ^{62c}, Y. Zhu ^{62a}, X. Zhuang ^{14a}, K. Zhukov ³⁷, N.I. Zimine ³⁸, J. Zinsser ^{63b}, M. Ziolkowski ¹⁴², L. Živković ¹⁵, A. Zoccoli ^{23b,23a}, K. Zoch ⁶¹, T.G. Zorbas ¹⁴⁰, O. Zormpa ⁴⁶, W. Zou ⁴¹, L. Zwalinski ³⁶.

¹Department of Physics, University of Adelaide, Adelaide; Australia.

²Department of Physics, University of Alberta, Edmonton AB; Canada.

³(^a)Department of Physics, Ankara University, Ankara; (^b)Division of Physics, TOBB University of Economics and Technology, Ankara; Türkiye.

⁴LAPP, Université Savoie Mont Blanc, CNRS/IN2P3, Annecy; France.

⁵APC, Université Paris Cité, CNRS/IN2P3, Paris; France.

⁶High Energy Physics Division, Argonne National Laboratory, Argonne IL; United States of America.

⁷Department of Physics, University of Arizona, Tucson AZ; United States of America.

⁸Department of Physics, University of Texas at Arlington, Arlington TX; United States of America.

⁹Physics Department, National and Kapodistrian University of Athens, Athens; Greece.

¹⁰Physics Department, National Technical University of Athens, Zografou; Greece.

¹¹Department of Physics, University of Texas at Austin, Austin TX; United States of America.

¹²Institute of Physics, Azerbaijan Academy of Sciences, Baku; Azerbaijan.

¹³Institut de Física d'Altes Energies (IFAE), Barcelona Institute of Science and Technology, Barcelona; Spain.

¹⁴(^a)Institute of High Energy Physics, Chinese Academy of Sciences, Beijing; (^b)Physics Department, Tsinghua University, Beijing; (^c)Department of Physics, Nanjing University, Nanjing; (^d)School of Science, Shenzhen Campus of Sun Yat-sen University; (^e)University of Chinese Academy of Science (UCAS), Beijing; China.

¹⁵Institute of Physics, University of Belgrade, Belgrade; Serbia.

¹⁶Department for Physics and Technology, University of Bergen, Bergen; Norway.

¹⁷(^a)Physics Division, Lawrence Berkeley National Laboratory, Berkeley CA; (^b)University of California,

Berkeley CA; United States of America.

¹⁸Institut für Physik, Humboldt Universität zu Berlin, Berlin; Germany.

¹⁹Albert Einstein Center for Fundamental Physics and Laboratory for High Energy Physics, University of Bern, Bern; Switzerland.

²⁰School of Physics and Astronomy, University of Birmingham, Birmingham; United Kingdom.

²¹(^a)Department of Physics, Bogazici University, Istanbul; (^b)Department of Physics Engineering, Gaziantep University, Gaziantep; (^c)Department of Physics, Istanbul University, Istanbul; Türkiye.

²²(^a)Facultad de Ciencias y Centro de Investigaciones, Universidad Antonio Nariño,

Bogotá; (^b)Departamento de Física, Universidad Nacional de Colombia, Bogotá; Colombia.

²³(^a)Dipartimento di Fisica e Astronomia A. Righi, Università di Bologna, Bologna; (^b)INFN Sezione di Bologna; Italy.

²⁴Physikalisches Institut, Universität Bonn, Bonn; Germany.

²⁵Department of Physics, Boston University, Boston MA; United States of America.

²⁶Department of Physics, Brandeis University, Waltham MA; United States of America.

²⁷(^a)Transilvania University of Brasov, Brasov; (^b)Horia Hulubei National Institute of Physics and Nuclear Engineering, Bucharest; (^c)Department of Physics, Alexandru Ioan Cuza University of Iasi, Iasi; (^d)National Institute for Research and Development of Isotopic and Molecular Technologies, Physics Department, Cluj-Napoca; (^e)University Politehnica Bucharest, Bucharest; (^f)West University in Timisoara, Timisoara; (^g)Faculty of Physics, University of Bucharest, Bucharest; Romania.

²⁸(^a)Faculty of Mathematics, Physics and Informatics, Comenius University, Bratislava; (^b)Department of Subnuclear Physics, Institute of Experimental Physics of the Slovak Academy of Sciences, Kosice; Slovak Republic.

²⁹Physics Department, Brookhaven National Laboratory, Upton NY; United States of America.

³⁰Universidad de Buenos Aires, Facultad de Ciencias Exactas y Naturales, Departamento de Física, y CONICET, Instituto de Física de Buenos Aires (IFIBA), Buenos Aires; Argentina.

³¹California State University, CA; United States of America.

³²Cavendish Laboratory, University of Cambridge, Cambridge; United Kingdom.

³³(^a)Department of Physics, University of Cape Town, Cape Town; (^b)iThemba Labs, Western Cape; (^c)Department of Mechanical Engineering Science, University of Johannesburg,

Johannesburg; (^d)National Institute of Physics, University of the Philippines Diliman

(Philippines); (^e)University of South Africa, Department of Physics, Pretoria; (^f)University of Zululand, KwaDlangezwa; (^g)School of Physics, University of the Witwatersrand, Johannesburg; South Africa.

³⁴Department of Physics, Carleton University, Ottawa ON; Canada.

³⁵(^a)Faculté des Sciences Ain Chock, Réseau Universitaire de Physique des Hautes Energies - Université Hassan II, Casablanca; (^b)Faculté des Sciences, Université Ibn-Tofail, Kénitra; (^c)Faculté des Sciences Semlalia, Université Cadi Ayyad, LPHEA-Marrakech; (^d)LPMR, Faculté des Sciences, Université Mohamed Premier, Oujda; (^e)Faculté des sciences, Université Mohammed V, Rabat; (^f)Institute of Applied Physics, Mohammed VI Polytechnic University, Ben Guerir; Morocco.

³⁶CERN, Geneva; Switzerland.

³⁷Affiliated with an institute covered by a cooperation agreement with CERN.

³⁸Affiliated with an international laboratory covered by a cooperation agreement with CERN.

³⁹Enrico Fermi Institute, University of Chicago, Chicago IL; United States of America.

⁴⁰LPC, Université Clermont Auvergne, CNRS/IN2P3, Clermont-Ferrand; France.

⁴¹Nevis Laboratory, Columbia University, Irvington NY; United States of America.

⁴²Niels Bohr Institute, University of Copenhagen, Copenhagen; Denmark.

⁴³(^a)Dipartimento di Fisica, Università della Calabria, Rende; (^b)INFN Gruppo Collegato di Cosenza, Laboratori Nazionali di Frascati; Italy.

- ⁴⁴Physics Department, Southern Methodist University, Dallas TX; United States of America.
- ⁴⁵Physics Department, University of Texas at Dallas, Richardson TX; United States of America.
- ⁴⁶National Centre for Scientific Research "Demokritos", Agia Paraskevi; Greece.
- ⁴⁷(^a) Department of Physics, Stockholm University; (^b) Oskar Klein Centre, Stockholm; Sweden.
- ⁴⁸Deutsches Elektronen-Synchrotron DESY, Hamburg and Zeuthen; Germany.
- ⁴⁹Fakultät Physik, Technische Universität Dortmund, Dortmund; Germany.
- ⁵⁰Institut für Kern- und Teilchenphysik, Technische Universität Dresden, Dresden; Germany.
- ⁵¹Department of Physics, Duke University, Durham NC; United States of America.
- ⁵²SUPA - School of Physics and Astronomy, University of Edinburgh, Edinburgh; United Kingdom.
- ⁵³INFN e Laboratori Nazionali di Frascati, Frascati; Italy.
- ⁵⁴Physikalisches Institut, Albert-Ludwigs-Universität Freiburg, Freiburg; Germany.
- ⁵⁵II. Physikalisches Institut, Georg-August-Universität Göttingen, Göttingen; Germany.
- ⁵⁶Département de Physique Nucléaire et Corpusculaire, Université de Genève, Genève; Switzerland.
- ⁵⁷(^a) Dipartimento di Fisica, Università di Genova, Genova; (^b) INFN Sezione di Genova; Italy.
- ⁵⁸II. Physikalisches Institut, Justus-Liebig-Universität Giessen, Giessen; Germany.
- ⁵⁹SUPA - School of Physics and Astronomy, University of Glasgow, Glasgow; United Kingdom.
- ⁶⁰LPSC, Université Grenoble Alpes, CNRS/IN2P3, Grenoble INP, Grenoble; France.
- ⁶¹Laboratory for Particle Physics and Cosmology, Harvard University, Cambridge MA; United States of America.
- ⁶²(^a) Department of Modern Physics and State Key Laboratory of Particle Detection and Electronics, University of Science and Technology of China, Hefei; (^b) Institute of Frontier and Interdisciplinary Science and Key Laboratory of Particle Physics and Particle Irradiation (MOE), Shandong University, Qingdao; (^c) School of Physics and Astronomy, Shanghai Jiao Tong University, Key Laboratory for Particle Astrophysics and Cosmology (MOE), SKLPPC, Shanghai; (^d) Tsung-Dao Lee Institute, Shanghai; (^e) School of Physics and Microelectronics, Zhengzhou University; China.
- ⁶³(^a) Kirchhoff-Institut für Physik, Ruprecht-Karls-Universität Heidelberg, Heidelberg; (^b) Physikalisches Institut, Ruprecht-Karls-Universität Heidelberg, Heidelberg; Germany.
- ⁶⁴(^a) Department of Physics, Chinese University of Hong Kong, Shatin, N.T., Hong Kong; (^b) Department of Physics, University of Hong Kong, Hong Kong; (^c) Department of Physics and Institute for Advanced Study, Hong Kong University of Science and Technology, Clear Water Bay, Kowloon, Hong Kong; China.
- ⁶⁵Department of Physics, National Tsing Hua University, Hsinchu; Taiwan.
- ⁶⁶IJCLab, Université Paris-Saclay, CNRS/IN2P3, 91405, Orsay; France.
- ⁶⁷Centro Nacional de Microelectrónica (IMB-CNM-CSIC), Barcelona; Spain.
- ⁶⁸Department of Physics, Indiana University, Bloomington IN; United States of America.
- ⁶⁹(^a) INFN Gruppo Collegato di Udine, Sezione di Trieste, Udine; (^b) ICTP, Trieste; (^c) Dipartimento Politecnico di Ingegneria e Architettura, Università di Udine, Udine; Italy.
- ⁷⁰(^a) INFN Sezione di Lecce; (^b) Dipartimento di Matematica e Fisica, Università del Salento, Lecce; Italy.
- ⁷¹(^a) INFN Sezione di Milano; (^b) Dipartimento di Fisica, Università di Milano, Milano; Italy.
- ⁷²(^a) INFN Sezione di Napoli; (^b) Dipartimento di Fisica, Università di Napoli, Napoli; Italy.
- ⁷³(^a) INFN Sezione di Pavia; (^b) Dipartimento di Fisica, Università di Pavia, Pavia; Italy.
- ⁷⁴(^a) INFN Sezione di Pisa; (^b) Dipartimento di Fisica E. Fermi, Università di Pisa, Pisa; Italy.
- ⁷⁵(^a) INFN Sezione di Roma; (^b) Dipartimento di Fisica, Sapienza Università di Roma, Roma; Italy.
- ⁷⁶(^a) INFN Sezione di Roma Tor Vergata; (^b) Dipartimento di Fisica, Università di Roma Tor Vergata, Roma; Italy.
- ⁷⁷(^a) INFN Sezione di Roma Tre; (^b) Dipartimento di Matematica e Fisica, Università Roma Tre, Roma; Italy.
- ⁷⁸(^a) INFN-TIFPA; (^b) Università degli Studi di Trento, Trento; Italy.

- ⁷⁹Universität Innsbruck, Department of Astro and Particle Physics, Innsbruck; Austria.
- ⁸⁰University of Iowa, Iowa City IA; United States of America.
- ⁸¹Department of Physics and Astronomy, Iowa State University, Ames IA; United States of America.
- ⁸²Istinye University, Sariyer, Istanbul; Türkiye.
- ⁸³(^a) Departamento de Engenharia Elétrica, Universidade Federal de Juiz de Fora (UFJF), Juiz de Fora; (^b) Universidade Federal do Rio De Janeiro COPPE/EE/IF, Rio de Janeiro; (^c) Instituto de Física, Universidade de São Paulo, São Paulo; (^d) Rio de Janeiro State University, Rio de Janeiro; (^e) Federal University of Bahia, Bahia; Brazil.
- ⁸⁴KEK, High Energy Accelerator Research Organization, Tsukuba; Japan.
- ⁸⁵Graduate School of Science, Kobe University, Kobe; Japan.
- ⁸⁶(^a) AGH University of Krakow, Faculty of Physics and Applied Computer Science, Krakow; (^b) Marian Smoluchowski Institute of Physics, Jagiellonian University, Krakow; Poland.
- ⁸⁷Institute of Nuclear Physics Polish Academy of Sciences, Krakow; Poland.
- ⁸⁸Faculty of Science, Kyoto University, Kyoto; Japan.
- ⁸⁹Research Center for Advanced Particle Physics and Department of Physics, Kyushu University, Fukuoka ; Japan.
- ⁹⁰L2IT, Université de Toulouse, CNRS/IN2P3, UPS, Toulouse; France.
- ⁹¹Instituto de Física La Plata, Universidad Nacional de La Plata and CONICET, La Plata; Argentina.
- ⁹²Physics Department, Lancaster University, Lancaster; United Kingdom.
- ⁹³Oliver Lodge Laboratory, University of Liverpool, Liverpool; United Kingdom.
- ⁹⁴Department of Experimental Particle Physics, Jožef Stefan Institute and Department of Physics, University of Ljubljana, Ljubljana; Slovenia.
- ⁹⁵School of Physics and Astronomy, Queen Mary University of London, London; United Kingdom.
- ⁹⁶Department of Physics, Royal Holloway University of London, Egham; United Kingdom.
- ⁹⁷Department of Physics and Astronomy, University College London, London; United Kingdom.
- ⁹⁸Louisiana Tech University, Ruston LA; United States of America.
- ⁹⁹Fysiska institutionen, Lunds universitet, Lund; Sweden.
- ¹⁰⁰Departamento de Física Teórica C-15 and CIAFF, Universidad Autónoma de Madrid, Madrid; Spain.
- ¹⁰¹Institut für Physik, Universität Mainz, Mainz; Germany.
- ¹⁰²School of Physics and Astronomy, University of Manchester, Manchester; United Kingdom.
- ¹⁰³CPPM, Aix-Marseille Université, CNRS/IN2P3, Marseille; France.
- ¹⁰⁴Department of Physics, University of Massachusetts, Amherst MA; United States of America.
- ¹⁰⁵Department of Physics, McGill University, Montreal QC; Canada.
- ¹⁰⁶School of Physics, University of Melbourne, Victoria; Australia.
- ¹⁰⁷Department of Physics, University of Michigan, Ann Arbor MI; United States of America.
- ¹⁰⁸Department of Physics and Astronomy, Michigan State University, East Lansing MI; United States of America.
- ¹⁰⁹Group of Particle Physics, University of Montreal, Montreal QC; Canada.
- ¹¹⁰Fakultät für Physik, Ludwig-Maximilians-Universität München, München; Germany.
- ¹¹¹Max-Planck-Institut für Physik (Werner-Heisenberg-Institut), München; Germany.
- ¹¹²Graduate School of Science and Kobayashi-Maskawa Institute, Nagoya University, Nagoya; Japan.
- ¹¹³Department of Physics and Astronomy, University of New Mexico, Albuquerque NM; United States of America.
- ¹¹⁴Institute for Mathematics, Astrophysics and Particle Physics, Radboud University/Nikhef, Nijmegen; Netherlands.
- ¹¹⁵Nikhef National Institute for Subatomic Physics and University of Amsterdam, Amsterdam; Netherlands.

- ¹¹⁶Department of Physics, Northern Illinois University, DeKalb IL; United States of America.
- ¹¹⁷^(a)New York University Abu Dhabi, Abu Dhabi;^(b)United Arab Emirates University, Al Ain; United Arab Emirates.
- ¹¹⁸Department of Physics, New York University, New York NY; United States of America.
- ¹¹⁹Ochanomizu University, Otsuka, Bunkyo-ku, Tokyo; Japan.
- ¹²⁰Ohio State University, Columbus OH; United States of America.
- ¹²¹Homer L. Dodge Department of Physics and Astronomy, University of Oklahoma, Norman OK; United States of America.
- ¹²²Department of Physics, Oklahoma State University, Stillwater OK; United States of America.
- ¹²³Palacký University, Joint Laboratory of Optics, Olomouc; Czech Republic.
- ¹²⁴Institute for Fundamental Science, University of Oregon, Eugene, OR; United States of America.
- ¹²⁵Graduate School of Science, Osaka University, Osaka; Japan.
- ¹²⁶Department of Physics, University of Oslo, Oslo; Norway.
- ¹²⁷Department of Physics, Oxford University, Oxford; United Kingdom.
- ¹²⁸LPNHE, Sorbonne Université, Université Paris Cité, CNRS/IN2P3, Paris; France.
- ¹²⁹Department of Physics, University of Pennsylvania, Philadelphia PA; United States of America.
- ¹³⁰Department of Physics and Astronomy, University of Pittsburgh, Pittsburgh PA; United States of America.
- ¹³¹^(a)Laboratório de Instrumentação e Física Experimental de Partículas - LIP, Lisboa;^(b)Departamento de Física, Faculdade de Ciências, Universidade de Lisboa, Lisboa;^(c)Departamento de Física, Universidade de Coimbra, Coimbra;^(d)Centro de Física Nuclear da Universidade de Lisboa, Lisboa;^(e)Departamento de Física, Universidade do Minho, Braga;^(f)Departamento de Física Teórica y del Cosmos, Universidad de Granada, Granada (Spain);^(g)Departamento de Física, Instituto Superior Técnico, Universidade de Lisboa, Lisboa; Portugal.
- ¹³²Institute of Physics of the Czech Academy of Sciences, Prague; Czech Republic.
- ¹³³Czech Technical University in Prague, Prague; Czech Republic.
- ¹³⁴Charles University, Faculty of Mathematics and Physics, Prague; Czech Republic.
- ¹³⁵Particle Physics Department, Rutherford Appleton Laboratory, Didcot; United Kingdom.
- ¹³⁶IRFU, CEA, Université Paris-Saclay, Gif-sur-Yvette; France.
- ¹³⁷Santa Cruz Institute for Particle Physics, University of California Santa Cruz, Santa Cruz CA; United States of America.
- ¹³⁸^(a)Departamento de Física, Pontificia Universidad Católica de Chile, Santiago;^(b)Millennium Institute for Subatomic physics at high energy frontier (SAPHIR), Santiago;^(c)Instituto de Investigación Multidisciplinario en Ciencia y Tecnología, y Departamento de Física, Universidad de La Serena;^(d)Universidad Andres Bello, Department of Physics, Santiago;^(e)Instituto de Alta Investigación, Universidad de Tarapacá, Arica;^(f)Departamento de Física, Universidad Técnica Federico Santa María, Valparaíso; Chile.
- ¹³⁹Department of Physics, University of Washington, Seattle WA; United States of America.
- ¹⁴⁰Department of Physics and Astronomy, University of Sheffield, Sheffield; United Kingdom.
- ¹⁴¹Department of Physics, Shinshu University, Nagano; Japan.
- ¹⁴²Department Physik, Universität Siegen, Siegen; Germany.
- ¹⁴³Department of Physics, Simon Fraser University, Burnaby BC; Canada.
- ¹⁴⁴SLAC National Accelerator Laboratory, Stanford CA; United States of America.
- ¹⁴⁵Department of Physics, Royal Institute of Technology, Stockholm; Sweden.
- ¹⁴⁶Departments of Physics and Astronomy, Stony Brook University, Stony Brook NY; United States of America.
- ¹⁴⁷Department of Physics and Astronomy, University of Sussex, Brighton; United Kingdom.

- ¹⁴⁸School of Physics, University of Sydney, Sydney; Australia.
- ¹⁴⁹Institute of Physics, Academia Sinica, Taipei; Taiwan.
- ¹⁵⁰(^a) E. Andronikashvili Institute of Physics, Iv. Javakhishvili Tbilisi State University, Tbilisi; (^b) High Energy Physics Institute, Tbilisi State University, Tbilisi; (^c) University of Georgia, Tbilisi; Georgia.
- ¹⁵¹Department of Physics, Technion, Israel Institute of Technology, Haifa; Israel.
- ¹⁵²Raymond and Beverly Sackler School of Physics and Astronomy, Tel Aviv University, Tel Aviv; Israel.
- ¹⁵³Department of Physics, Aristotle University of Thessaloniki, Thessaloniki; Greece.
- ¹⁵⁴International Center for Elementary Particle Physics and Department of Physics, University of Tokyo, Tokyo; Japan.
- ¹⁵⁵Department of Physics, Tokyo Institute of Technology, Tokyo; Japan.
- ¹⁵⁶Department of Physics, University of Toronto, Toronto ON; Canada.
- ¹⁵⁷(^a) TRIUMF, Vancouver BC; (^b) Department of Physics and Astronomy, York University, Toronto ON; Canada.
- ¹⁵⁸Division of Physics and Tomonaga Center for the History of the Universe, Faculty of Pure and Applied Sciences, University of Tsukuba, Tsukuba; Japan.
- ¹⁵⁹Department of Physics and Astronomy, Tufts University, Medford MA; United States of America.
- ¹⁶⁰Department of Physics and Astronomy, University of California Irvine, Irvine CA; United States of America.
- ¹⁶¹University of Sharjah, Sharjah; United Arab Emirates.
- ¹⁶²Department of Physics and Astronomy, University of Uppsala, Uppsala; Sweden.
- ¹⁶³Department of Physics, University of Illinois, Urbana IL; United States of America.
- ¹⁶⁴Instituto de Física Corpuscular (IFIC), Centro Mixto Universidad de Valencia - CSIC, Valencia; Spain.
- ¹⁶⁵Department of Physics, University of British Columbia, Vancouver BC; Canada.
- ¹⁶⁶Department of Physics and Astronomy, University of Victoria, Victoria BC; Canada.
- ¹⁶⁷Fakultät für Physik und Astronomie, Julius-Maximilians-Universität Würzburg, Würzburg; Germany.
- ¹⁶⁸Department of Physics, University of Warwick, Coventry; United Kingdom.
- ¹⁶⁹Waseda University, Tokyo; Japan.
- ¹⁷⁰Department of Particle Physics and Astrophysics, Weizmann Institute of Science, Rehovot; Israel.
- ¹⁷¹Department of Physics, University of Wisconsin, Madison WI; United States of America.
- ¹⁷²Fakultät für Mathematik und Naturwissenschaften, Fachgruppe Physik, Bergische Universität Wuppertal, Wuppertal; Germany.
- ¹⁷³Department of Physics, Yale University, New Haven CT; United States of America.
- ^a Also Affiliated with an institute covered by a cooperation agreement with CERN.
- ^b Also at An-Najah National University, Nablus; Palestine.
- ^c Also at Borough of Manhattan Community College, City University of New York, New York NY; United States of America.
- ^d Also at Center for High Energy Physics, Peking University; China.
- ^e Also at Center for Interdisciplinary Research and Innovation (CIRI-AUTH), Thessaloniki; Greece.
- ^f Also at Centro Studi e Ricerche Enrico Fermi; Italy.
- ^g Also at CERN, Geneva; Switzerland.
- ^h Also at Département de Physique Nucléaire et Corpusculaire, Université de Genève, Genève; Switzerland.
- ⁱ Also at Departament de Física de la Universitat Autònoma de Barcelona, Barcelona; Spain.
- ^j Also at Department of Financial and Management Engineering, University of the Aegean, Chios; Greece.
- ^k Also at Department of Physics, Ben Gurion University of the Negev, Beer Sheva; Israel.
- ^l Also at Department of Physics, California State University, Sacramento; United States of America.
- ^m Also at Department of Physics, King's College London, London; United Kingdom.

- ⁿ Also at Department of Physics, Stanford University, Stanford CA; United States of America.
- ^o Also at Department of Physics, Stellenbosch University; South Africa.
- ^p Also at Department of Physics, University of Fribourg, Fribourg; Switzerland.
- ^q Also at Department of Physics, University of Thessaly; Greece.
- ^r Also at Department of Physics, Westmont College, Santa Barbara; United States of America.
- ^s Also at Hellenic Open University, Patras; Greece.
- ^t Also at Institutio Catalana de Recerca i Estudis Avancats, ICREA, Barcelona; Spain.
- ^u Also at Institut für Experimentalphysik, Universität Hamburg, Hamburg; Germany.
- ^v Also at Institute for Nuclear Research and Nuclear Energy (INRNE) of the Bulgarian Academy of Sciences, Sofia; Bulgaria.
- ^w Also at Institute of Applied Physics, Mohammed VI Polytechnic University, Ben Guerir; Morocco.
- ^x Also at Institute of Particle Physics (IPP); Canada.
- ^y Also at Institute of Physics and Technology, Ulaanbaatar; Mongolia.
- ^z Also at Institute of Physics, Azerbaijan Academy of Sciences, Baku; Azerbaijan.
- ^{aa} Also at Institute of Theoretical Physics, Ilia State University, Tbilisi; Georgia.
- ^{ab} Also at Lawrence Livermore National Laboratory, Livermore; United States of America.
- ^{ac} Also at National Institute of Physics, University of the Philippines Diliman (Philippines); Philippines.
- ^{ad} Also at Technical University of Munich, Munich; Germany.
- ^{ae} Also at The Collaborative Innovation Center of Quantum Matter (CICQM), Beijing; China.
- ^{af} Also at TRIUMF, Vancouver BC; Canada.
- ^{ag} Also at Università di Napoli Parthenope, Napoli; Italy.
- ^{ah} Also at University of Colorado Boulder, Department of Physics, Colorado; United States of America.
- ^{ai} Also at Washington College, Chestertown, MD; United States of America.
- ^{aj} Also at Yeditepe University, Physics Department, Istanbul; Türkiye.
- * Deceased